
THE UNIVERSITY OF QUEENSLAND

# SCHOOL OF CIVIL ENGINEERING

**REPORT CH103/16**

# INTERACTIONS BETWEEN LARGE BOUNDARY ROUGHNESS AND HIGH INFLOW TURBULENCE IN OPEN CHANNEL: A PHYSICAL STUDY INTO TURBULENCE PROPERTIES TO ENHANCE UPSTREAM FISH MIGRATION

AUTHORS: Hang WANG, Laura K. BECKINGHAM, Caitlyn Z. JOHNSON, Urvisha R. KIRI, and Hubert CHANSON

HYDRAULIC MODEL REPORTS

This report is published by the School of Civil Engineering at the University of Queensland. Lists of recently-published titles of this series and of other publications are provided at the end of this report. Requests for copies of any of these documents should be addressed to the Civil Engineering Secretary.



School of Civil Engineering
The University of Queensland
Brisbane QLD 4072
AUSTRALIA

Telephone: (61 7) 3365 4163
Fax: (61 7) 3365 4599

URL: http:/http://www.civil.uq.edu.au//

First published in 2016 by
School of Civil Engineering
The University of Queensland, Brisbane QLD 4072, Australia



ISBN No. 978-1-74272-156-9

The University of Queensland, St Lucia QLD, Australia

# Interactions between Large Boundary Roughness and High Inflow Turbulence in Open channel: a Physical Study into Turbulence Properties to Enhance Upstream Fish Migration

by

Hang WANG

Research Fellow, The University of Queensland, School of Civil Engineering, Brisbane QLD 4072, Australia

Laura K. BECKINGHAM

Undergraduate student, The University of Queensland, School of Civil Engineering, Brisbane QLD 4072, Australia

Caitlyn Z. JOHNSON

Undergraduate student, The University of Queensland, School of Civil Engineering, Brisbane QLD 4072, Australia

Urvisha R. KIRI

Undergraduate student, The University of Queensland, School of Civil Engineering, Brisbane QLD 4072, Australia

and

Hubert CHANSON

Professor, The University of Queensland, School of Civil Engineering, Brisbane QLD 4072, Australia, Email: h.chanson@uq.edu.au

HYDRAULIC MODEL REPORT No. CH103/16

ISBN 978-1-74272-156-9

The University of Queensland, School of Civil Engineering,

May 2016

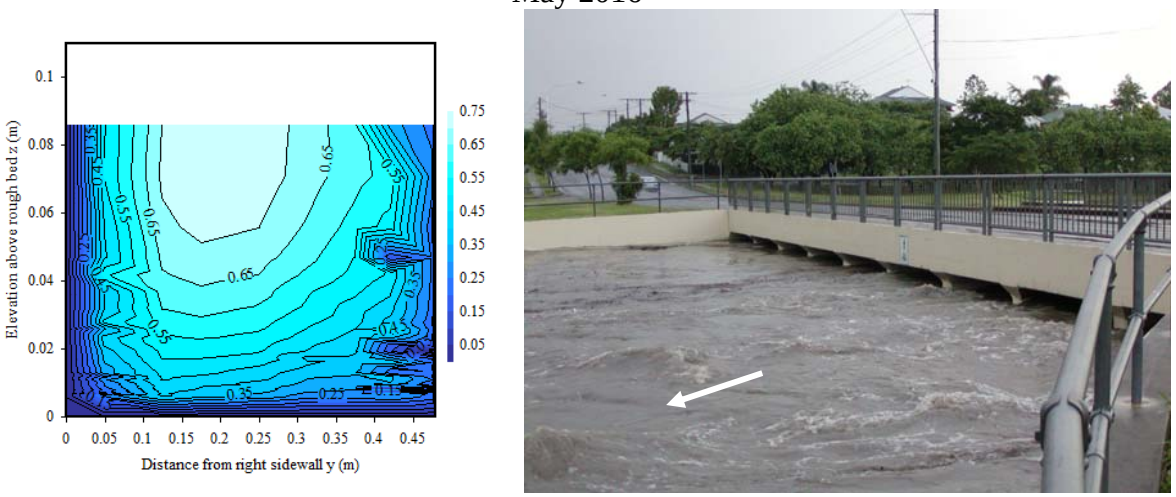


Left: Contour curves of constant longitudinal velocity in the 12 m long channel with rough bed and sidewall (Configuration 3) for Q = 0.0261 $m^3/s$ at x = 8 m

Right: Culvert operation beneath Cornwall Street, Stones Corner on 31 December 2001

**ABSTRACT**

Culverts are road crossings passing underneath an embankment (e.g. roadway, railroad) to allow continuous flow of water. Although the discharge capacity is based upon hydrological and hydraulic engineering considerations, large velocities in the structure may create a fish passage barrier. In this study, the effects of boundary roughness on turbulent properties were tested in channels with high inflow turbulence. Physical modelling was conducted in laboratory under controlled flow conditions to test systematically three boundary roughness configurations, with the aim to facilitate upstream fish migration by maximising slow flow and recirculation regions suitable to small fish (<10 cm total length) passage. The project focused on the development of a simple solution to retrofit of existing box culverts. Three test channels were investigated in a bio-hydrodynamics laboratory at the University of Queensland, equipped by a fish-friendly water reticulation system. A key feature was the presence of upstream and downstream screens to contain fish movements in designated test areas, resulting in inflow conditions with large turbulence levels. Three boundary roughness configurations were tested: (1) smooth boundaries, (2) rough invert and (3) rough invert and sidewall. The measurements showed the marked effect of boundary roughness on the distributions of time-averaged velocity and velocity fluctuations. With the rough bed and sidewall (Configuration 3), the results showed an asymmetrical velocity field, the existence of the velocity dip and the presence of secondary currents This roughness configuration appeared to provide excellent recirculation regions next to the rough sidewall and at the corner between the rough sidewall and channel bed, which might be suitable to the upstream passage of small body mass fish, typical of Australian streams. Preliminary experiments in a water tunnel showed that fish swimming performance data depended critically upon a careful testing protocol, as well as upon a sound velocity measurement technique.

Keywords: Open channel flows, Large boundary roughness, Secondary currents, Turbulence, Fish passage, Culverts, Physical study.

**TABLE OF CONTENTS**

**LIST OF SYMBOLS**

The following symbols are used in this report:

| | |
|---|---|
| A | channel cross-section area ($m^2$); |
| B | channel width (m); |
| $D_H$ | hydraulic diameter depth (m); |
| d | water depth (m); |
| $d_c$ | critical flow depth (m); |
| $d_o$ | inflow depth (m); |
| Fr | Froude number; for a rectangular channel: $Fr = \frac{V}{\sqrt{g \times d}}$ |
| f | Darcy-Weisbach friction factor; |
| g | gravity acceleration ($m/s^2$): g = 9.80 $m/s^2$ in Brisbane, Australia; |
| $k_s$ | equivalent sand roughness height (m); |
| L | channel length (m); |
| Q | water discharge ($m^3/s$); |
| P | pressure (Pa); |
| q | water discharge per unit width ($m^2/s$); |
| $S_f$ | friction slope; |
| $S_o$ | bed slope; |
| $T_f$ | amount of time (s) that the fish swam in the final increment; |
| Tu | turbulence intensity: $Tu = v_x'/V_x$; |
| $U_{crit}$ | critical swimming speed (m/s); |
| $U_f$ | penultimate velocity (m/s) during fish swimming performance testing; |
| V | flow velocity (m/s) positive downstream; |
| $V_c$ | critical flow velocity (m/s); |
| $V_{fs}$ | free-surface velocity (m/s); |
| $V_{max}$ | maximum velocity (m/s); |
| | free-stream velocity (m/s) above boundary layer |
| $V_{mean}$ | cross-sectional mean velocity (m/s): $V_{mean} = Q/A$; |
| $V_o$ | inflow velocity (m/s); |
| $V_x$ | longitudinal velocity component (m/s); |
| $V_y$ | transverse velocity component (m/s); |
| $V_z$ | vertical velocity component (m/s); |
| $\overline{V}$ | mean velocity (m/s) |
| $v_o'$ | standard deviation (m/s) of $V_o$; |
| $v_x'$ | standard deviation (m/s) of $V_x$; |
| $v_y'$ | standard deviation (m/s) of $V_y$; |
| $v_z'$ | standard deviation (m/s) of $V_z$; |

| | |
|---|---|
| x | longitudinal distance (m) positive downstream; |
| $Y_{Vmax}$ | transverse distance (m) where $V_x = V_{max}$; |
| y | transverse distance (m) measured from the right sidewall positive towards the left sidewall; |
| $Z_{Vmax}$ | vertical elevation (m) where $V_x = V_{max}$; |
| $Z_{Vx'm}$ | vertical elevation (m) where $v_x' = (v_x')_{max}$; |
| $Z_{Vy'm}$ | vertical elevation (m) where $v_y' = (v_y')_{max}$; |
| $Z_{Vz'm}$ | vertical elevation (m) where $v_z' = (v_z')_{max}$; |
| z | vertical distance (m) positive upwards with z = 0 at the invert; |

| | |
|---|---|
| $\Delta H$ | manometer reading (m); |
| $\Delta T$ | time increment (s); |
| $\delta$ | boundary layer thickness (m); |
| $\mu$ | dynamic viscosity (Pa.s) of water; |
| $\rho$ | water density ($kg/m^3$); |
| $\sigma$ | surface tension (N/m) between air and water; |
| Ø | diameter (m); |

*Subscript*

| | |
|---|---|
| max | maximum value; |
| min | minimum value; |
| o | inflow conditions; |
| x | longitudinal direction positive downstream; |
| y | transverse direction positive towards the left sidewall; |
| z | vertical direction positive upwards; |
| 1 | upstream flow conditions; |

*Abbreviations*

| | |
|---|---|
| ADV | acoustic Doppler velocimeter; |
| C | Celsius; |
| PVC | polyvinyl chloride; |
| s | second; |
| TL | total length. |

# 1. INTRODUCTION

## 1.1 PRESENTATION

Culverts are road crossings passing underneath an embankment (e.g. roadway, railroad) to allow continuous flow of water. Numerous waterway culverts are installed worldwide. Figure 1-1 presents typical examples. Culvert designs are diverse, using various shapes and materials determined by stream width, peak flows, stream gradient, and minimum cost (CHANSON 2004). For the past two decades, concerns regarding the ecological impact of culvert crossings have led to an evolution in their design. Although the overall culvert discharge capacity is based upon hydrological and hydraulic engineering considerations, large culvert flow velocities may create a fish passage barrier. In some cases, the environmental impact on fish passage may affect the upstream catchment with adverse impact on the stream ecology, because the installation of road crossings can limit the longitudinal connectivity of streams for fish movement (WARREN and PARDEW 1998, BRIGG and GALAROWICZ 2013). Common culvert fish passage barriers include excessive vertical drop at the culvert outlet (perched outlet), high velocity or inadequate flow depth within the culvert barrel, excessive turbulence, and debris accumulation at the culvert inlet (OLSEN and TULLIS 2013). The increased velocities in the barrel can also produce reduced flow depths (potentially inadequate flow depths for fish passage) relative to the culvert size. Higher culvert exit velocities may also increase perched outlet fall heights (fish barrier) with increased scour hole development downstream. Hydraulic jumps in the culvert inlet or outlet could generate further hindrance to fish massage. Figure 1-1H shows a hydraulic jump in a culvert inlet.

One of the primary ecological concerns regarding culvert crossings is the potential velocity barrier to upstream fish passage resulting from the constriction of the channel as illustrated in Figure 1-1. In an effort to minimize the impact of culvert crossings on stream ecology, several jurisdictions have developed guidelines to ensure that their design will allow for the upstream passage of fish. In Canada, these guidelines are based on a number of criteria including average flow velocity and minimum embedment depth (HUNT et al. 2012). For culvert rehabilitation applications where fish passage may be a concern, baffles installed along the invert may provide a more fish-friendly alternative, provided that adequate culvert discharge capacity is maintained (OLSEN and TULLIS 2013, CHANSON and UYS 2016). At low flows, baffles would decrease the flow velocity and increase the water depth for fish passage. For medium to larger discharges, baffles would induced locally lower velocities and generate recirculation regions.

(A) 

 (B)

(C)

(D) 

 (E)

(F) 

 (G)

(H) 


Fig. 1-1 - Culvert operation during small to medium rainstorms in Queensland, Australia - (A) Inlet of culvert in St Lucia on 31 Dec. 2001 at 5:40am; (B) Outlet of culvert beneath Cornwall Street, Stones Corner on 31 Dec. 2001 around 6:10am; (C) Outlet of culvert beneath Cornwall Street, Stones Corner on 20 May 2009 between 8:40 and 8:45am; (D) Details of culvert inlet flow beneath Cornwall Street on 20 May 2009 between 10:35 and 10:40am; (E) Outlet of culvert beneath Ridge Street, Stones Corner on 31 Dec. 2001 around 6:10am; (F) Culvert inlet operation upstream of Ridge Street, Stones Corner on 7 Nov. 2004 around 13:15; (G) Culvert outlet downstream of Ridge Street, Stones Corner on 20 May 2009 between 10:25 and 10:35am; (H) Inlet operation of culvert beneath Ridge Street, Stones Corner on 20 May 2009 at 11:00am with details of hydraulic jump roller in front of culvert barrel - White arrows show flow direction

Although culvert type may not have a major role influencing the fish longitudinal movement, a general data trend indicated that box culverts (e.g. Fig 1-1B and 1-1C) were most effective (BRIGG and GALAROWICZ 2013). The culvert length is another important factor in allowing upstream passage of some fish species. For example, in northeastern Kansas streams, fish movement data supported culvert length as an important factor since the culverts limiting upstream fish passage were the longest culverts in the study (BRIGG and GALAROWICZ 2013). The behavioural response by some fish species to culvert length and flow turbulence could play a role in their swimming ability and culvert passage rate. The critical parameters of a culvert in terms of fish passage are the dimensions of the barrel, including its length and cross-sectional characteristics and the invert slope. These geometric characteristics, together with the water levels upstream and downstream of the structure, determine the hydraulic behaviour of the culvert, i.e. the flow discharge, the head loss through the culvert, the flow pattern and the turbulent velocity field in the barrel (HENDERSON 1966, HEE 1969, CHANSON 2004). The variability of the culvert dimensions is linked to the characteristics and constraints of the site where the road crossing has to be built, the flow discharge passing through the facility and the compliance with specifications for

volumetric power dissipation. This variability results in a wide diversity in flow patterns that can be observed in existing culverts. These flow patterns are one of the elements determining the capacity of the facility to allow the targeted fish species to pass successfully. A recent discussion paper recommended that three-dimensional analysis of culvert flows should be considered to gain an understanding of the turbulence and secondary flow motion (PAPANICOLAOU and TALEBBEYDOKHTI 2002). The authors recommended an in-depth examination of the spanwise and vertical velocity distributions as well as turbulent intensities and kinetic energy, in view of the importance of these parameters to fish passage.

## 1.2 CULVERT FISH PASS DESIGN

The selection of the type of culvert fish pass and of the fish pass characteristics depends on the swimming capacities of the fish species. If the fish swimming power is greater than the maximum volumetric power (BATES 2000), the fish will be able to pass the successive baffles and rest in each pool, thus successfully negotiate a fish pass consisting of a large number of pools without difficulty. Currently there is no simple technical means for measuring the characteristics of turbulence in fish pass, although it is acknowledged that the turbulence in fish pass plays a key role in fish behaviour (LIU et al. 2006, YASUDA 2011, BRETON et al. 2013). A number of key turbulence characteristics, which are deemed most important to migrating fish, have been identified: turbulence intensity, Reynolds stresses, turbulent kinetic energy, vorticity, dissipation (PAVLOV et al. 2000. HOTCHKISS 2002, NIKORA et al. 2003). Recent observations further showed that fish may take advantage of the unsteady character of turbulent flows (WANG et al. 2010, TARRADE et al. 2011).

In Australia, national guidelines on fish passage requirements for waterway crossings developed in 2003 were based on limited data for native Australian fish. The biological information which underpinned these recommendations was based on research and evaluation of overseas fish species (e.g. salmonids) that display vastly superior swimming capabilities compared to most Australian native fish. Current Australian national recommendations provide little guidance concerning specific culvert design parameters. They merely indicate that water depth should range between 0.2 to 0.5 m with bulk velocity less than 0.3 m/s during base flows, and that culvert cross-sectional area should maximise geometric similarities of the natural waterway profile (FAIRFULL and WITHERIDGE 2003), thus yielding uneconomical culvert designs. Newer research suggested that bulk velocity maxima should to be revised down to 0.1 m/s for culvert lengths up to 15 m (RODGERS et al. 2014).

## 1.3 ROLE OF BOUNDARY ROUGHNESS

In recent years, rock-ramp fish passes were introduced as naturelike fish passage (BAKI et al. 2014), while a number of studies investigated the effects of large bed roughness (LACEY and RENNIE 2012, CASSAN et al. 2014). The large bed roughness induced characteristic coherent flow structures, creating or masking trails that can be tracked by fish (JOHNSON and RICE 2014). Observations in fishways indicated that fish behaviour was strongly affected by the turbulent flow and its structure (DAVID et al. 2012). Substrate roughening was observed to increase the likelihood of successful passage of small-bodied ([1]) native Australian fish species (HEASLIP 2015). To date most studies considered the effects of bed roughness, and the role of sidewall roughness was not considered.

On the other hand, carefully-controlled experiments suggested that the bed roughness and inflow turbulence might have little effects on fish swimming velocities (NIKORA et al. 2003). The same study hinted however the potential interplay between turbulence length scales and fish dimensions.

## 1.4 STRUCTURE OF THE REPORT

In this report, the effects of boundary roughness on turbulent properties were tested in channels with high inflow turbulence. Physical modelling was conducted in laboratory under controlled flow conditions to test systematically three boundary roughness configurations, with the aim to facilitate upstream fish migration by maximising slow flow and recirculation regions suitable to small fish passage. The project focused on the development of a simple solution to retrofit of existing box culverts.

[1] That is, small-bodied and/or juvenile fish less than 100 mm long. Examples of small-bodied Australia native fish species include Empire Gudgeon, Firetail Gudgeon, Western Carp Gudgeon, Striped Gudgeon, Mountain Galaxias, Southern Pygmy Perch, Unspecked Hardyhead, Common Jollytail, Olive Perchlet, Fly-specked Hardyhead, Australian Smelt and Duboulay's Rainbowfish.

# 2. EXPERIMENTAL STUDY, INSTRUMENTATION AND METHODOLOGY

## 2.1 PRESENTATION

Physical models are commonly used in hydraulic engineering to optimise a structure and to ensure a sound operation of the open channel system. In laboratory, the flow conditions must be similar to those at full-scale: that is, a similarity of form, of motion and of forces (NOVAK and CABELKA 1981, HUGHES 1993, CHANSON 2004, NOVAK et al. 2010). In many hydraulic engineering applications, including the present one, the physical model is smaller than the prototype, and scale effects might take place.

For any dimensional analysis, the relevant parameters include the fluid properties and physical constants, the channel geometry and initial flow conditions. Considering the simple case of a steady flow in a rectangular, horizontal channel, a dimensional analysis yields a series of relationship between the flow properties at a location (x,y,z) and the initial flow conditions, channel geometry and fluid properties:

$$\frac{d}{d_c}, \frac{P}{\rho \times g \times d_c}, \frac{V_x}{V_c}, \frac{V_y}{V_c}, \frac{V_z}{V_c}, , \frac{v_x'}{V_c}, \frac{v_y'}{V_c}, \frac{v_z'}{V_c} = F\left( \frac{x}{d_c}, \frac{y}{d_c}, \frac{z}{d_c}, \frac{V_o}{\sqrt{g \times d_o}}, \frac{v_o'}{V_c}, \rho \times \frac{q}{\mu}, \frac{B}{d_c}, \frac{k_s}{d_c}, \frac{g \times \mu^4}{\rho \times \sigma^3}, ... \right) \quad (2\text{-}1)$$

where d is the flow depth, P is the instantaneous pressure at a location (x, y, z), with x the longitudinal coordinate positive downstream, y the transverse coordinate positive towards the left sidewall and z the vertical elevation positive upwards, $V_x$, $V_y$, $V_z$ are respectively the time-averaged longitudinal, transverse and vertical velocity components, $v_x'$, $v_y'$, $v_z'$ are respectively some characteristic longitudinal, transverse and vertical velocity fluctuations, $d_c$ and $V_c$ are respectively the critical flow depth and velocity ([2]), $d_o$ and $V_o$ are the inflow depth and velocity respectively, $v_o'$ is an initial characteristic velocity fluctuations, B is the channel width, $k_s$ is the equivalent sand roughness height of the channel boundary, g is the gravity acceleration, q is the water discharge per unit width ($q = V_c \times d_c$), $\rho$ and $\mu$ are the water density and dynamic viscosity respectively, and $\sigma$ is the surface tension between air and water. Equation (2-1) describes the dimensionless steady flow properties at a position as functions of a number of dimensionless parameters, including the inflow Froude number (4th term), the inflow turbulence intensity (5th term) the Reynolds number (6th term) and the Morton number (9th term).

In a geometrically similar model, a true dynamic similarity is achieved only if each dimensionless parameter has the same value in both model and prototype. Scale effects may exist when one or

[2] For a rectangular channel: $d_c = (Q^2/(g \times B^2)^{1/3}$ and $V_c = (g \times Q/B)^{1/3}$ (HENDERSON 1966, CHANSON 2004).

more dimensionless numbers have different values between the model and prototype. In free-surface flows, a Froude similitude is commonly used (NOVAK and CABELKA 1981, LIGGETT 1994). When the same fluids (air and water) are used in both model and prototype, the Morton number becomes a constant. Herein Froude and Morton number similarities were applied and the experiments were conducted in a large size facility operating at relatively large Reynolds numbers. These conditions may correspond to a 1:4 to 1:5 scale study of box culvert cells shown in Figures 1-1B to 1-1H, thus ensuring that the extrapolation of the laboratory data to prototype conditions is unlikely to be adversely affected by significant scale effects.

## 2.2 EXPERIMENTAL FACILITIES

New experiments were conducted in the Seddon bio-hydrodynamics laboratory at the University of Queensland. Three experimental facilities were used: (1) a 12 m long 0.5 m wide flume, (2) a 3.2 m long 0.25 m wide flume and (3) a recirculating water tunnel with a 0.259×0.251 $m^2$ cross-section. The bulk of the measurements were conducted in the 12 m long flume, tests with juvenile silver perch fish (*Bidyanus bidyanus*) were performed in the water tunnel, and calibration tests were undertaken in the 3.2 m long flume.

### 2.2.1 12 m long flume

Several experiments were conducted in a relatively large rectangular tilting flume (Fig. 2-1A). The channel was 12 m long 0.5 m wide and the channel bed was horizontal herein. The flume was made of smooth PVC bed and glass walls. The waters were supplied by a constant head tank feeding a large intake basin (2.1 m long, 1.1 m wide, 1.1 m deep) leading to the test section through a series of flow straighteners, followed by a bottom and sidewall convergent. The channel ended with a free overfall at x = 12 m. Both upstream and downstream of the flume, stainless steel screens were installed to ensure the safety of small fish. The mesh wire had a 1.6 mm diameter, the mesh pattern was square and the mesh opening was 6.75 mm (inside dimensions). Figure 2-2 presents photographs of the screens. The upstream screen was located in the intake basin immediately upstream of the bottom and sidewall convergent. The downstream screen was located 0.57 m upstream of the free overfall. The same flume was previously used by SIMON and CHANSON (2013) and LENG and CHANSON (2014), without upstream and downstream screens.

The water discharge was supplied by a constant head reticulation system, equipped with a biological filter system, enabling fish-friendly chemical-free water. The flow rate was measured with an orifice meter that was designed based upon the British Standards (British Standard 1943) and calibrated on site against a V-notch weir, and the integration of the measured velocity profiles

obtained with the acoustic Doppler velocimeter and with the Prandtl-Pitot tube ([3]). The percentage of error was expected to be less than 2%.

(A) 12 m long flume looking upstream; (Left) Rough bed configuration - note in the background the intake structure, the upstream screen and flow straighteners behind; (Right) Rough bed and rough left sidewall configuration

(B1) General overview - Arrow shows flow direction in working section

[3] The calibration data sets are reported in Appendix A.

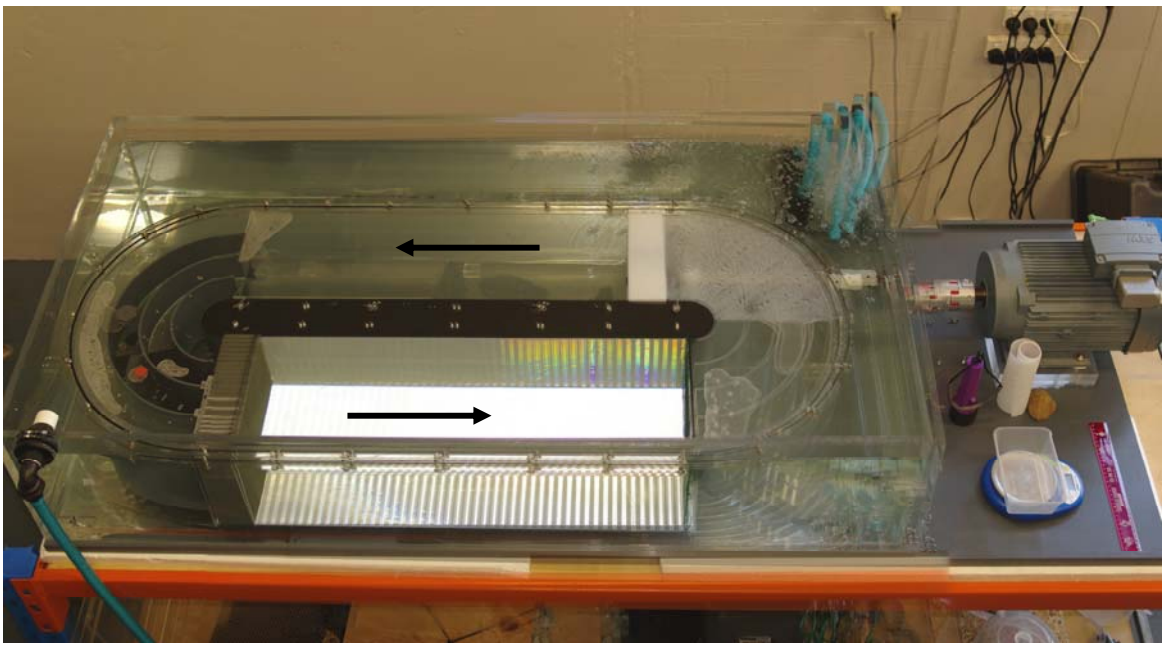

(B2) View in elevation - Arrows indicate flow direction

(B) Recirculating water tunnel

Fig. 2-1 - Sketch of the experimental facilities

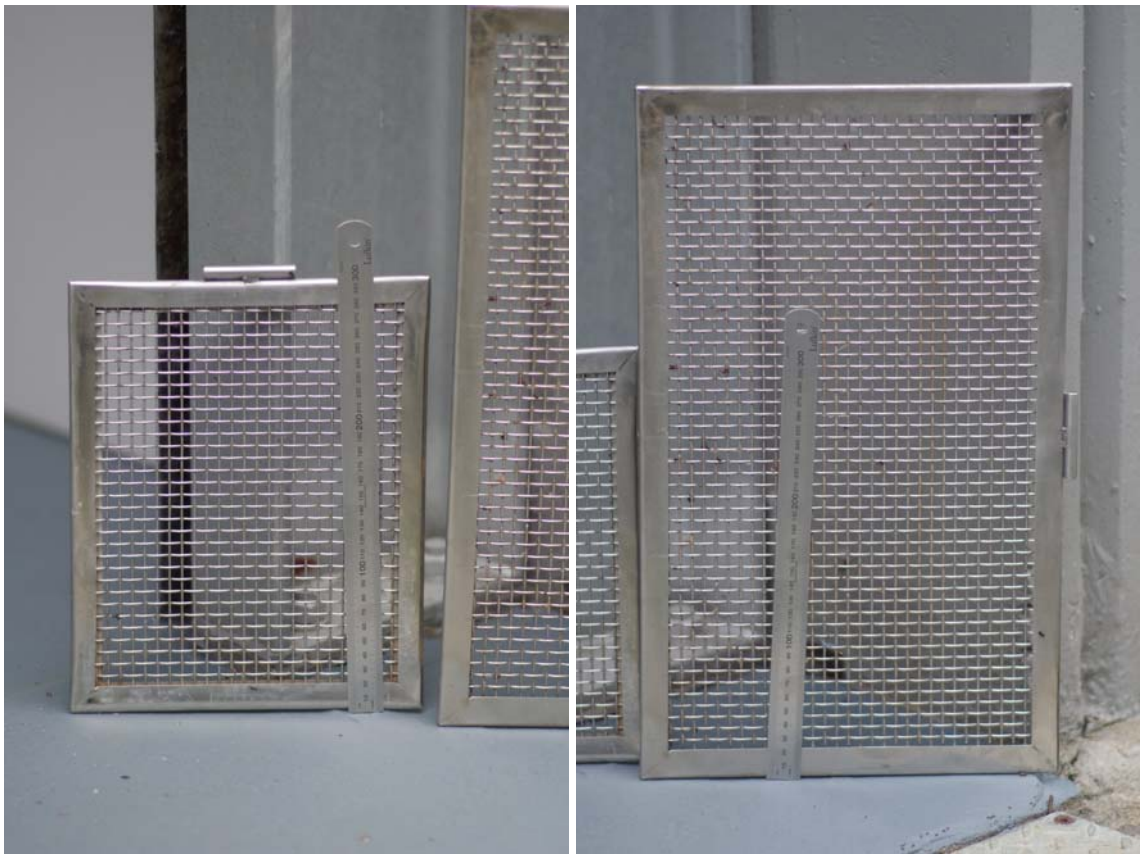

Fig. 2-2 - Details of the stainless steel mesh screens - Mesh wire diameter: 1.6 mm, square opening, opening size: 6.75 mm

2.2.2 3.2 m long flume

Calibration tests were performed in a 3.2 m long 0.25 m wide rectangular tilting flume. The PVC channel bed was horizontal herein and the sidewalls were made out of glass. The waters were supplied by the constant head tank system feeding a small intake basin leading to the test section through a series of flow straighteners, followed by a convergent. The channel ended with a free overfall at x = 3.2 m. Both upstream and downstream of the flume, stainless steel screens ([4]) were installed to ensure the safety of small fish. The upstream screen was located in the intake basin immediately upstream of the bed and sidewall convergent. The downstream screen was located 0.21 m upstream of the free overfall. The flow rate was measured with a Venturi meter that was designed based upon the British Standards (British Standard 1943) and calibrated on site (Appendix A).

2.2.3 Water tunnel

The fish swimming tests were conducted using a small Loligo$^{TM}$ recirculating water tunnel with a 0.86 m long 0.251 m wide and 0.259 m high working section made of perspex (Fig. 2-1B). The volume of the water tunnel system was 0.185 m$^3$ and it was placed in a 0.4 m$^3$ rectangular water tank. The top section was equipped with a 0.215 m diameter access panel to insert the velocimeter. Screens and mesh were installed at both test section ends to restrict the fish movements.

Water quality was maintained using a continuous flow of filtered fresh water from an external reservoir enabling a constant temperature of 24 C ±0.5 C. A continuous flow motion in the tunnel test section was delivered by a screw pump.

The flow hydrodynamics in the water tunnel were assessed before swimming tests with direct measurements covering a velocity range from 0.1 m/s to 1.1 m/s.

## 2.3 INSTRUMENTATION

2.3.1 Presentation

The water depths were measured using rail mounted pointer gauges.

In the 12 m long and 3.2 m long flumes, the velocity measurements were conducted with either a Prandtl-Pitot tube or an acoustic Doppler velocimeter (ADV). The Pitot tube was a Dwyer® 166 Series Prandtl-Pitot tube with a 3.18 mm diameter tube made of corrosion resistant stainless steel, and featured a hemispherical total pressure tapping (Ø = 1.19 mm) at the tip with four equally spaced static pressure tappings (Ø = 0.51 mm) located 25.4 mm behind the tip. The tip design met

[4] The same screen mesh was used for both 12 m long and 3.2 m log flumes, with a mesh wire diameter: 1.6 mm, square opening, opening size: 6.75 mm (Fig. 2-2).

AMCA and ASHRAE specifications and the tube did not require calibration ([5]). The acoustic Doppler velocimeter was a Nortek™ Vectrino+ (Serial No. VNO 0436) unit equipped with a three-dimensional side-looking head (Fig. 2-3). The velocity range was ±1.0 m/s and the sampling rate was 200 Hz. The ADV was set up with a transmit length of 0.3 mm and a sampling volume of 1.5 mm height. The ADV signal was sampled at 200 Hz for 180 s at each point. The translation of the Pitot-Prandtl and ADV probes in the vertical direction was controlled by a fine adjustment travelling mechanism connected to a Mitutoyo™ digimatic scale unit. The error on the vertical position of the probes was $\Delta z < 0.025$ mm. The accuracy on the longitudinal position was estimated as $\Delta x < \pm 2$ mm. The accuracy on the transverse position of the probe was less than 1 mm.

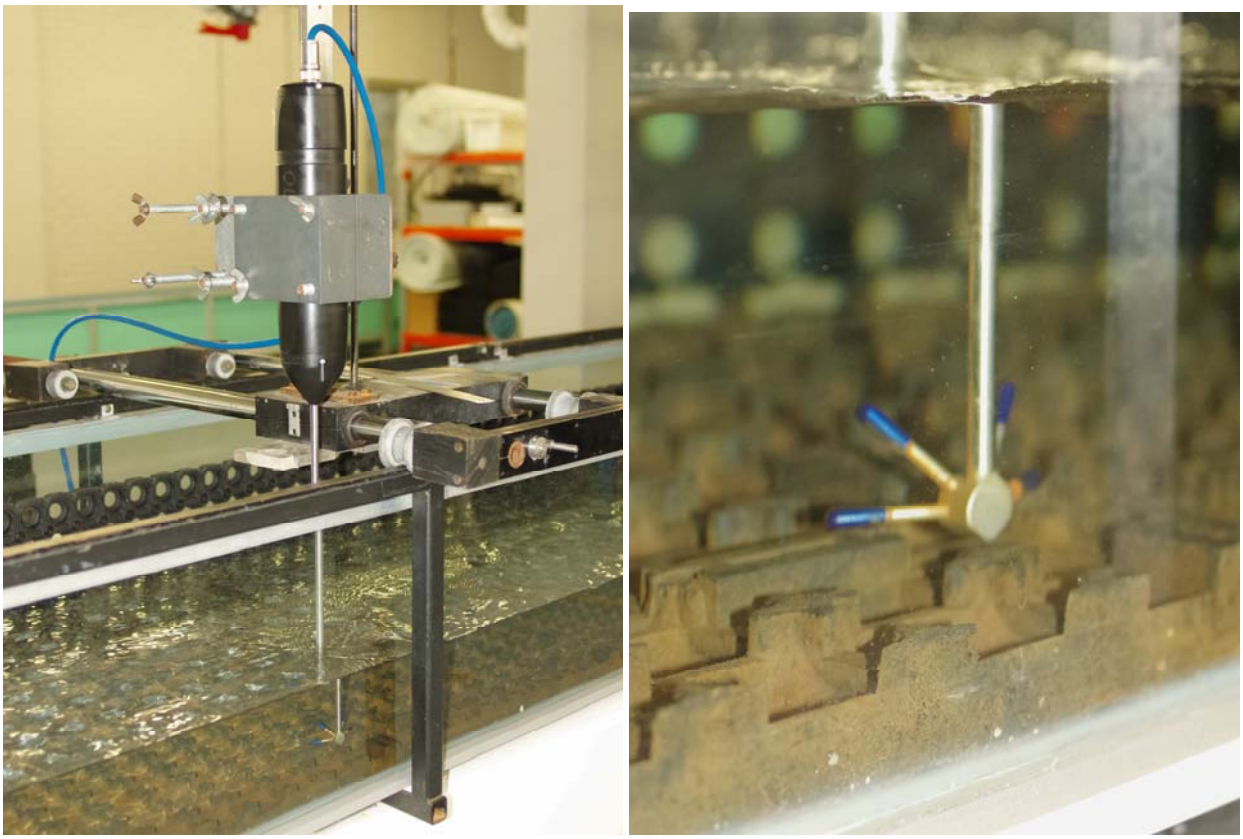

(A, Left) General view of the ADV unit, flow from left to right

(B, Right) Details of the ADV head above the roughness bed

[5] Reference: http://www.dwyer-inst.com/Product/TestEquipment/PitotTubes/Series160.

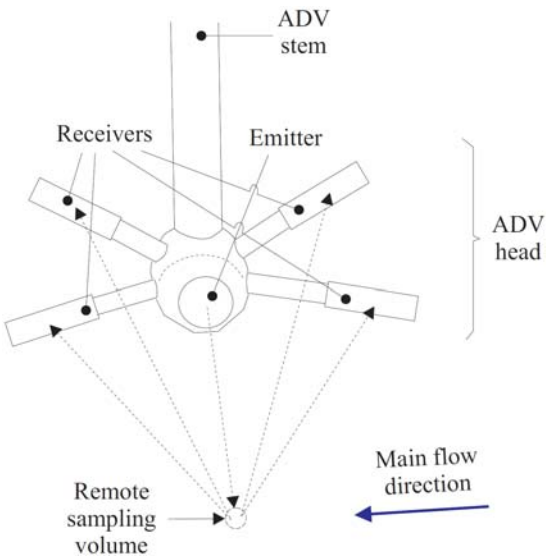


(C) Sketch of the ADV side-looking head

Fig. 2-3 - Acoustic Doppler velocimeter

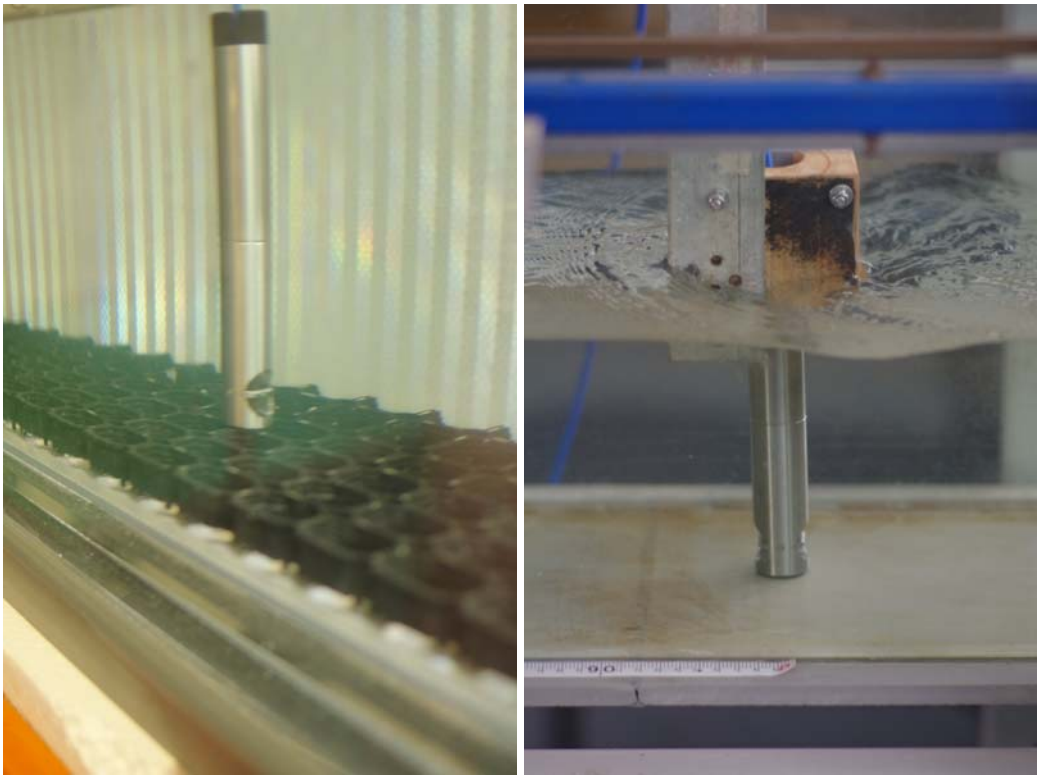

Fig. 2-4 - Propeller velocimeter - Left: in the recirculating water tunnel; Right: in the 3.2 m long flume, with flow direction from left to right

In the water tunnel, the velocity was measured using a Hontzsch$^{TM}$ vane wheel AC10002 meter. The meter consisted of a 30 mm diameter body with a 25 mm circular housing and a 22 mm

diameter propeller ([6]). The propeller meter was also tested in the 3.2 m long flume against the ADV and Pitot tube data (Appendix B). Figure 2-4 shows photographs of the propeller meter.
Additional information was obtained with digital cameras Pentax™ K-3 and Casio™ Exlim EX-10, with movie mode set at 240 fps (512×384 pixels).

2.3.2 Acoustic Doppler velocimetry and data processing

The acoustic Doppler velocimeter (ADV) operation is based on the Doppler shift effect. The velocity measurements are inferred from the Doppler shift measurements of particles in a remote sampling volume (VOULGARIS and TROWBRIDGE 1998, McLELLAND and NICHOLAS 2000). For each velocity component sample, the ADV system records the level of signal strength, correlation value and signal-to-noise ratio. These parameters are indicative of the quality and reliability of velocity measurements (McLELLAND and NICHOLAS 2000, CHANSON 2008). Past and present experiences demonstrated some recurrent issues because the ADV signal outputs combined the effects of velocity fluctuations, Doppler noise, signal aliasing, turbulent shear and other errors (LEMMIN and LHERMITTE 1999, GORING and NIKORA 2002, CHANSON et al. 2007,2008, DOROUDIAN et al. 2007, DOCHERTY and CHANSON 2010).
For all experiments, the present experience highlighted some problems with the velocity data, including low correlations and low signal to noise ratios. Initially this was primarily caused by a lack of particles in the channel water at the start of the experiments. After several days of operation, natural particles circulated into the reticulation system and no further problem was observed.
The post processing of ADV data was conducted with the software WinADV™ version 2.030. The signal post processing included the removal of communication errors, the removal of average signal to noise ratio data less than 5 dB and the removal of average correlation values less than 60%. In addition, the phase-space thresholding technique developed by GORING and NIKORA (2002) and implemented by WAHL (2003) was used to remove spurious points in the data set.
The proximity of a solid boundary may affect adversely the ADV probe output. Several studies discussed the effects of boundary proximity on sampling volume characteristics and the impact on the time-averaged velocity (FINELLI et al. 1999, LIU et al. 2002, CHANSON et al. 2007). The findings highlighted that acoustic Doppler velocimeter outputs were adversely affected when the solid boundary was less than 30 to 50 mm from the probe sampling volume. Herein, with the side-looking head, the vertical velocity component $V_z$ data were adversely affected by the bed proximity for $z < 0.030$ m, where z is the vertical elevation above the bed, as documented by CHANSON (2010), DOCHERTY and CHANSON (2012) and LENG and CHANSON (2014). Further all

[6] When the propeller casing sat on the bed, the propeller axis was 17.3 mm above the invert.

velocity components were affected when the control volume was located less than 50 mm from the sidewalls ([7]), with a significant drop in average signal correlations, in average signal-to-noise ratios and in average signal amplitudes.

## 2.4 BED CONFIGURATIONS AND CHARACTERISTICS

Three types of bed roughness were tested in the 12 m long flume and water tunnel. Some experiments were performed with the smooth PVC invert and smooth sidewalls (Configuration 1). Further experiments were conducted with a rough bed and smooth sidewalls (Configuration 2). The last configuration consisted of a rough bed, a rough sidewall and a smooth sidewall (Configuration 3). All these boundary roughness configurations are illustrated in Figure 2-5. For Configurations 2 and 3, the smooth channel bed was covered with a series of industrial rubber floor mats for 0.05 m < x < 10.65 m. The rubber mats consisted of square patterns (Fig. 2-5). They were cut to the channel width and laid on the PVC. With Configuration 3, a series of rubber mats were glued to one sidewall.

Herein the water depths were measured above the top of the rubber mats, that is z = 0 as shown in Figure 2-6. On rough walls, the effective origin of the boundary layer is not known (PERRY et al. 1987). In line with studies of d-type roughness (DJENIDI et al. 1999), the assumption of z = 0 at the top of the mats was used and it was supported by visual observations suggesting zero to negligible flow motion through the mats themselves.

The hydraulic roughness of the three boundary roughness configurations was tested in the 12 m long flume for a range of steady flow conditions. The gradually-varied flow profiles were recorded in the fully-developed flow region for a range of steady flow rates. The boundary shear stress was deduced from the measured free-surface profiles and estimated friction slopes ([8]). The estimates of Darcy-Weisbach friction factor f for the smooth boundary Configuration 1 ranged from 0.015 to 0.017, corresponding to mean equivalent sand roughness height $k_s$ = 0.2 mm. The equivalent Darcy friction factor of the rough bed Configuration 2 was f = 0.07 to 0.10 (Config. 2), while the friction factor of the rough boundary Configuration 3 was f = 0.08 to 0.12 (Config. 3). The results corresponded to an equivalent sand roughness height $k_s \approx$ 20 mm (Config. 2) and 30 mm (Config. 3) on average ([9]). The equivalent rugosity height of Configuration 2 was close to the earlier findings

---

[7] The same issue was experience with both glass sidewall and rough sidewall herein.

[8] The friction slope $S_f$ is the slope of the total head line. $S_f$ is related to the Darcy-Weisbach friction factor f by: $S_f = f \times V^2/(2 \times g \times D_H)$ where $D_H$ is the equivalent pipe diameter (HENDERSON 1966, CHANSON 2004).

[9] Further experiments with Configuration 3 and 0.015 < Q < 0.053 $m^3/s$ yielded an equivalent Darcy friction factor 0.07 < f < 0.11 corresponding to an equivalent sand roughness height 20 < $k_s$ < 25 mm.

of LENG and CHANSON (2014) with the same bed roughness configuration ([10]).

(A) Configuration 1: smooth bed and sidewalls

(B) Configuration 2: rough bed and smooth sidewalls

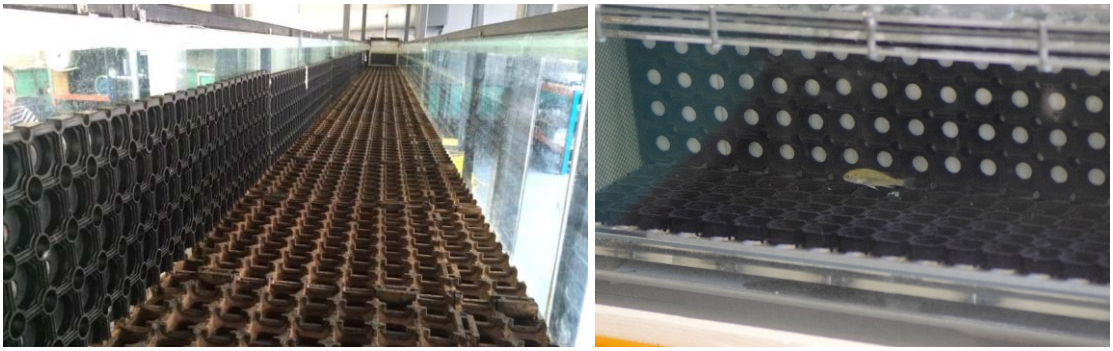

(C) Configuration 3: rough bed, and combination of rough and smooth sidewall

Fig. 2-5 - Roughness configurations in the 12 m long flume (Left) and water tunnel (Right)

[10] In the same flume with the same bed materials, LENG and CHANSON (2014) reported Darcy friction factors f = 0.09 to 0.18 corresponding to an equivalent sand roughness height $k_s$ = 39 mm. However the inflow conditions differed: no upstream screen was located in the intake basin during their experiments.

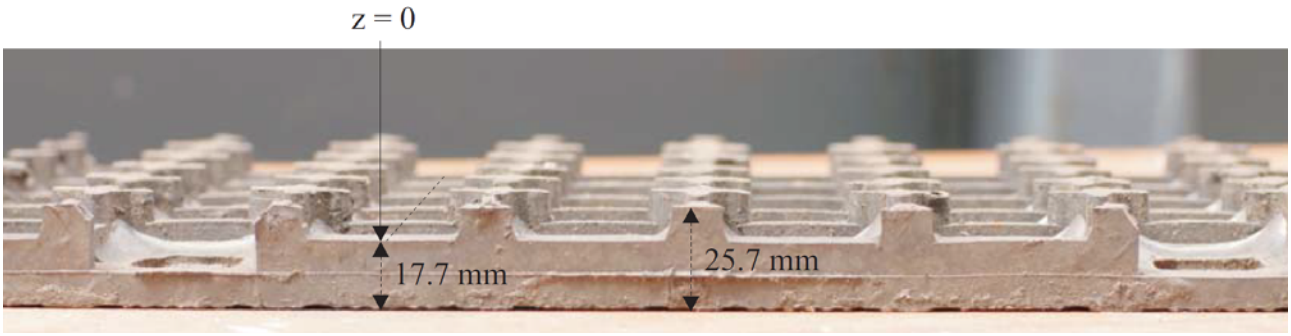


(A) Rubber mat used on the 12 m long channel bed (after LENG and CHANSON 2014) - Note the rubber 'spikes' protuding above the vertical origin (z = 0)

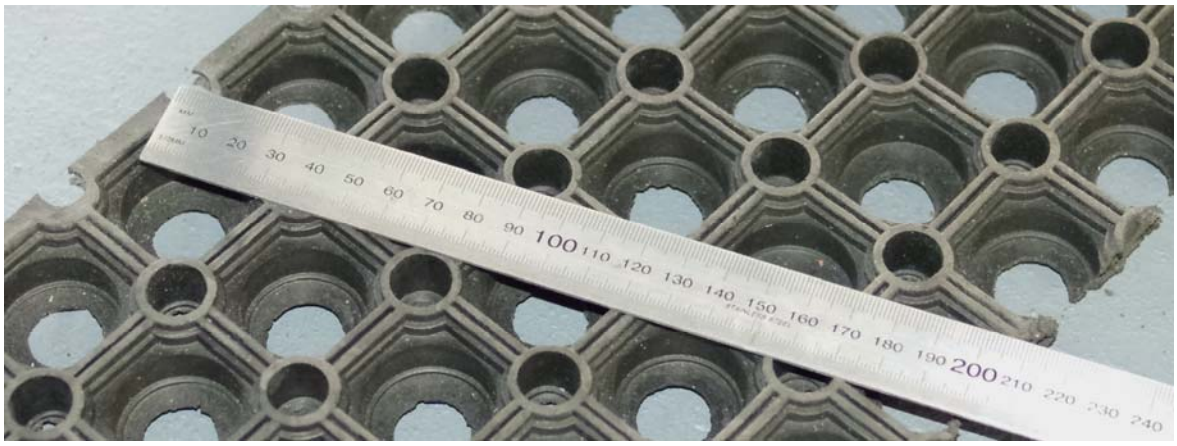

(B) Rubber mat used in the water tunnel and along the 12 m long flume sidewall - The vertical origin (z = 0) was set at the top of the mat where the ruler is


(C) Rubber mat used in the water tunnel and along the 12 m long flume sidewall

Fig. 2-6 - Rubber mat details

## 2.5 EXPERIMENTAL FLOW CONDITIONS

Several series of experiments were conducted. In the 12 m long flume, the measurements focused on the effects of boundary roughness on the turbulent flow properties, with some relatively high inflow turbulence. The 3.2 m long flume was used to perform comparative tests of velocimeters with a smooth bed and sidewalls (Appendix B). The small recirculating water tunnel was used to undertake fish swimming performance tests (Appendix D).

Table 2-1 summarises the experimental flow conditions.

Table 2-1 - Experimental flow conditions and boundary conditions

| Facility | Q<br>$m^3/s$ | B<br>m | Boundary conditions | Velocity measurement technique |
|---|---|---|---|---|
| 12 m long flume | 0.261<br>0.556 | 0.50 ([a])<br>0.478 ([b]) | PVC bed & glass sidewalls<br>Rough bed & glass sidewalls<br>Rough bed & rough sidewall | Flow meter, Pitot tube, acoustic Doppler velocimeter |
| 3.2 m long flume | 0.010<br>0.020 | 0.25 | PVC bed & glass sidewalls | Flow meter, Pitot tube, acoustic Doppler velocimeter, Propeller |
| Recirculating water tunnel | -- | 0.25 ([a])<br>0.225 ([b]) | Smooth bed & sidewalls<br>Rough bed & smooth sidewalls<br>Rough bed & rough sidewall | Propeller |

Notes: B: channel width; Q: water discharge; (--) data not available; ([a]) Configurations 1 and 2 with smooth sidewalls; ([b]): Configuration 3 with rough left sidewall.

# 3. TIME-AVERAGED VELOCITY AND TURBULENCE MEASUREMENTS

## 3.1 PRESENTATION

In the 12 m and 3.2 m long channels, the upstream flow was relatively turbulent, because of the upstream screens, located at the upstream end of the intake convergent. The inflow turbulence was measured with the acoustic Doppler velocimeter. At the upstream end of the channels, the turbulence intensity Tu ranged from 17% to 20% in the 3.2 m long channel, while Tu ≈ 16% in the 12 m long flume irrespective of the channel roughness configuration ([1]). Herein the turbulence intensity is defined as $Tu = v_x'/V_x$, where $v_x'$ is the standard deviation of the longitudinal velocity component and $V_x$ is the time-averaged longitudinal velocity component. For comparison, DOCHERTY and CHANSON (2012) and SIMON and CHANSON (2013) measured some inflow turbulence in the 12 m long channel in absence of screens: i.e., about Tu ~ 5-10%, depending upon the discharge.

The flow was subcritical along both channels, with decreasing water depth with increasing downstream distance. The longitudinal free-surface profiles presented a H2 backwater profile (BRESSE 1860, CHOW 1959). This is illustrated in Figure 3-1. In presence of boundary roughness, the boundary friction induced a greater rate of decrease in water depth with increasing downstream distance.

Another flow feature was the 'backwater effect' induced by the downstream screen, because the downstream screen induced some energy loss. Herein the downstream screen was regularly cleaned to prevent any clogging.

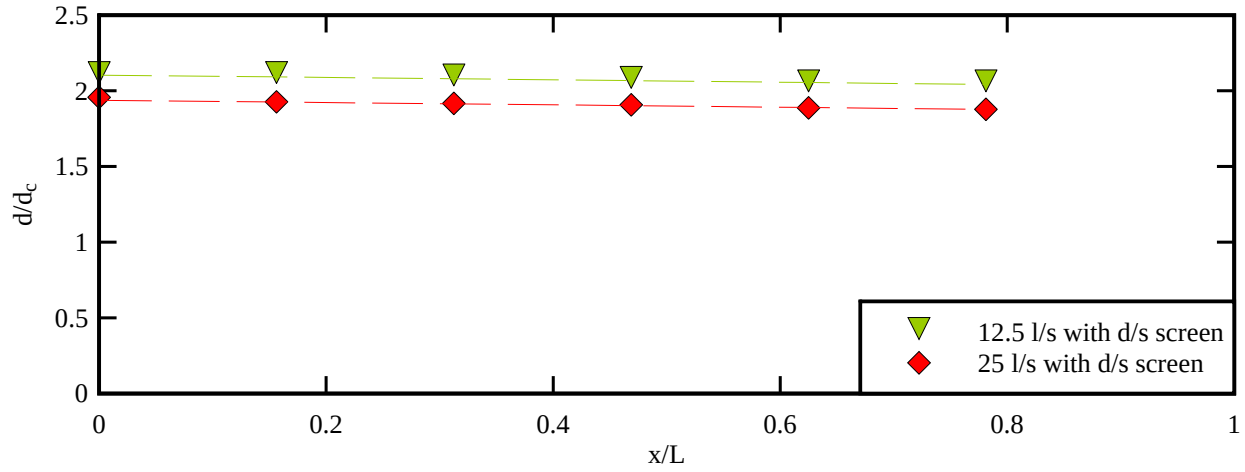


(A) 3.2 m long flume with smooth PVC bed and glass sidewalls

[1] The data were recorded with the ADV unit in the free-stream on the channel centreline at x = 0.65 m in 12 m long channel and x = 0.5 m in 3.2 m long flume.

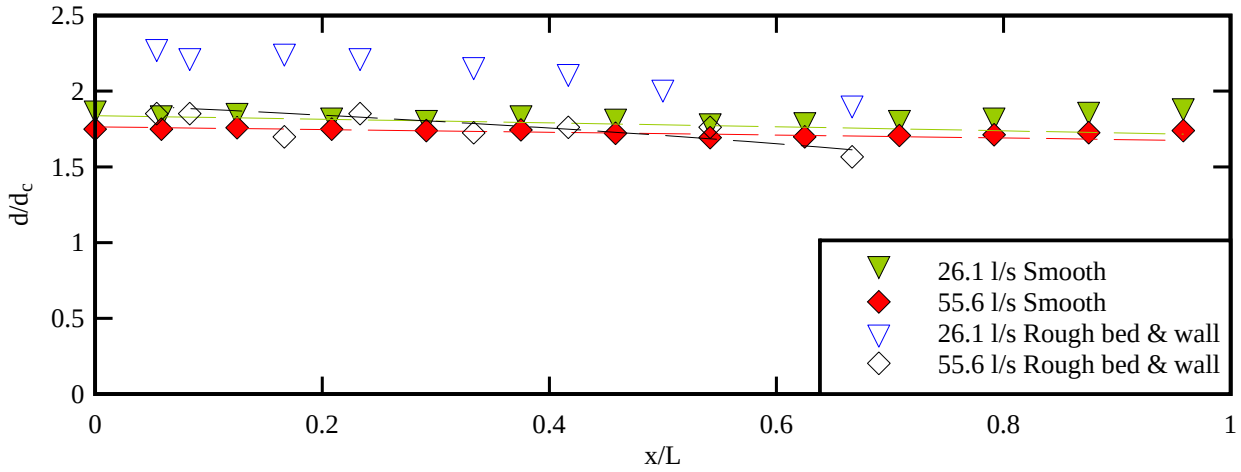


(B) 12 m long flume: comparison between Configuration 1 (smooth PVC bed and glass sidewalls) and Configuration 3 (rough bed and rough left sidewall)

Fig. 3-1 - Dimensionless longitudinal free-surface profiles - Comparison between experimental observations and backwater calculations (dashed lines)

Detailed velocity measurements were conducted on the channel centreline with smooth and rough bed configurations (Config. 1 & 2). Experimental flow conditions are summarised in Table 3-1 and compared with relevant laboratory studies. In the 3.2 m long flume, the flow was partially-developed for the whole length of the channel for all flow conditions (Table 3-1). That is, the vertical velocity distributions exhibited a sharp velocity gradient in a relatively thin region next to the bed, called boundary layer, and the velocity profile was uniform above the boundary layer.

In the 12 m long flume, the results indicated that the upstream part of the channel flow was characterised by a developing boundary layer with an ideal fluid flow region above. Further downstream the outer edge of the boundary layer interacted with the free-surface and the downstream flow became fully-developed. The longitudinal flow pattern is sketched in Figure 3-2A. Typical vertical distributions of time-averaged longitudinal velocity $V_x$ and standard deviations of velocity components $v_x'$, $v_y'$ and $v_z'$ are shown in Figures 3-2B and 3-2C for smooth and rough bed configurations respectively. In the 12 m long flume, the flow became fully-developed for x > 6.5-8 m on the smooth bed configuration (Config. 1) and for x > 4-5 m on the rough bed configuration (Config. 2).

Table 3-1 - Experimental flow conditions for velocity measurements in open channels

| Facility | Boundary conditions | $S_o$ | B m | Q $m^3/s$ | d m | B/d |
|---|---|---|---|---|---|---|
| Present Study 12 m long flume | PVC bed & glass sidewalls | 0 | 0.50 | 0.261 | 0.121-0.124 | 4.03-4.13 |
| | | | | 0.556 | 0.185-0.193 | 2.54-2.7 |
| | Rough bed & glass sidewalls | 0 | 0.50 | 0.261 | 0.112-0.129 | 3.9-4.48 |
| | | | | 0.556 | 0.192-0.206 | 2.43-2.6 |
| | Rough bed & rough sidewall | 0 | 0.478 | 0.261 | 0.129-0.154 | 3.15-3.7 |
| | | | | 0.556 | 0.174-0.222 | 2.6-2.87 |
| Present Study 3.2 m long flume | PVC bed & glass sidewalls | 0 | 0.25 | 0.010 | 0.115-0.120 | 2.08-2.17 |
| | | | | 0.020 | 0.165-0.170 | 1.47-1.51 |
| NEZU & RODI (1985) | Smooth invert | -- | 0.60 | 0.018 | 0.060 | 10 |
| | | | | 0.0052 | 0.060 | 10 |
| | | | | 0.029 | 0.100 | 6 |
| | | | 0.20 | 0.011 | 0.101 | 2 |
| | | | 0.175 | 0.025 | 0.103 | 1.69 |
| | | | 0.2 | 0.020 | 0.195 | 1.0 |
| APELT & XIE (2011) 13.5 m long flume | Smooth plywood | 0.0003 | 0.40 | 0.015 | 0.125 | 3.2 |

Notes: B: channel width; d: water depth measured above invert; Q: water discharge; $S_o$: bed slope; (--): information not available.

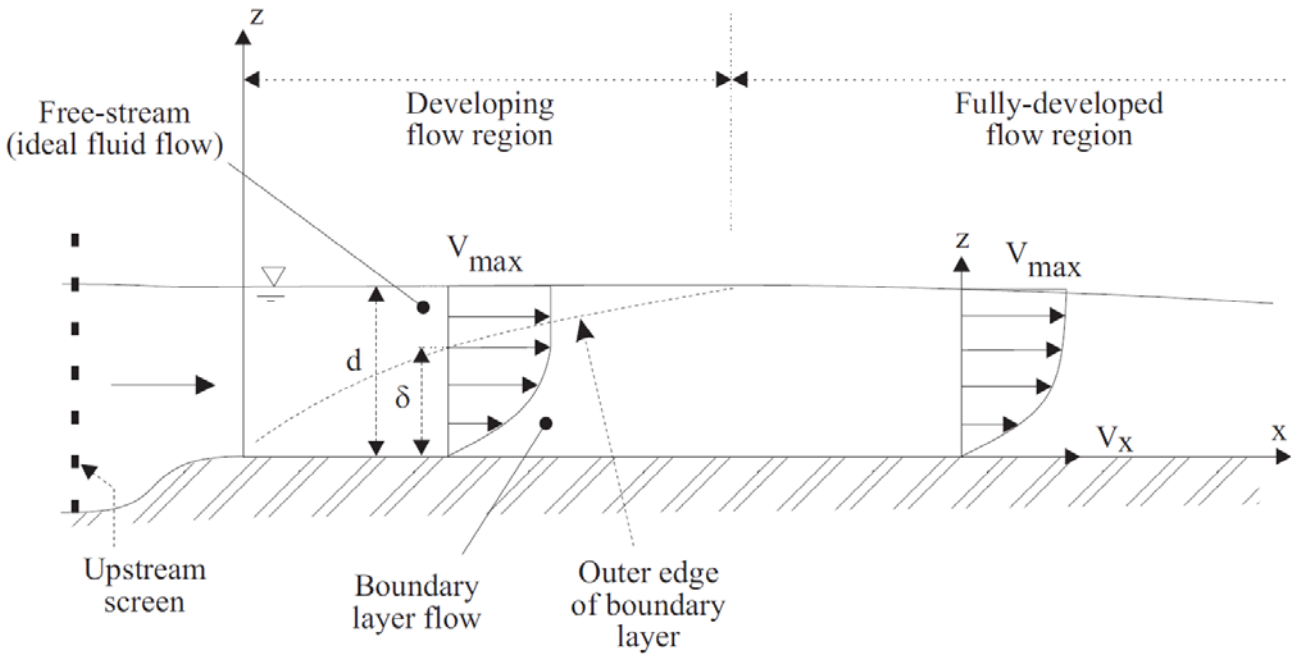


(A) Definition sketch

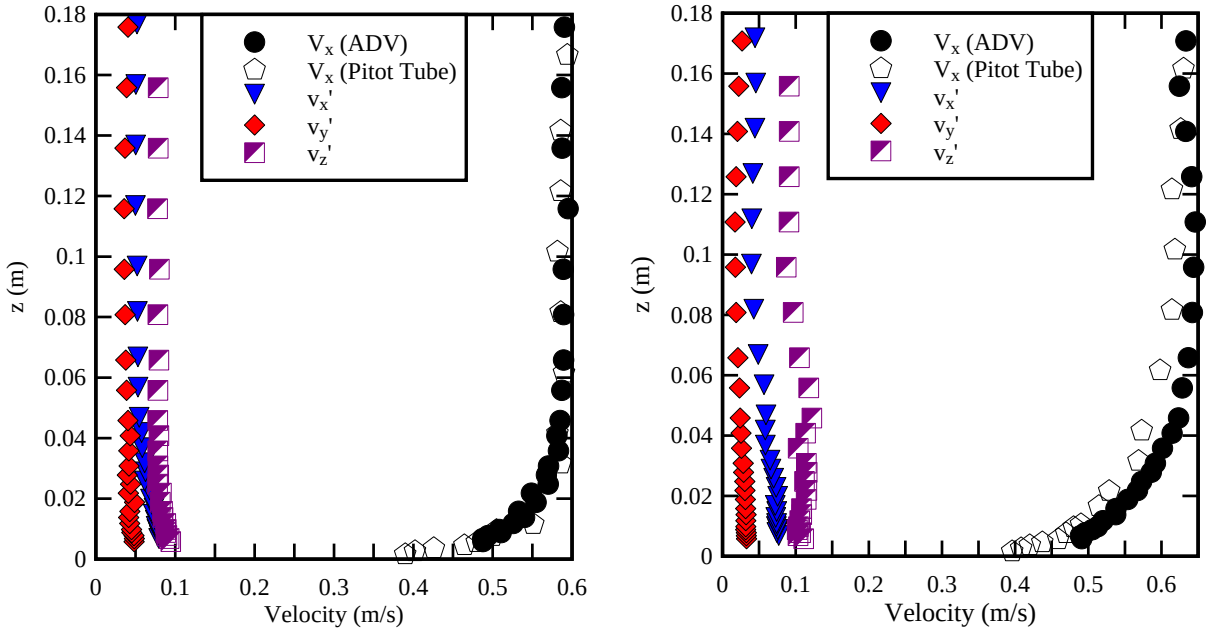


(B) Vertical distributions of time-averaged velocity $V_x$ and standard deviations of velocity components $v_x'$, $v_y'$ and $v_z'$ in the 12 m long flume for Q = 0.0556 m3/s, smooth PVC bed (Config. 1) - Left: partially-developed flow at x = 2.8 m, Right: fully-developed flow at x = 8 m

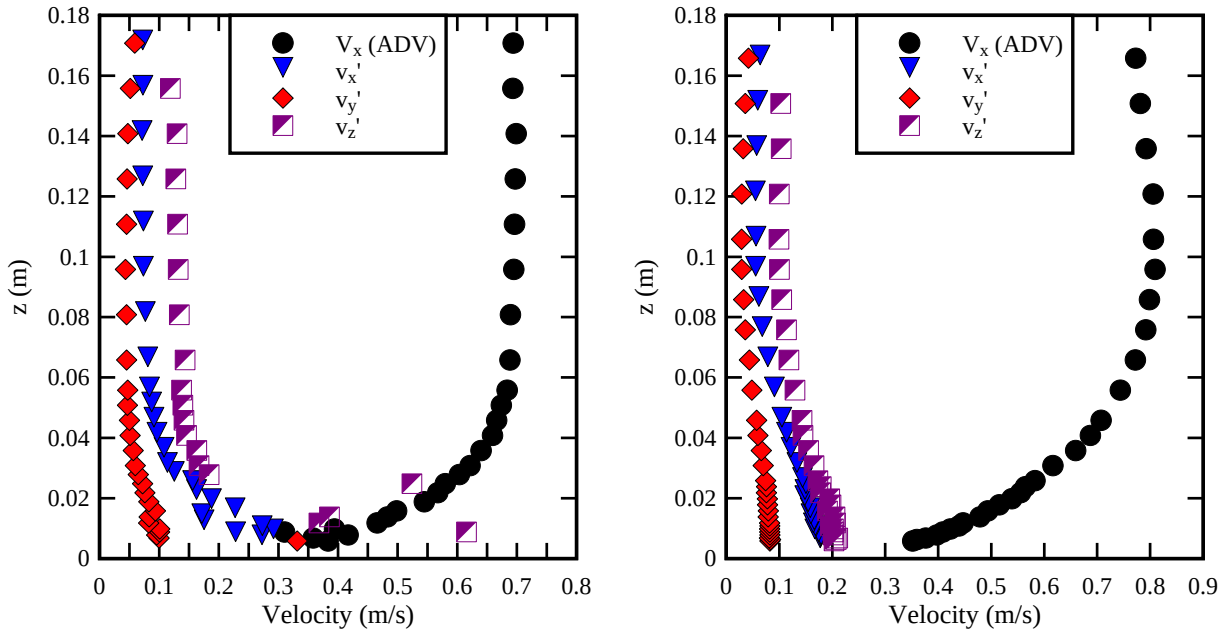


(C) Vertical distributions of time-averaged velocity $V_x$ and standard deviations of velocity components $v_x'$, $v_y'$ and $v_z'$ in the 12 m long flume for Q = 0.0556 $m^3$/s, rough PVC bed (Config. 2) - Left: partially-developed flow at x = 2.8 m, Right: fully-developed flow at x = 6.5 m

Fig. 3-2 - Centreline velocity profiles on smooth and rough bed configurations (Config. 1 and 2)

In the developing flow region, the boundary shear stress was derived from the momentum integral equation applied to the developing boundary layer flow (SCHLICHTING 1979, CHANSON 2009).

Typical results are presented in Figure 3-3 for the 12 m long flume, where $\tau_o$ is the boundary shear stress, $\rho$ is the water density, $V_{max}$ is the free-stream velocity (i.e. ideal fluid flow velocity) and L is the channel length (L = 12 m). In Figure 3-3, the smooth bed configuration data are compared with the analytical solution for a turbulent developing boundary layer above a smooth plate in absence of pressure gradient (dashed black line). The data showed a relatively close agreement between the smooth bed data and theoretical solution, as well as a marked increase in dimensionless boundary shear stress for the rough bed configuration. The results were little affected by the flow rate within the range of investigated flow conditions (Table 3-1).

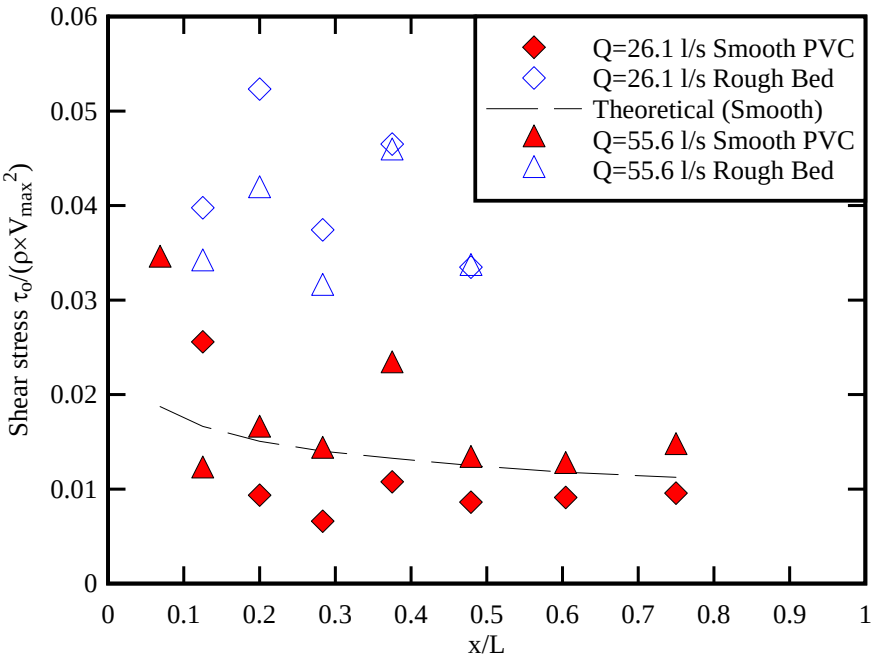


Fig. 3-3 - Dimensionless longitudinal distribution of boundary shear stress in the developing flow region in the 12 m long flume - Comparison between smooth and rough bed configuration data (Config. 1 and 2) and analytical solution for a turbulent developing boundary layer above a smooth plate in absence of pressure gradient

## 3.2 ROUGH BED AND SIDEWALL CONFIGURATION OBSERVATIONS

For the Configuration 3, the boundary roughness was asymmetrical, with a rough invert, a rough left wall and a smooth right wall. Owing to the presence of the free-surface and of differences in boundary friction along the wetted perimeter, the velocities in the channel were not uniformly distributed and the velocity field was not symmetrical about the channel centreline. This was clearly evidenced with dye injection showing a slower flow motion next to the rough invert and next to the rough left sidewall, with some complicated flow pattern next to the left corner. Visual observations suggested the development of a sidewall boundary layer at the upstream end of the channel, which

interacted with the bottom boundary layer. The resulting flow motion led to a complicated secondary flow pattern. Next to a rough boundary, the flow was retarded, and some complicated flow patterns developed: e.g., next to the corners. In turn, some flow motion was generated at right angle to the longitudinal current: i.e., secondary currents. Secondary flow velocities are typically very small (e.g. 1 to 2% of mean flow velocity), but the secondary currents transport some momentum from the channel centre towards the corners and sidewalls (SCHLICHTING 1979, LIGGETT 1994). It is well-known that secondary currents play a major role in open channel flows including both natural rivers and man-made waterways (KNIGHT et al. 1984, MACINTOSH 1990, NEZU and NAKAGAWA 1993, APELT and XIE 1995,2011, XIE 1998) ([2]). Laboratory and field observations showed the existence of large streamwise vortices with lateral length scale of between 1.5 and 3 times the water depth (NEZU and RODI 1985, TAMBURRINO and GULLIVER 2007, TREVETHAN et al. 2008).

The time-averaged longitudinal velocity contours are illustrated in Figure 3-4. In Figure 3-4, the left graphs correspond to Q = 0.0261 $m^3/s$ while the right graphs were obtained for Q = 0.0556 $m^3/s$. On each graph, the left axis corresponds to the smooth right wall and the right axis to the rough left wall. At the upstream end of the channel, the effects of boundary friction were confined to a narrow region close to the bed and sidewalls (e.g. Fig.. 3-4A and 3-4B). With increasing downstream distance, the flow region affected by boundary friction extended to the entire cross-section area. The velocity data showed a complicated velocity pattern in the left bottom corner with the rough bed and rough left sidewall.

A phenomenon of velocity dip is seen in Figure 3-4, in which the maximum velocity $V_{max}$ at each transverse location was observed at a vertical elevation $Z_{Vmax}/d < 1$, where d is the depth of flow. The dip in velocity profile was believed to be caused by the presence of secondary currents (NEZU and RODI 1985, APELT and XIE 2011). Low momentum fluid was transported from near the side walls to the centre and high momentum fluid was moved from the free surface toward the bed (GIBSON 1909, NEZU and RODI 1985, XIE 1998).

In Configuration 3, the maximum velocity and its location were found to be functions of the transverse locations (Fig. 3-5). Figure 3-5 regroups experimental observations in fully-developed flows for Configurations 1, 2 and 3, where B is the channel width and $V_{mean}$ is cross-sectional averaged velocity: $V_{mean} = Q/(B \times d)$. On average, the cross sectional maximum velocity was observed at about $Z_{Vmax}/d \approx 0.62$ and $Y_{Vmax}/B = 1/3$, where $V_{max}/V_{mean} \approx 1.6$. That is, the cross-sectional maximum was observed below the free-surface towards the right smooth sidewall. The relative elevation of cross-sectional maximum velocity was close to the observations of XIE (1998)

[2] For a historical account, see MONTES (1998).

in a smooth channel: $Z_{Vmax}/d \approx 0.66$ (also APELT and XIE 2011).

On the channel centreline (y/B = 0.5), the ratio of maximum velocity to free-surface velocity equalled 1.03 on average (Configuration 3), close to $V_{max}/V_{fs} \approx 1.02$ in Configuration 2 ([3]). For comparison, NEZU and RODI (1985) reported $V_{max}/V_{fs} \approx 1.1$ in a smooth and wide channel (B/d = 10). Close to the sidewalls, the ratio of maximum velocity to free-surface velocity was larger than or equal to 1.1, and the relative elevation of maximum velocity was within $Z_{Vmax}/d \approx 0.3$-$0.5$ (Fig. 3-4B). Full results are summarised in Appendix C.

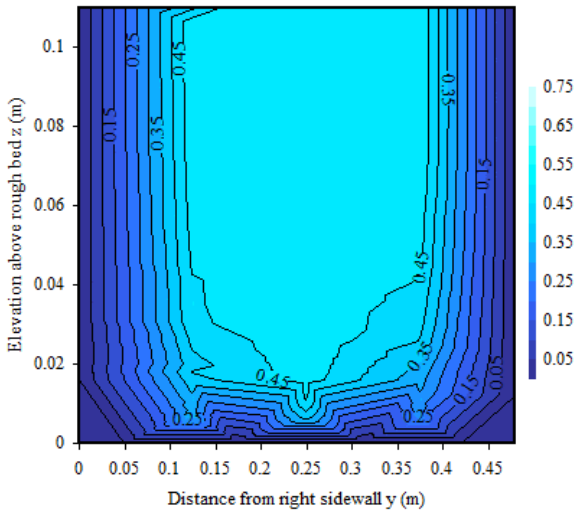


(A) x = 0.65 m - Left: Q = 0.0261 $m^3/s$

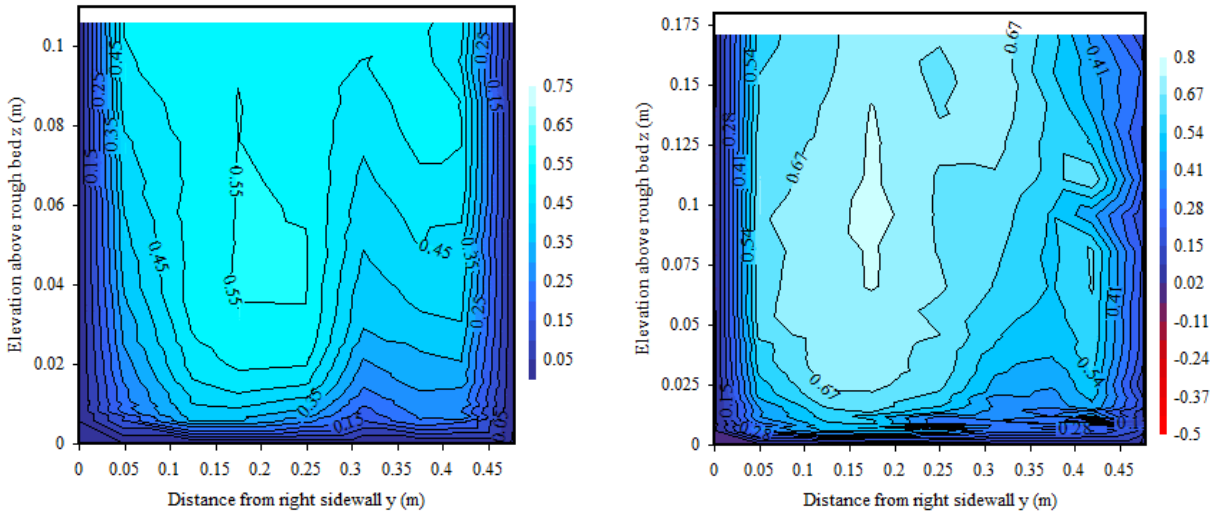


(B) x = 2.0 m - Left: Q = 0.0261 $m^3/s$; Right: Q = 0.0556 $m^3/s$

[3] Observations in the fully-developed flow region (x > 4-4.5 m).

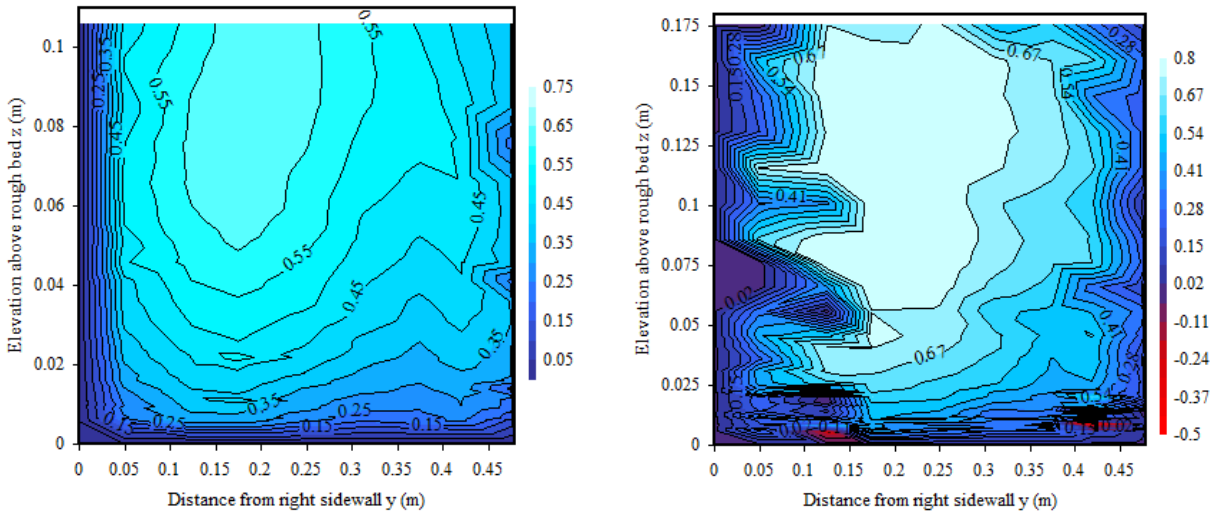


(C) x = 5.0 m - Left: Q = 0.0261 $m^3/s$; Right: Q = 0.0556 $m^3/s$

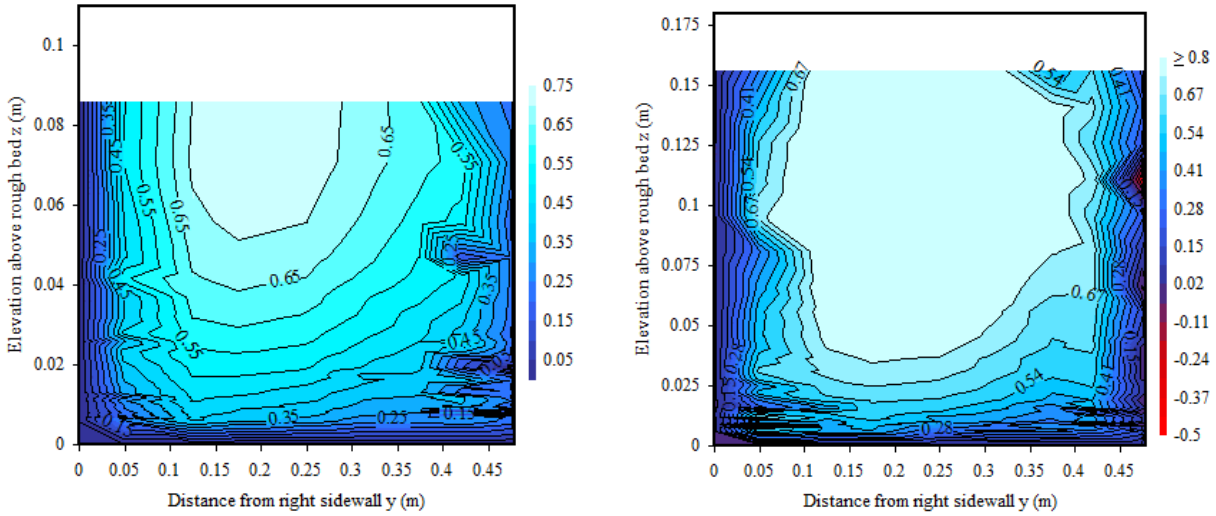


(D) x = 8.0 m - Left: Q = 0.0261 $m^3/s$; Right: Q = 0.0556 $m^3/s$

Fig. 3-4 - Contour curves of constant longitudinal velocity $V_x$ in the 12 m long channel with rough bed and sidewall (Configuration 3) - y = 0 at the right smooth sidewall, velocity scale in m/s - Note the vertical distortion

Visual observations, supported with dye injection, showed some recirculation motion next to the left rough sidewall and at the corner between the rough bed and sidewall. A strong longitudinal vortex stretched near the channel bed and a smaller vortex took place on the left side near the free surface. No similar vortex pattern was seen in the right side of the channel, possibly because the transverse velocity gradient $\partial V_x/\partial y$ was large and dye recirculation was not visible. These vortical structures are called 'bottom vortex' and 'free surface vortex' respectively (APELT and XIE 2011). The free surface vortex was studied by many researchers (GIBSON 1909, NEZU and RODI 1985) while the bottom vortex was first evidenced by NEZU and RODI (1985) (XIE 1998, APELT and

XIE 2011).

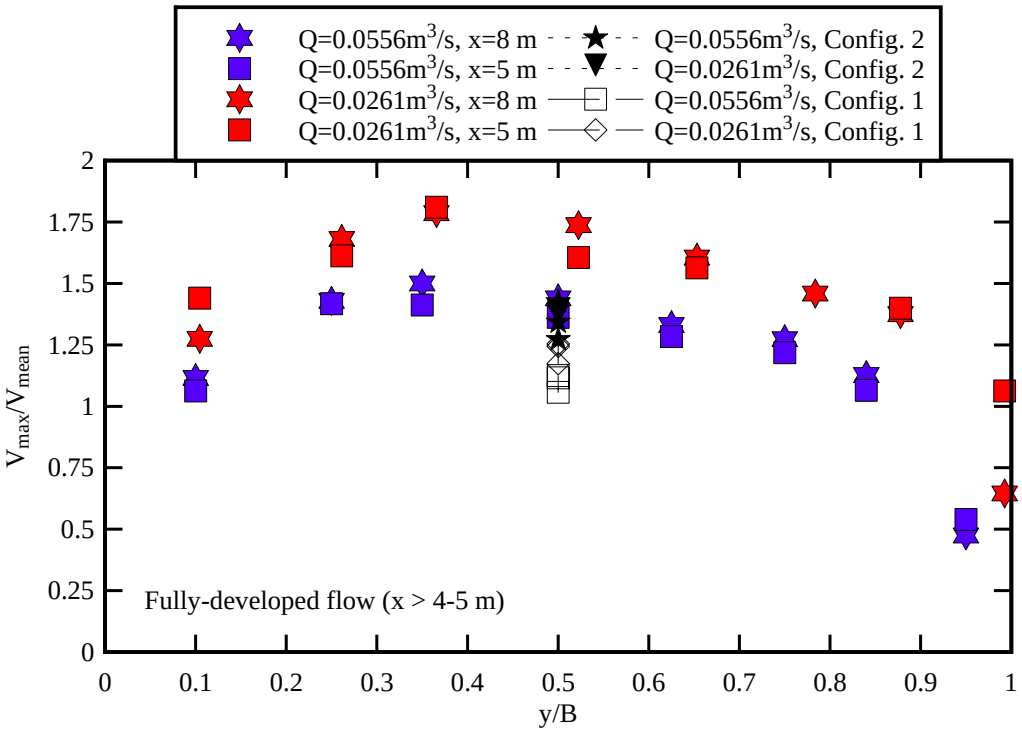


(A) Maximum velocity $V_{max}$

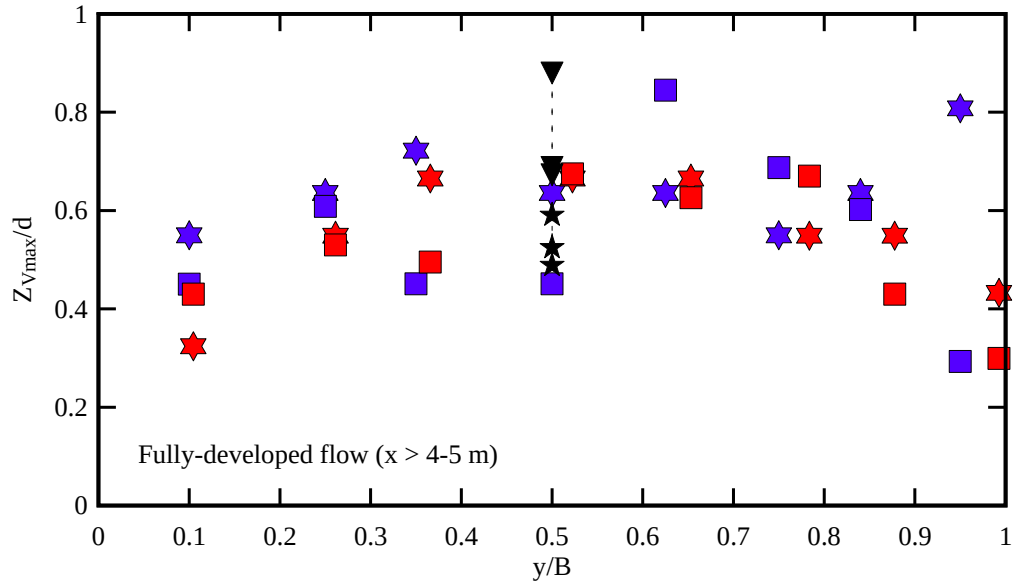


(B) Vertical elevation of maximum velocity $Z_{Vmax}$

Fig. 3-5 - Transverse distribution of maximum velocity and its location as function of the transverse location in the 12 m long channel with rough bed and sidewall (Configuration 3), with the same legend for all graphs - Comparison with centreline data for Configurations 1 and 2 - Note y = 0 at the right smooth sidewall

Contours of distributions of longitudinal velocity fluctuations $v_x'$ are shown in Figure 3-6. The graphs show the distributions of $v_x'$ at three different longitudinal locations for the same discharge. Maximum velocity fluctuations were recorded close to the rough bed and rough sidewall. Along most vertical lines away from side walls, the longitudinal velocity fluctuations $v_x'$ presented a local minimum below the free surface, at about the same elevation where the longitudinal velocity $V_x$ was maximum. From this local minimum, $v_x'$ increased slightly towards the free surface and increased substantially with depth to its maximum close the invert ([4]). The trend was also seen with the smooth bed and rough bed data, and previously reported by APELT and XIE (2011).

The cross sectional minimum values of longitudinal velocity fluctuations were about the centre line with $(v_x')_{min}/V_{mean} \sim 0.10\text{-}0.12$. Such minimum values were close to the smooth bed and rough bed data. The cross-sectional maximum value of $(v_x')_{max}/V_{mean}$ was observed close to the bottom left rough wall, with values about 1.6-2.0. Physically the magnitude of $v_x'$ increased in regions where the velocity gradients $\partial V_x/\partial y$ and $\partial V_x/\partial z$ increased. The change in boundary roughness along the wetted perimeter affected these gradients and resulted in a re-distribution of turbulent kinetic energy. The boundary roughness change had a most significant effect on the turbulence intensity. The magnitude of velocity fluctuations was large near the rough side wall across most of the water column, but it became much smaller near the channel centreline.

Contours of distributions of transverse and vertical velocity fluctuations, $v_y'$ and $v_z'$ respectively, are presented in Figure 3-7. The graphs show data in the fully-developed flow region (x = 8 m) for the same flow conditions as in Figure 3-6C. Compared to the distributions of longitudinal velocity fluctuations, the data were similar except for the following differences The vertical velocity fluctuation $v_z'$ was reduced next to the free surface while $v_x'$ was enhanced due to the water surface, as observed by XIE (1998). Another difference was the magnitudes of $v_z'$, consistently larger than those of $v_x'$. The reason remains unclear but it might have been linked to the instrumentation. While it is hard to find precise data of the transverse velocity fluctuations $v_y'$ in the literature, the present $v_y'$ data in most parts away from solid boundaries of each cross section were small, consistently smaller than $v_x'$.

A comparison between the distributions of $v_x'$ and $v_y'$ suggested similar distribution patterns. Along most vertical lines away from sidewalls, the transverse velocity fluctuation $v_y'$ had a local minimum below the free surface. This local minimum was located in the region where the time-averaged longitudinal velocity $V_x$ was maximum. From this local minimum, $v_y'$ increases towards the free surface and increased with depth to its maximum next to the channel bed. The minima of $v_y'$ at all

[4] Theoretically, $v_x'$, $v_y'$ and $v_z'$ should be zero at z =0, but the lowest ADV sampling elevation was z = 0.0058 m.

locations in the fully-developed flow region were about $(v_y')_{min}/V_{mean}$ ~ 0.05-0.07 on average. Near the sidewalls, $v_y'$ exhibited high values over most parts of the water column.

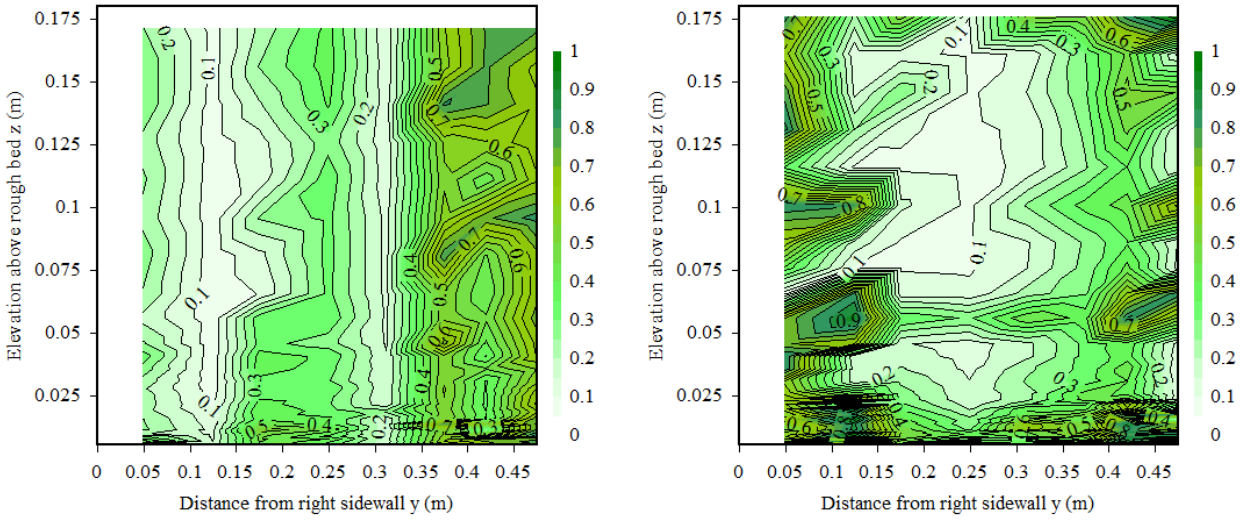


(A) x = 2 m (B) x = 5 m

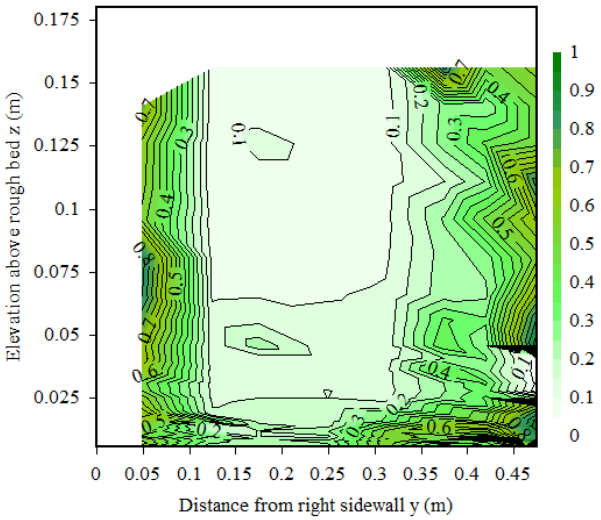


(C) x = 8 m

Fig. 3-6 - Contour curves of constant longitudinal velocity fluctuations $v_x'$ in the 12 m long channel with rough bed and sidewall (Configuration 3) - Q = 0.0556 $m^3/s$, y = 0 at the right smooth sidewall, velocity scale in m/s - Note the vertical distortion

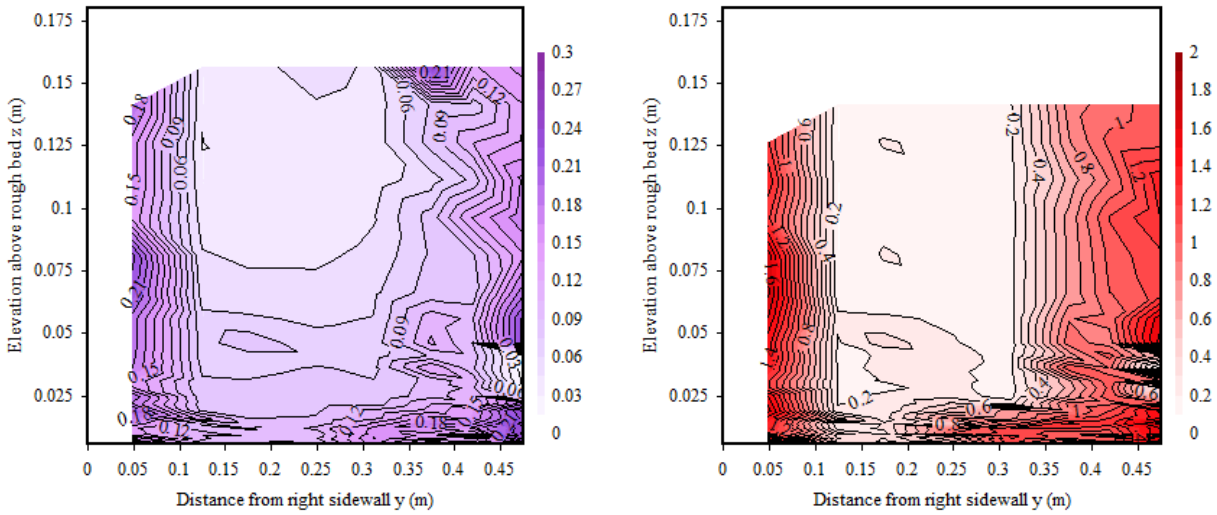


(A) Transverse velocity fluctuation $v_y'$ (B) Vertical velocity fluctuation $v_z'$

Fig. 3-7 - Contour curves of constant transverse and vertical velocity fluctuations $v_x'$ at x = 8 m in the 12 m long channel with rough bed and sidewall (Configuration 3) - Q = 0.0556 $m^3/s$, x = 8 m, y = 0 at the right smooth sidewall, velocity scale in m/s - Note the vertical distortion

# 4. SUMMARY

A physical study was undertaken to characterise the turbulence properties in open channels, aiming to find suitable flow conditions to maximise slow and recirculation regions, which might facilitate the passage of fish with small body mass ([1]), in particular upstream migration. Three test channels were investigated in the new Seddon bio-hydrodynamics laboratory at the University of Queensland, characterised by a fish-friendly water reticulation system. A key feature was the presence of upstream and downstream screens to contain fish movements in designated test areas without harm, resulting in inflow conditions with large turbulence levels. A total of three boundary roughness configurations were tested, consisting of the smooth boundary Configuration 1, the rough bed Configuration 2 and the rough bed and sidewall Configuration 3. The latter consisted of a very rough bed plus a very rough sidewall and a smooth sidewall.

Both free-surface and velocity measurements implied a fully-rough turbulent flow motion. In boundary roughness Configurations 1 and 2, the data showed that the upstream channel flow consisted of a developing boundary layer with an ideal fluid flow region above. When the outer edge of the boundary layer interacted with the free-surface, the flow became fully-developed and remained fully-developed further downstream. With the smooth bed Configuration 1, the velocity data were close to those for a developing boundary layer on a smooth plate, albeit higher turbulence levels in the free-stream: i.e., free-stream turbulence intensity Tu ranging from 16% to 20%. The experimental measurements showed a marked increase in dimensionless boundary shear stress for the rough bed Configuration 2, in both the developing and fully-developed flow regions.

With the rough bed and sidewall Configuration 3, the analysis of the results showed an asymmetrical velocity field, the existence of the velocity dip and the presence of secondary currents in the three-dimensional turbulent flows. Visual observations and dye injection indicated a recirculation motion next to the left rough sidewall and at the corner between the rough bed and sidewall. The maximum velocity and its location were found to be functions of the transverse locations. The cross-sectional maximum was observed below the free-surface towards the right smooth sidewall. The relative elevation of cross-sectional maximum velocity was close to past observations in smooth channels. Maximum velocity fluctuations were recorded close to the rough bed and rough sidewall. Along most vertical lines away from side walls, the longitudinal and transverse velocity fluctuations, $v_x'$ and $v_y'$ respectively, presented a local minimum below the free surface. This minimum was observed at the same elevation where the longitudinal velocity $V_x$ was maximum. The trend was also seen with the smooth bed and rough bed configuration data. The

[1] That is, small-bodied and juvenile fish less than 100 mm total length.

minima of $v_x'$ and $v_y'$ at all locations in the fully-developed flow region were about $(v_x')_{min}/V_{mean}$ ~ 0.10-0.12. and $(v_y')_{min}/V_{mean}$ ~ 0.05-0.07 on average. The vertical velocity fluctuation $v_z'$ was reduced next to the free surface while the vertical velocity fluctuation $v_x'$ was enhanced locally due to the water surface, as observed by XIE (1998).

Overall and based upon the physical modelling, the boundary roughness Configuration 3 appeared to provide excellent recirculation regions next to the rough sidewall and at the corner between the rough sidewall and channel bed, which might be suitable to the upstream passage of small body mass fish, typical of Australian streams. Preliminary experiments in a water tunnel showed that fish swimming performance data depended critically upon a careful testing protocol, as well as upon a sound velocity measurement technique. It must be acknowledged that the present findings are preliminary. Further testing must be conducted to develop quantitative design guidelines, with tests encompassing real fish to be complemented by field monitoring of prototype structures.

## 5. ACKNOWLEDGEMENTS

The authors thank Prof. Artur RADECKI-PAWLIK (Agricultural University of Cracow, Poland) for his review of the report and most valuable comments. They acknowledge the helpful inputs of Dr Pippa KERN (The University of Queensland, Australia). The authors acknowledge the technical assistance of Jason VAN DER GEVEL, Stewart MATTHEWS and Jabin WATSON (The University of Queensland). Hubert CHANSON acknowledges helpful discussions with UQ Biological Sciences and NSW Department of Fisheries colleagues, in particular Prof. Craig FRANKLIN and Dr Rebecca CRAMP. The financial support through the Australian Research Council (Grant LP140100225) is acknowledged.

# APPENDIX A - DISCHARGE CALIBRATION OF THE SEDDON BIO-HYDRODYNAMICS FLUMES

The Seddon bio-hydraulics laboratory includes five flumes for experimentation: two 12 m by 0.5 m (upper and lower) flumes and three 3.2 m by 0.25 m (#1 blue, #2 green and #3 yellow) flumes. All the flumes were made of a smooth PVC bed and glass side walls, and were supplied by a constant head tank. The 12 m long flumes and two 3.2 m long flumes (#2 green & #3 yellow) had an orifice meter installed on the supply line to measure the water discharge, whereas the other 3.2 m long flume (#1 blue) had a Venturi meter. Within this report, the focus of the experiments was the 12 m long (lower) flume and 3.2 m long (#1 blue) channel.

The water discharge was calibrated on site using different methods: a sharp crest weir, a free overfall, Pitot tube and acoustic Doppler velocimeter. The sharp crest weir method was used for low flow rates to maintain the air pocket on the downstream side of the weir and the free overfall method was used for higher flow rates, where the air pocket was not present. The Pitot tube and ADV were used to measure longitudinal velocities, and the vertical distributions of velocity were integrated.

The results are summarised in Table A-1 and two calibration data sets are reported in Figures A-1 and A-2. Present results were compared with previous calibrations of the same devices. Note that, herein, the free fall method was less reliable than the sharp crest weir method, because of the interference of support structures built on the channel sidewalls to the downstream screen.

Table A-1 - Summary of flume calibration curves

| Flume | Calibration curve<br>Q in [L/s], ΔH in [mm] | $R^2$ | Comments |
|---|---|---|---|
| 12 m long (Lower) | $Q=1.1892 \times \Delta H^{0..5107}$ | N/A | Orifice meter. Vertical (90°) air-water manometer. |
| 12 m long (Upper) | Including free overfall data: $Q=1.2422 \times \Delta H^{0.4920}$ | 0.9993 | Orifice meter.Vertical (90°) air-water manometer. |
| | Excluding free overfall data: $Q=1.1787 \times \Delta H^{0.4997}$ | 0.9990 | |
| 3.2 m long #1 [Blue] | $Q=0.8077 \times \Delta H^{0.5144}$ | 0.9997 | Venturi meter. 30° inclined air-water manometer. Free fall method could not be used as the flow converged for values of ΔH larger than that used in the sharp-crest weir method |
| 3.2 m long #2 [Green] | $Q=0.3495 \times \Delta H^{0.5404}$ | 0.9989 | Orifice meter. 30° inclined air-water manometer. Free fall data not used as it didn't follow the trend of the sharp-crest weir data |
| 3.2 m long #3 [Yellow] | $Q=0.3809 \times \Delta H^{0.5182}$ | 0.9999 | Orifice meter. 30° inclined air-water manometer. Free fall data was not used as it didn't follow the trend of the sharp-crest weir data |

Notes: Q: water discharge; ΔH: reading on manometer, as set per column 4.

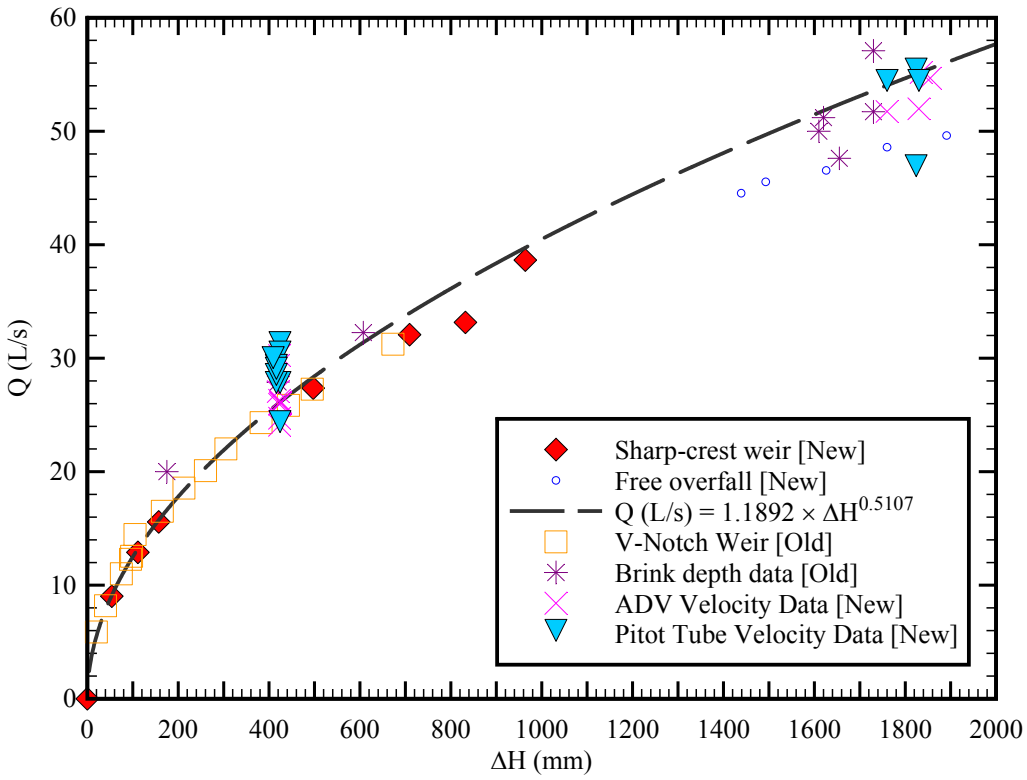


Fig. A-1 - Flow meter calibration of the 12 m long (lower) flume

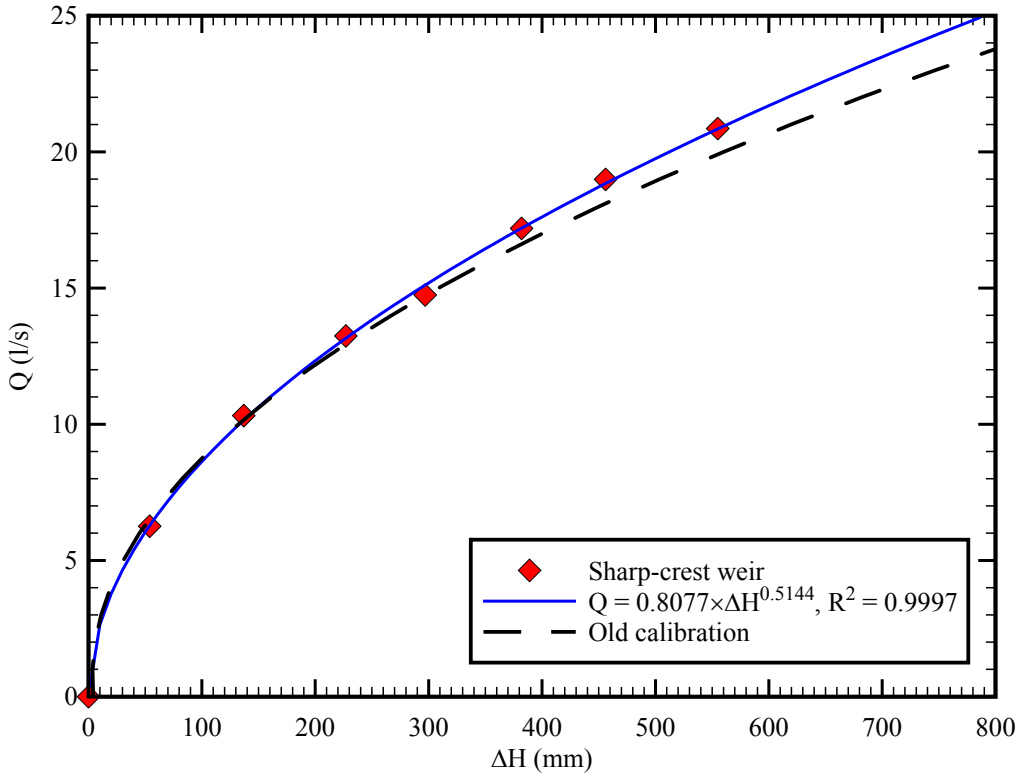


Fig. A-2 - Flow meter calibration of the 3.2 m long (#1 blue) flume

# APPENDIX B - VELOCITY MEASUREMENTS: COMPARISON BETWEEN DIFFERENT TECHNIQUES

Water velocities were measured by different techniques and instruments. These included cross-sectional-averaged velocity $V_{mean}$ and local time-averaged longitudinal velocity $V_x$. A series of tests were conducted to compare the different techniques, and the key results are presented below.

INSTRUMENTATION AND EXPERIMENTAL CONDITIONS

The cross-sectional-averaged velocity was deduced from the equation of conservation of mass for an incompressible flow:

$$V_{mean} = \frac{Q}{A} \qquad \text{(B-1)}$$

where Q is the water discharge measured with a flow meter (Appendix A) and A is the flow cross-section area. For an open channel flow in a rectangular channel: A = B×d, with B the channel width and d the flow depth measured with a pointer gauge.

In the 12 m long and 3.2 m long flumes, the local time-averaged velocities were recorded using either a Prandtl-Pitot tube or an acoustic Doppler velocimeter (ADV). The Pitot tube was a Dwyer® 166 Series Prandtl-Pitot tube with a 3.18 mm diameter tube made of corrosion resistant stainless steel, and featured a hemispherical total pressure tapping (Ø = 1.19 mm) at the tip with four equally spaced static pressure tappings (Ø = 0.51 mm) located 25.4 mm behind the tip. The tip design met AMCA and ASHRAE specifications and the tube did not require calibration ([1]). The acoustic Doppler velocimeter was a Nortek™ Vectrino+ (Serial No. VNO 0436) unit equipped with a three-dimensional side-looking head. The velocity range was ±1.0 m/s and the sampling rate was 200 Hz ([2]). The translation of the Pitot-Prandtl and ADV probe in the vertical direction was controlled by a fine adjustment travelling mechanism connected to a Mitutoyo™ digimatic scale unit. The error on the vertical position of the probe was $\Delta z < 0.025$ mm. The accuracy on the longitudinal position was estimated as $\Delta x < \pm 2$ mm. The accuracy on the transverse position of the probe was less than 1 mm.

In the water tunnel and 3.2 m long flume, the local time-averaged velocity was measured with a Hontzsch™ vane wheel FA ZS meter. The meter consisted of a 30 mm diameter body with a 25 mm

[1] Reference: http://www.dwyer-inst.com/Product/TestEquipment/PitotTubes/Series160.

[2] See more details, including on the signal processing, in Section 2.

circular housing and a 22 mm diameter propeller ([3]).

Comparative measurements were conducted between four techniques in the 3.2 m long 0.25 m wide flume, while vertical and transverse velocity profiles were conducted in the water tunnel using the propeller meter. A summary of the testing conditions is presented in Table B-1.

Table B-1 - Summary of testing flow conditions

| Flume | Flow conditions | Instrumentation |
|---|---|---|
| 3.2 m long (#1 Blue) | Q = 0.010 $m^3/s$<br>x = 2.5 m<br>d = 0.1175 m<br>Smooth PVC bed | Flow meter and pointer gauge<br>Pitot tube<br>ADV<br>Hontzsch$^{TM}$ propeller meter |
| | Q = 0.020 $m^3/s$<br>x = 2.5 m<br>d = 0.168 m<br>Smooth PVC bed | Flow meter and pointer gauge<br>Pitot tube<br>ADV<br>Hontzsch$^{TM}$ propeller meter |
| Water tunnel | Smooth walls<br>0.251 m wide 0.259 m high test section | Hontzsch$^{TM}$ propeller meter |
| | Rough bed<br>0.251 m wide 0.233 m high test section | Hontzsch$^{TM}$ propeller meter |
| | Rough bed and left wall<br>0.225 m wide 0.233 m high test section | Hontzsch$^{TM}$ propeller meter |

Notes: d: water depth; Q: water discharge; x: longitudinal location.

COMPARATIVE RESULTS

Different velocity measurement techniques were tested in the 3.2 m long 0.25 m wide flume: namely the flow meter (Eq. (B-1)), Pitot tube, ADV system, and propeller meter. The results are reported in Figure B-1. In Figure B-1, the thick blue line shows the water surface, while the thick black line indicates the cross-sectional-averaged velocity V (Eq. (B-1)).

The flow meter, ADV and Pitot tube data gave very close results. Further the vertical distributions of Pitot tube-and ADV velocity measurements were integrated over the water depth:

$$V_{avg} = \frac{1}{d} \times \int_{z=0}^{d} V_x \times dz \qquad \text{(B-2)}$$

where the no-slip condition was applied to the channel boundaries: e.g., $V_x(z=0) = 0$. With both

[3] When the propeller casing sat on the bed, the propeller axis was 17.3 mm above the invert.

Pitot tube and ADV data, the depth-averaged velocity $V_{avg}$ was within 2% of the cross-sectional-averaged velocity $V_{mean}$ deduced from the flow meter.

The propeller data tended to overestimate the velocity, as well as showing a trend of slightly decreasing velocity with increasing elevation.

Discussion

The propeller casing was a 30 mm diameter solid body, but for the propeller opening. The size of the casing induced some blockage effect, evidenced visually when the propeller was inserted in the flow. The blockage tended to generate a local fluid acceleration around the propeller, and the local velocity may be estimated from continuity:

$$V_{local} = \frac{A_1}{A_1 - \Delta A} \times V_x \qquad \text{(B-2)}$$

where $A_1$ is the upstream cross-section area: $A_1 = B \times d_1$, $\Delta A$ is the propeller casing's submerged projected area ([4]), B is the channel width and $d_1$ is the upstream water depth. Equation (B-2) is shown in Figure B-1 in a thick red line, based upon the ADV data. The trend shows that the blockage effect decreased with increasing propeller elevation, as expected since the propeller casing projected area decreased.

A comparison between propeller data and Equation (B-2) suggested that the propeller readings overestimated the cross-sectional average velocity by 5% to 20% depending upon the propeller elevation, in the 3.2 m long 0.25 m wide smooth channel. The worst overestimates were observed when the propeller was close to the bed.

[4] The submerged projected area of propeller casing is: $\Delta A = 0.030 \times l$, where l is the height of casing submerged in water. When the casing lies on the bed, l = d with d the water depth.

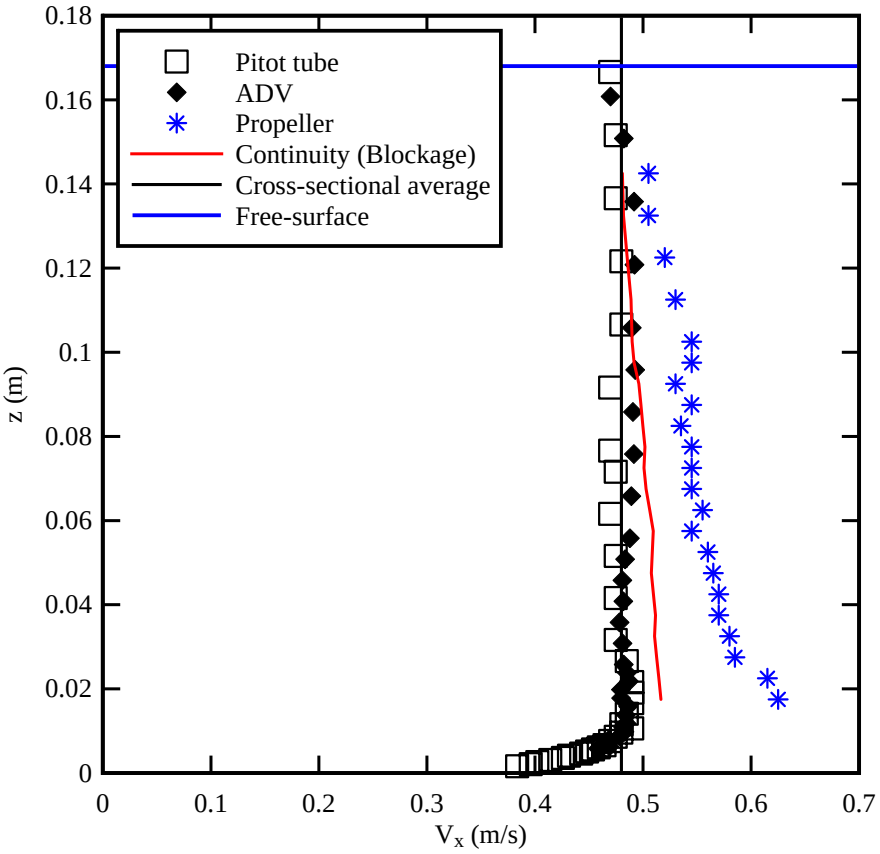


(A) Q = 0.010 $m^3$/s, x = 2.5 m, d = 0.1175 m, smooth PVC bed

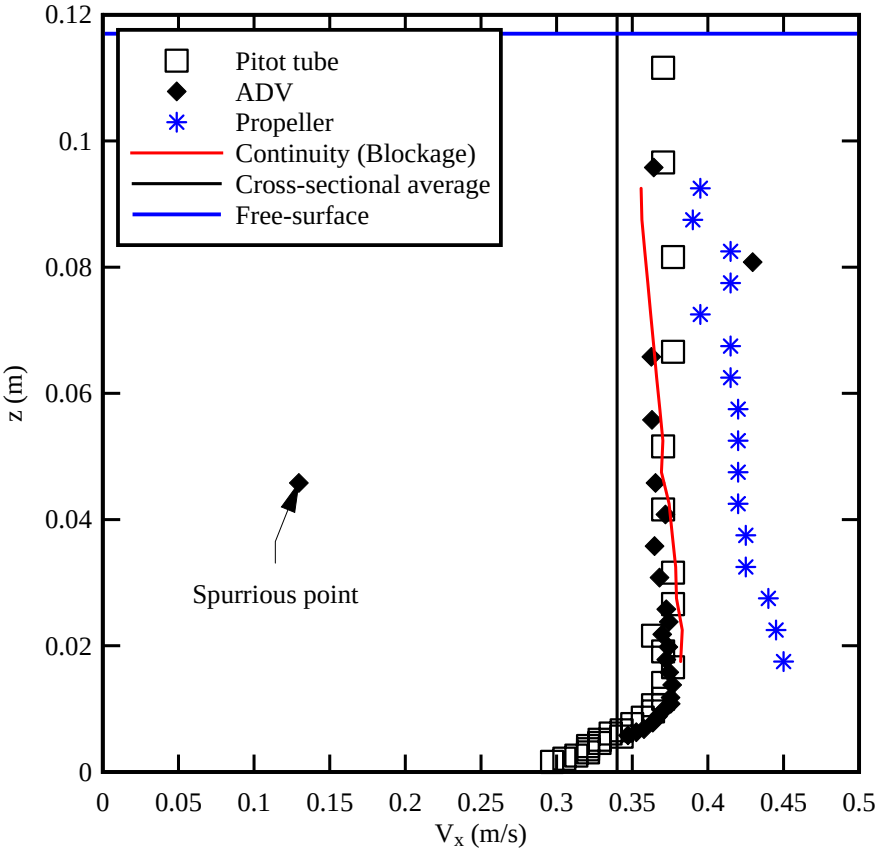


(B) Q = 0.020 $m^3$/s, x = 2.5 m, d = 0.168 m, smooth PVC bed

Fig. B-1 - Comparison between different velocity measurements (Flow meter (Eq. (B-1), Pitot tube,

ADV, propeller meter) in the 3.2 m long flume - Equation (B-1) is reported in thick red line

VELOCITY MEASUREMENTS IN THE WATER TUNNEL

Propeller velocity measurements were conducted in the water tunnel at several locations for several flow conditions with three different boundary conditions. Figure B-2 illustrates the three boundary roughness configurations. In Configurations 1 and 2, measurements were conducted at three vertical elevations along the test section centreline ([5]). In Configuration 3, velocity recordings were performed at three elevations ant at three transverse locations for each elevation. Typical results are shown in Figure B-3. Note that herein all propeller velocity data were corrected for the blockage effect induced by the propeller casing using.

$$V_x = \frac{A_1 - \Delta A}{A_1} \times V_{local} \qquad \text{(B-3)}$$

where $V_{local}$ is the propeller observation.

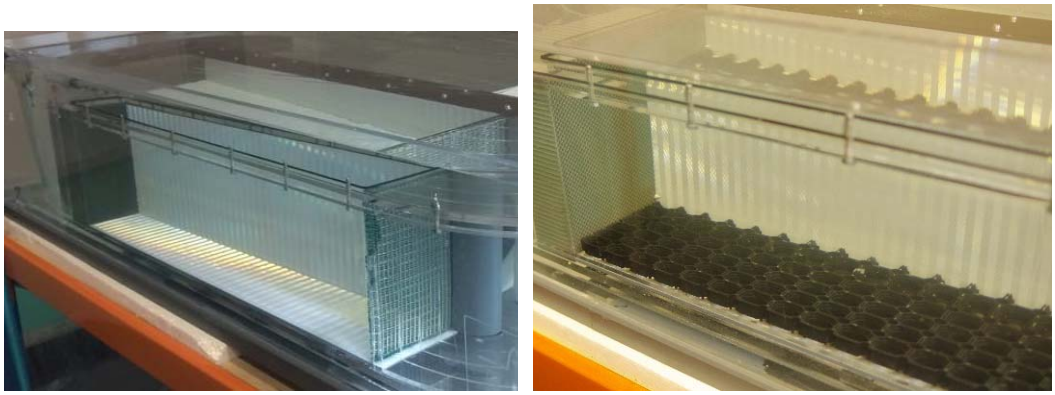

(A, Left) Configuration 1: smooth bed and sidewalls

(B, Right) Configuration 2: rough bed and smooth sidewalls

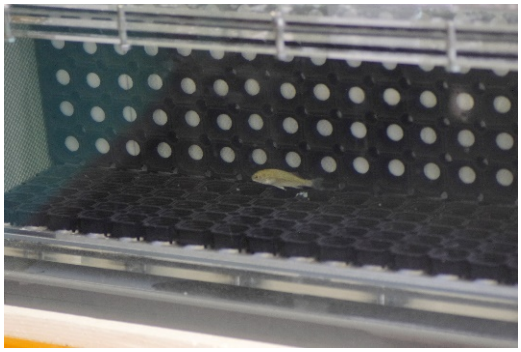

(C) Configuration 3: rough bed, and combination of rough and smooth sidewall

Fig. B-2 - Roughness configurations in the 12 m long flume (Left) and water tunnel (Right)

[5] All measurements were conducted at 0.50 m downstream of the upstream screen.

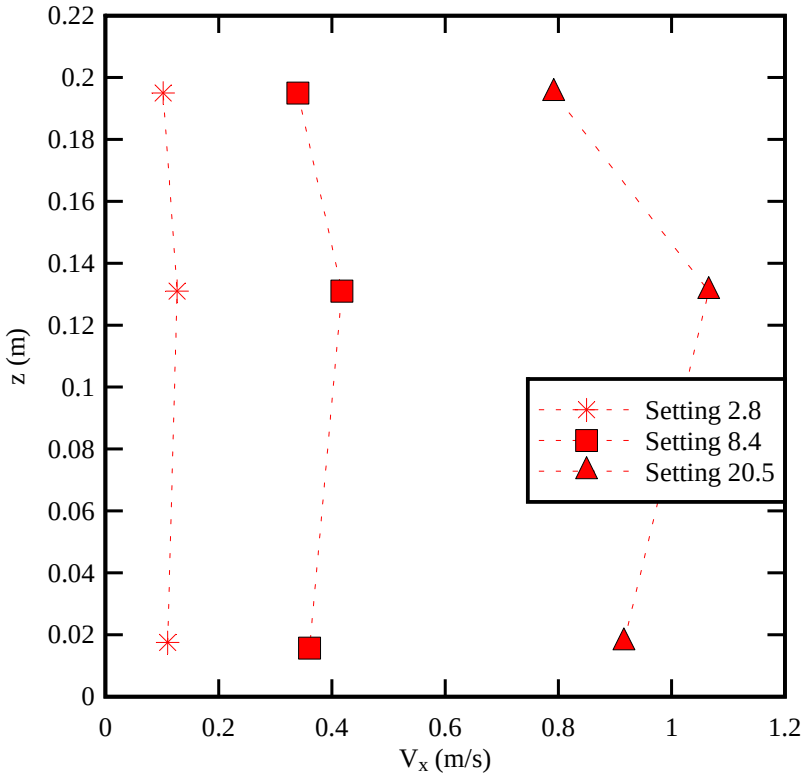


Fig. B-3 - Velocity measurements in the water tunnel with a rough bed (Configuration 2) - All velocity data corrected for blockage effect (Eq. (B-3))

The velocity distributions were integrated over the full height and width of the water tunnel's test section to obtain the cross-sectional-averaged velocity:

$$\overline{V} = B \times \int_0^D V_x \times dz \qquad \text{Two-dimensional flow (B-4a)}$$

$$\overline{V} = \int_0^B \int_0^D V_x \times dz \times dy \qquad \text{Three-dimensional flow (B-4b)}$$

where D is the internal height and B is the internal width of the water tunnel. Equation (B-4) was integrated using the velocity data corrected for the blockage effect induced by the propeller casing ([6]) and assuming the no-slip condition at the solid boundaries: $V_x(z=0) = V_x(z=D) = 0$ and $V_x(y=0) = V_x(y=B) = 0$.

Typical results are reported in Figure B-4, showing the cross-sectional averaged velocity $\overline{V}$ as a function of the motor setting. The data are compared with the propeller observation on the channel centreline when the propeller casing sat on the bed for the same motor setting: that is, $V_{local}$(z=15.7 mm, y=B/2). For completeness, the observations in the 3.2 m long flume are compared to the water

[6] using Equation (B-3).

tunnel data for Configuration 1 (Fig. B-4A). Depending upon the bed roughness configuration, the local propeller observation overestimated the cross-sectional-averaged velocity between 20% and 80%, with a 50% overestimation on average. This simple comparison suggested that a single-point velocity measurement was unlikely to be representative of the cross-sectional-averaged velocity, particularly in a three-dimensional flow like Configuration 3.

Importantly the above results assumed that the propeller was correctly calibrated at the time. This crude assumption was questionable, as seen in Figure B-1.

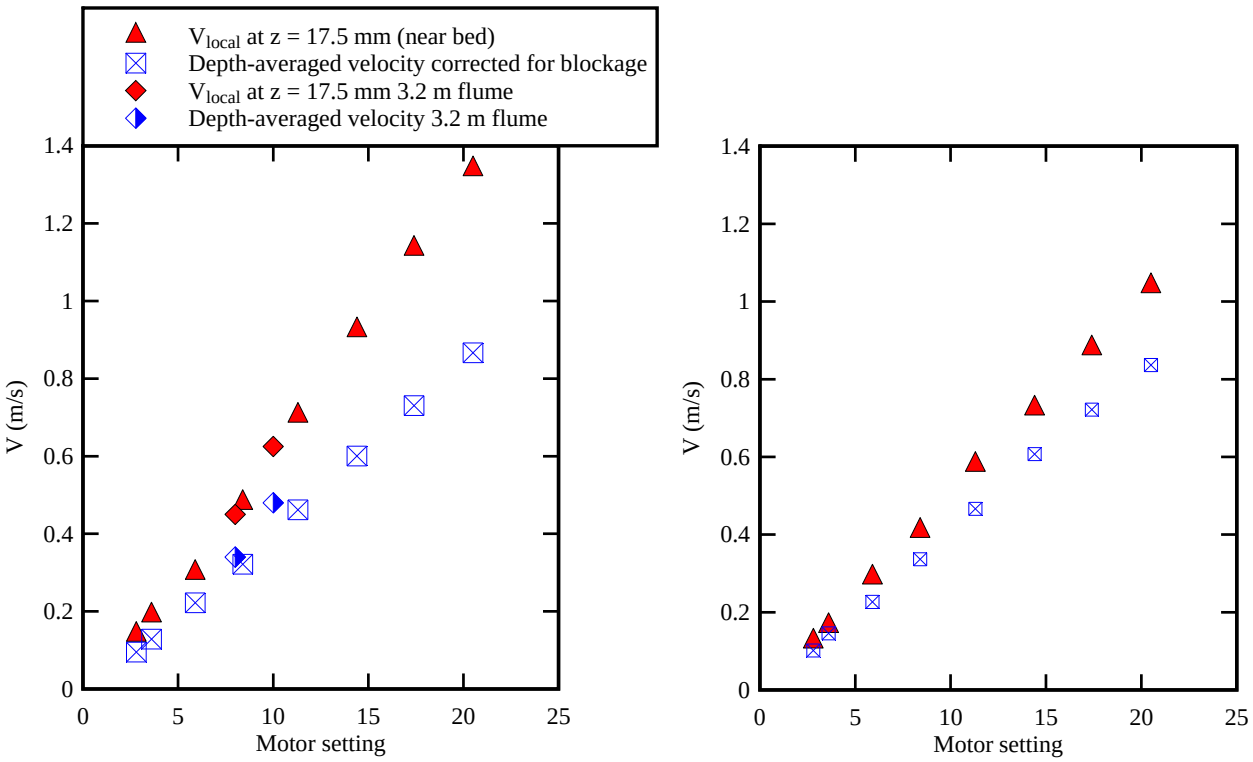


(A, Left) Configuration 1: smooth bed and sidewalls - Comparison with 3.2 m long observations (smooth PVC bed and glass sidewalls), with $\overline{V}$ deduced from water discharge flow meter

(B, Right) Configuration 2: rough bed and smooth sidewalls

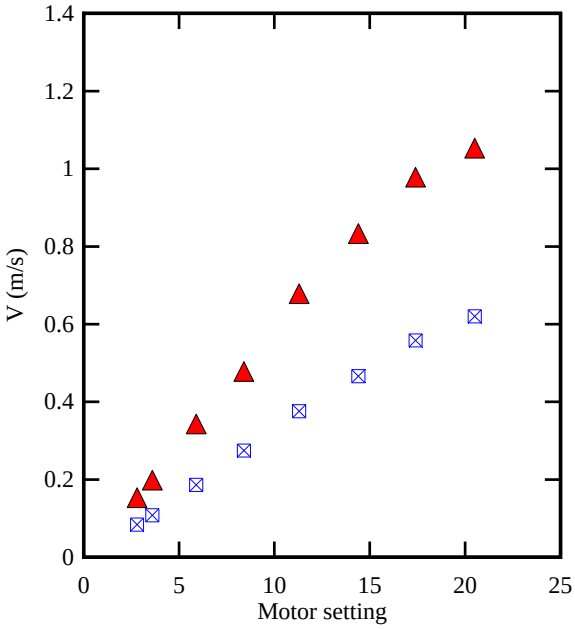


(C) Configuration 3: rough bed, and combination of rough and smooth sidewall

Fig. B-4 - Cross-sectional averaged velocity in the water tunnel as a function of the motor setting - Comparison with the propeller observation on the channel centreline when the propeller casing sat on the bed $V_{local}$(z=15.7 mm, y=B/2)

# APPENDIX C - SUMMARY OF VELOCITY DISTRIBUTION DATA IN THE 12 M LONG CHANNEL

## C.1 PRESENTATION

Detailed velocity measurements were conducted in a 12 m long 0.5 m wide horizontal channel. The flume was made of smooth PVC bed and glass walls. The waters were supplied by a constant head tank feeding a large intake basin (2.1 m long, 1.1 m wide, 1.1 m deep) leading to the test section through a series of flow straighteners, followed by a bottom and sidewall convergent. The channel ended with a free overfall at x = 12 m. Both upstream and downstream of the flume, stainless screens were installed to ensure the safety of small fish. The mesh wire had a 1.6 mm diameter, the mesh pattern was square and the mesh opening was 6.75 mm (inside dimensions).

The water depths were measured using rail mounted pointer gauges. The velocity measurements were conducted with an acoustic Doppler velocimeter (ADV) and the time-averaged velocity data were checked against a Prandtl-Pitot tube.

The post processing of ADV data was conducted with the software WinADV$^{TM}$ version 2.030. The signal post processing included the removal of communication errors, the removal of average signal to noise ratio data less than 5 dB and the removal of average correlation values less than 60%. In addition, the phase-space thresholding technique developed by GORING and NIKORA (2002) and implemented by WAHL (2003) was used to remove spurious points in the data set. Herein, with the side-looking head, the vertical velocity component $V_z$ data were adversely affected by the bed proximity for $z < 0.030$ m. Further all velocity components were affected when the control volume was located less than 50 mm from the sidewalls, with a significant drop in average signal correlations, in average signal-to-noise ratios and in average signal amplitudes.

## C.2 BOUNDARY CONDITIONS

Three types of bed roughness were tested in the 12 m long flume and water tunnel. Some experiments were performed with the smooth PVC invert and smooth sidewalls (Configuration 1). Further experiments were conducted with a rough bed and smooth sidewalls (Configuration 2). The last configuration consisted of a rough bed, a rough sidewall and a smooth sidewall (Configuration 3). For Configurations 2 and 3, the smooth channel bed was covered with a series of industrial rubber floor mats for $0.05 \text{ m} < x < 10.65$ m. The rubber mats consisted of square patterns, cut to the channel width and laid on the PVC. With Configuration 3, a series of rubber mats were glued to one sidewall.

Herein the water depths were measured above the top of the rubber mats. The hydraulic roughness

of the three boundary roughness configurations was tested for a range of steady flow conditions. The gradually-varied flow profiles were recorded in the fully-developed flow region for a range of steady flow rates. The bed shear stress was deduced from the measured free-surface profiles and estimated friction slopes. The estimates of Darcy-Weisbach friction factor f for the smooth boundary Configuration 1 ranged from 0.015 to 0.017, corresponding to mean equivalent sand roughness height $k_s$ = 0.2 mm. The equivalent Darcy friction factor of the rough bed Configuration 2 was f = 0.07 to 0.10 (Config. 2), while the friction factor of the rough boundary Configuration 3 was f = 0.08 to 0.12 (Config. 3). The results corresponded to an equivalent sand roughness height $k_s$ ≈ 20 mm (Config. 2) and 30 mm (Config. 3) on average ([1]). The equivalent rugosity height of Configuration 2 was close to the earlier findings of LENG and CHANSON (2014) with the same bed roughness configuration ([2]).

## C.3 BASIC RESULTS

In the 12 m long flume, the results indicated that the upstream part of the channel was characterised by a developing boundary layer with an ideal fluid flow region above. Further downstream the outer edge of the boundary layer interacted with the free-surface and the downstream flow became fully-developed. The experimental data indicated that the flow became fully-developed for x > 6.5-8 m on the smooth bed configuration (Config. 1) and for x > 4-5 m on the rough bed configuration (Config. 2). With the rough bed and sidewall configuration (Config. 3), both sidewall and bed boundary layer developments were observed together with strong interactions between the two boundary layer processes. The velocity data suggested that an ideal fluid flow core was observed at x = 2 m, and that the flow was fully-three-dimensional for x > 4 m.

Table C-1 summarises some basic result in terms of maximum velocity and its location, free-surface velocity ([3]), maximum standard deviation of velocity component and corresponding location. Figure C-1 presents a number of results.

---

[1] Further experiments with Configuration 3 and 0.015 < Q < 0.053 $m^3/s$ yielded an equivalent Darcy friction factor 0.07 < f < 0.11 corresponding to an equivalent sand roughness height 20 < $k_s$ < 25 mm.

[2] In the same flume with the same bed materials, LENG and CHANSON (2014) reported Darcy friction factors f = 0.09 to 0.18 corresponding to an equivalent sand roughness height $k_s$ = 39 mm. However the inflow conditions differed: no upstream screen was located in the intake basin during their experiments.

[3] Herein the 'free-surface velocity' is the nearest data from the free-surface.

Table C-1 - Basic velocity distribution results

| Rough. config (1) | Description (2) | Q $m^3/s$ (3) | x m (4) | d m (5) | $V_{mean}$ m/s (6) | y/B (7) | $V_{max}/V_{mean}$ (8) | $V_{max}/V_{fs}$ (9) | $(v_x')_{max}/V_{mean}$ (10) | $(v_y')_{max}/V_{mean}$ (11) | $(v_z')_{max}/V_{mean}$ (12) | $Z_{Vmax}$ /d (13) | $Z_{vx'm}$ /d (14) | $Z_{vy'm}$ /d (15) | $Z_{vz'm}$ /d (16) |
|---|---|---|---|---|---|---|---|---|---|---|---|---|---|---|---|
| 1 | Smooth boundaries | 0.0261 | 0.65 | 0.121 | 0.4314 | 0.5 | 1.059 | -- | 0.180 | 0.101 | 0.362 | 0.131 | 0.626 | 0.874 | 0.792 |
| | | | 1 | 0.123 | 0.4244 | 0.5 | 1.052 | -- | 0.166 | 0.095 | 0.334 | 0.706 | 0.047 | 0.868 | 0.051 |
| | | | 2 | 0.123 | 0.4244 | 0.5 | 1.077 | -- | 0.165 | 0.085 | 0.311 | 0.104 | 0.047 | 0.868 | 0.047 |
| | | | 2.8 | 0.1235 | 0.4227 | 0.5 | 1.108 | -- | 0.186 | 0.078 | 0.412 | 0.181 | 0.047 | 0.869 | 0.383 |
| | | | 4 | 0.1235 | 0.4227 | 0.5 | 1.108 | -- | 0.259 | 0.078 | 0.472 | 0.177 | 0.047 | 0.047 | 0.055 |
| | | | 5 | 0.124 | 0.421 | 0.5 | 1.117 | -- | 0.290 | 0.089 | 0.544 | 0.248 | 0.047 | 0.047 | 0.063 |
| | | | 6.5 | 0.118 | 0.4424 | 0.5 | 1.174 | 1.05 | 0.251 | 0.075 | 0.571 | 0.354 | 0.142 | 0.142 | 0.125 |
| | | | 8 | 0.123 | 0.4244 | 0.5 | 1.254 | 1.02 | 0.250 | 0.076 | 1.758 | 0.380 | 0.173 | 0.104 | 0.157 |
| | | | 10 | 0.122 | 0.4279 | 0.5 | 1.245 | 1.02 | 0.537 | 0.152 | 1.324 | 0.498 | 0.064 | 0.064 | 0.056 |
| 1 | Smooth boundaries | 0.0556 | 0.65 | 0.197 | 0.5645 | 0.5 | 1.161 | -- | 0.246 | 0.155 | 0.369 | 0.892 | 0.095 | 0.085 | 0.126 |
| | | | 1 | 0.185 | 0.6011 | 0.5 | 1.016 | -- | 0.139 | 0.126 | 0.174 | 0.977 | 0.031 | 0.075 | 0.031 |
| | | | 2 | 0.189 | 0.5884 | 0.5 | 1.017 | -- | 0.136 | 0.093 | 0.159 | 0.957 | 0.036 | 0.073 | 0.036 |
| | | | 2.8 | 0.191 | 0.5822 | 0.5 | 1.022 | -- | 0.137 | 0.084 | 0.162 | 0.920 | 0.036 | 0.098 | 0.030 |
| | | | 4 | 0.192 | 0.5792 | 0.5 | 1.033 | -- | 0.132 | 0.069 | 0.164 | 0.499 | 0.051 | 0.098 | 0.030 |
| | | | 5 | 0.192 | 0.5792 | 0.5 | 1.021 | -- | 0.141 | 0.065 | 0.171 | 0.655 | 0.030 | 0.082 | 0.030 |
| | | | 6.5 | 0.191 | 0.5822 | 0.5 | 1.057 | 1.06 | 0.123 | 0.059 | 0.205 | 0.397 | 0.030 | 0.030 | 0.397 |
| | | | 8 | 0.192 | 0.5792 | 0.5 | 1.116 | 1.04 | 0.133 | 0.057 | 0.211 | 0.577 | 0.030 | 0.030 | 0.239 |
| | | | 10 | 0.193 | 0.5762 | 0.5 | 1.125 | 1.04 | 0.137 | 0.061 | 0.217 | 0.574 | 0.051 | 0.051 | 0.046 |
| 2 | Rough bed | 0.0261 | 0.65 | 0.129 | 0.4047 | 0.5 | 1.186 | -- | 0.355 | 0.165 | 0.432 | 0.820 | 0.060 | 0.049 | 0.045 |
| | | | 1 | 0.12863 | 0.4058 | 0.5 | 1.228 | -- | 0.396 | 0.157 | 0.511 | 0.900 | 0.061 | 0.061 | 0.061 |
| | | | 2 | 0.12625 | 0.4135 | 0.5 | 1.263 | -- | 0.591 | 0.195 | 0.895 | 0.838 | 0.062 | 0.062 | 0.062 |
| | | | 2.8 | 0.1235 | 0.4227 | 0.5 | 1.293 | -- | 0.324 | 0.147 | 0.445 | 0.695 | 0.051 | 0.063 | 0.079 |
| | | | 4 | 0.1235 | 0.4227 | 0.5 | 1.377 | 1.01 | 0.543 | 0.191 | 0.848 | 0.695 | 0.047 | 0.047 | 0.047 |
| | | | 5 | 0.11925 | 0.4377 | 0.5 | 1.363 | 1.00 | 0.908 | 0.288 | 2.422 | 0.887 | 0.149 | 0.183 | 0.049 |
| | | | 6.5 | 0.1115 | 0.4682 | 0.5 | 1.380 | 1.01 | 0.279 | 0.144 | 0.376 | 0.680 | 0.052 | 0.052 | 0.196 |
| 2 | Rough bed | 0.0556 | 0.65 | 0.206 | 0.5398 | 0.5 | 1.186 | -- | 0.354 | 0.174 | 0.418 | 0.683 | 0.038 | 0.033 | 0.033 |
| | | | 1 | 0.206 | 0.5398 | 0.5 | 1.241 | -- | 0.368 | 0.156 | 0.464 | 0.756 | 0.028 | 0.028 | 0.028 |
| | | | 2 | 0.189 | 0.5884 | 0.5 | 1.165 | -- | 0.330 | 0.146 | 0.394 | 0.904 | 0.031 | 0.031 | 0.031 |
| | | | 2.8 | 0.206 | 0.5398 | 0.5 | 1.295 | -- | 1.298 | 0.614 | 3.336 | 0.683 | 0.028 | 0.028 | 0.028 |

| | | | | | | | | | | | | | | |
|---|---|---|---|---|---|---|---|---|---|---|---|---|---|---|
| | | | 4 | 0.192 | 0.5792 | 0.5 | 1.272 | 1.00 | 0.370 | 0.153 | 0.473 | 0.525 | 0.030 | 0.030 | 0.030 |
| | | | 5 | 0.196 | 0.5673 | 0.5 | 1.343 | 0.99 | 0.384 | 0.161 | 0.527 | 0.591 | 0.032 | 0.035 | 0.032 |
| | | | 6.5 | 0.196 | 0.5673 | 0.5 | 1.426 | 1.10 | 0.315 | 0.147 | 0.371 | 0.489 | 0.035 | 0.032 | 0.035 |
| 3 | Rough bed and sidewall | 0.0261 | 2 | 0.149 | 0.3661 | 0.1045 | 1.374 | -- | 0.738 | 0.263 | 1.742 | 0.710 | 0.039 | 0.039 | 0.046 |
| | | | | 0.152 | 0.3589 | 0.2612 | 1.457 | -- | 0.293 | 0.166 | 0.349 | 0.564 | 0.038 | 0.041 | 0.038 |
| | | | | 0.153 | 0.3565 | 0.3657 | 1.558 | -- | 0.352 | 0.157 | 0.404 | 0.267 | 0.041 | 0.038 | 0.038 |
| | | | | 0.151 | 0.3612 | 0.5225 | 1.534 | -- | 0.601 | 0.231 | 0.905 | 0.303 | 0.038 | 0.038 | 0.038 |
| | | | | 0.153 | 0.3565 | 0.6531 | 1.396 | -- | 0.304 | 0.148 | 0.386 | 0.626 | 0.041 | 0.077 | 0.038 |
| | | | | 0.149 | 0.3661 | 0.7837 | 1.438 | -- | 0.203 | 0.124 | 0.181 | 0.643 | 0.079 | 0.093 | 0.240 |
| | | | | 0.152 | 0.3589 | 0.8777 | 1.396 | -- | 1.261 | 0.390 | 2.920 | 0.499 | 0.334 | 0.038 | 0.334 |
| | | | | 0.153 | 0.3565 | 0.9927 | 0.942 | -- | 0.382 | 0.150 | 1.002 | 0.365 | 0.051 | 0.038 | 0.064 |
| 3 | Rough bed and sidewall | 0.0261 | 5 | 0.153 | 0.3565 | 0.1045 | 1.440 | 1.09 | 1.334 | 0.396 | 2.743 | 0.430 | 0.058 | 0.058 | 0.058 |
| | | | | 0.143 | 0.3814 | 0.2612 | 1.612 | 1.08 | 0.321 | 0.158 | 0.373 | 0.530 | 0.048 | 0.055 | 0.044 |
| | | | | 0.153 | 0.3565 | 0.3657 | 1.810 | 1.02 | 0.362 | 0.173 | 0.405 | 0.495 | 0.038 | 0.064 | 0.044 |
| | | | | 0.142 | 0.3841 | 0.5225 | 1.606 | 1.01 | 0.419 | 0.185 | 0.585 | 0.675 | 0.044 | 0.044 | 0.076 |
| | | | | 0.153 | 0.3565 | 0.6531 | 1.564 | 1.00 | 0.343 | 0.158 | 0.392 | 0.626 | 0.038 | 0.051 | 0.038 |
| | | | | 0.143 | 0.3814 | 0.7837 | 1.292 | 1.00 | 0.170 | 0.278 | 0.190 | 0.670 | 0.285 | 0.083 | 0.083 |
| | | | | 0.153 | 0.3565 | 0.8777 | 1.399 | 1.11 | 0.343 | 0.154 | 0.589 | 0.430 | 0.064 | 0.044 | 0.041 |
| | | | | 0.153 | 0.3565 | 0.9927 | 1.063 | 1.04 | 1.848 | 0.494 | 3.121 | 0.299 | 0.267 | 0.267 | 0.038 |
| 3 | Rough bed and sidewall | 0.0261 | 8 | 0.129 | 0.4228 | 0.1045 | 1.275 | 1.08 | 1.664 | 0.457 | 3.425 | 0.324 | 0.091 | 0.091 | 0.053 |
| | | | | 0.129 | 0.4228 | 0.2612 | 1.681 | 1.01 | 0.323 | 0.166 | 0.375 | 0.549 | 0.053 | 0.045 | 0.068 |
| | | | | 0.129 | 0.4228 | 0.3657 | 1.786 | 1.00 | 0.368 | 0.167 | 0.407 | 0.665 | 0.049 | 0.068 | 0.045 |
| | | | | 0.129 | 0.4228 | 0.5225 | 1.737 | 1.00 | 0.393 | 0.181 | 0.444 | 0.665 | 0.053 | 0.045 | 0.045 |
| | | | | 0.129 | 0.4228 | 0.6531 | 1.605 | 1.00 | 0.347 | 0.182 | 0.417 | 0.665 | 0.049 | 0.053 | 0.134 |
| | | | | 0.129 | 0.4228 | 0.7837 | 1.459 | 1.22 | 0.291 | 0.146 | 0.417 | 0.549 | 0.134 | 0.134 | 0.134 |
| | | | | 0.129 | 0.4228 | 0.8777 | 1.375 | 1.75 | 2.048 | 0.536 | 3.981 | 0.549 | 0.099 | 0.099 | 0.057 |
| | | | | 0.129 | 0.4228 | 0.9927 | 0.645 | 1.20 | 1.544 | 0.410 | 3.296 | 0.433 | 0.150 | 0.072 | 0.150 |
| 3 | Rough bed and sidewall | 0.0556 | 2 | 0.189 | 0.5884 | 0.1 | 1.128 | -- | 0.726 | 0.227 | 1.371 | 0.507 | 0.036 | 0.036 | 0.041 |
| | | | | 0.189 | 0.5884 | 0.25 | 1.214 | -- | 0.261 | 0.139 | 0.309 | 0.242 | 0.031 | 0.031 | 0.031 |
| | | | | 0.189 | 0.5884 | 0.35 | 1.310 | -- | 0.914 | 0.271 | 1.970 | 0.507 | 0.062 | 0.062 | 0.062 |
| | | | | 0.189 | 0.5884 | 0.5 | 1.156 | -- | 0.764 | 0.218 | 1.880 | 0.348 | 0.062 | 0.031 | 0.062 |
| | | | | 0.189 | 0.5884 | 0.625 | 1.239 | -- | 0.453 | 0.170 | 1.441 | 0.904 | 0.099 | 0.099 | 0.084 |
| | | | | 0.222 | 0.5009 | 0.75 | 1.182 | -- | 1.590 | 0.463 | 3.424 | 0.634 | 0.062 | 0.062 | 0.364 |
| | | | | 0.222 | 0.5009 | 0.84 | 1.319 | -- | 1.475 | 0.442 | 3.116 | 0.499 | 0.432 | 0.035 | 0.432 |
| | | | | 0.222 | 0.5009 | 0.95 | 0.544 | -- | 1.679 | 0.487 | 3.508 | 0.702 | 0.044 | 0.031 | 0.031 |
| 3 | Rough bed and sidewall | 0.0556 | 5 | 0.1905 | 0.5837 | 0.1 | 1.063 | -- | 1.448 | 0.493 | 2.971 | 0.450 | 0.214 | 0.345 | 0.529 |

| | | | | | | | | | | | | | | |
|---|---|---|---|---|---|---|---|---|---|---|---|---|---|---|
| | | | | 0.1903 | 0.5843 | 0.25 | 1.418 | 1.13 | 1.737 | 0.446 | 3.338 | 0.609 | 0.036 | 0.036 | 0.083 |
| | | | | 0.1903 | 0.5843 | 0.35 | 1.412 | 1.19 | 0.865 | 0.273 | 2.035 | 0.451 | 0.057 | 0.057 | 0.104 |
| | | | | 0.1903 | 0.5843 | 0.5 | 1.362 | 1.06 | 0.687 | 0.227 | 1.527 | 0.451 | 0.036 | 0.036 | 0.041 |
| | | | | 0.1903 | 0.5843 | 0.625 | 1.284 | 1.51 | 1.088 | 0.308 | 2.450 | 0.845 | 0.062 | 0.062 | 0.073 |
| | | | | 0.1903 | 0.5843 | 0.75 | 1.218 | 1.29 | 1.001 | 0.290 | 2.433 | 0.687 | 0.057 | 0.057 | 0.062 |
| | | | | 0.1923 | 0.5783 | 0.84 | 1.065 | 1.95 | 1.678 | 0.419 | 2.987 | 0.602 | 0.030 | 0.030 | 0.072 |
| | | | | 0.1903 | 0.5843 | 0.95 | 0.540 | 2.56 | 1.563 | 0.463 | 3.559 | 0.293 | 0.036 | 0.041 | 0.041 |
| 3 | Rough bed and sidewall | 0.0556 | 8 | 0.1743 | 0.638 | 0.1 | 1.116 | 1.46 | 1.639 | 0.405 | 2.995 | 0.550 | 0.045 | 0.045 | 0.378 |
| | | | | 0.1743 | 0.638 | 0.25 | 1.429 | 1.06 | 0.580 | 0.197 | 0.846 | 0.636 | 0.091 | 0.091 | 0.091 |
| | | | | 0.1743 | 0.638 | 0.35 | 1.500 | 1.06 | 0.378 | 0.162 | 0.559 | 0.722 | 0.050 | 0.050 | 0.263 |
| | | | | 0.1743 | 0.638 | 0.5 | 1.439 | 1.05 | 0.424 | 0.170 | 1.590 | 0.636 | 0.045 | 0.068 | 0.056 |
| | | | | 0.1743 | 0.638 | 0.625 | 1.331 | 1.07 | 0.866 | 0.259 | 1.919 | 0.636 | 0.050 | 0.050 | 0.050 |
| | | | | 0.1743 | 0.638 | 0.75 | 1.273 | 1.70 | 0.965 | 0.285 | 2.058 | 0.550 | 0.079 | 0.079 | 0.079 |
| | | | | 0.1743 | 0.638 | 0.84 | 1.127 | 1.17 | 1.044 | 0.281 | 1.978 | 0.636 | 0.050 | 0.050 | 0.050 |
| | | | | 0.1743 | 0.638 | 0.95 | 0.474 | 1.56 | 1.565 | 0.386 | 2.741 | 0.808 | 0.045 | 0.091 | 0.079 |

Notes: $V_{max}$: maximum longitudinal velocity component in a vertical profile; $V_{mean}$: cross-sectional averaged velocity; $V_{fs}$: free-surface velocity; x: longitudinal distance from the channel's upstream end; y: transverse distance from right smooth sidewall; Z: vertical elevation above the invert.

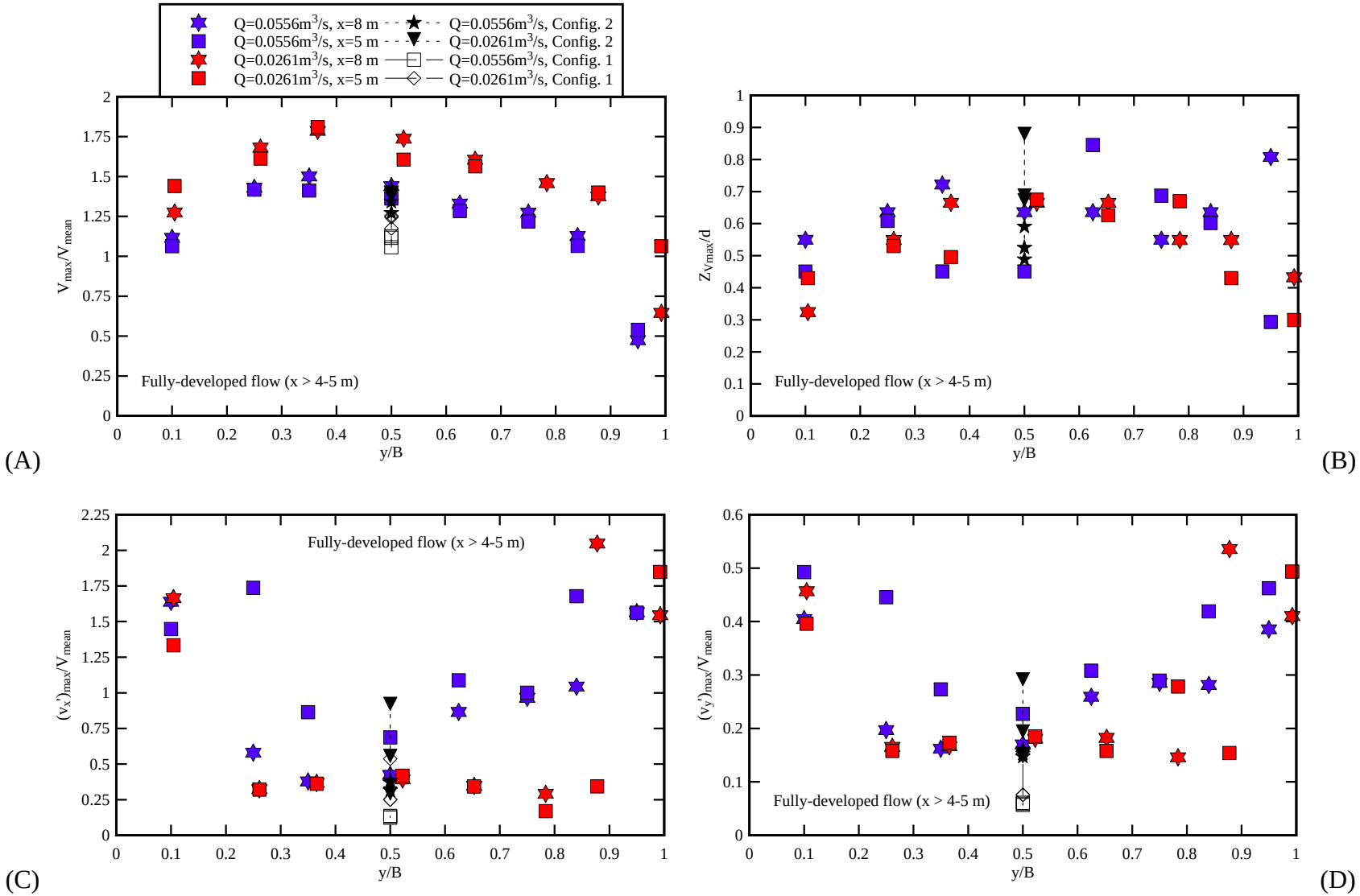


Fig.C-1 - Fig. 3-5 - Transverse distribution of maximum longitudinal velocity, maximum velocity fluctuations and elevation of maximum velocity as function of the transverse location in the 12 m long channel with rough bed and sidewall (Configuration 3) - Same legend for all graphs - Comparison with centreline data for Configurations 1 and 2 - Note y = 0 at the right smooth sidewall

# APPENDIX D - FISH SWIMMING PERFORMANCE TESTS

## D.1 PRESENTATION

The swimming performances of juvenile Silver Perch (*Bidyanus bidyanus*) were tested in a small Loligo$^{TM}$ recirculating water tunnel with a 0.86 m long 0.251 m wide and 0.259 m high working section. The water tunnel volume was 0.185 $m^3$ and it was placed in a 0.4 $m^3$ rectangular water tank. Screens and mesh were installed at both test section ends to restrict the fish movements. Water quality was maintained via a continuous flow of filtered fresh water from an external reservoir enabling a constant temperature of 24 C ±0.5 C. A continuous flow motion was delivered by a screw pump.

The tests were conducted on Silver Perch juveniles, following a clearly defined protocol (Table D-1). Each trial began with an acclimation period, consisting of 30 minutes at zero bulk velocity to allow each fish to become accustomed to the flow tank and display normal rheotaxic behaviour. When no adverse behaviour was observed during this acclimation period, the bulk water velocity was subsequently increased incrementally every 5 min until the fish fatigued (Table D-1). Fatigue was defined as when the fish rested against the downstream screen mesh for more than 3 s. The critical swimming speed ($U_{crit}$) of each individual was calculated as (BRETT 1964):

Table D-1 - Fish testing procedure in the water tunnel

| Step No. | Procedure |
|---|---|
| 1 | Fish were rested and fasted for 24 hours prior to experimentation |
| 2 | The fish were placed into the recirculating water tunnel test section and left for 30 minutes with zero flow to adjust to the change in temperature (24 C herein) |
| 3 | Using the calibration curves developed for the recirculating flume, accounting for blockage effects and three-dimensional velocity profile, the bulk velocity was increased in increments (4-4.5 cm/s in configuration 2; 2.5-3.5 cm/s in configuration 3) every 5 minutes |
| 4 | Photographs and videos (240 fps) were taken of the fish, particularly between 35 cm/s and 55 cm/s |
| 5 | The water tunnel was immediately stopped if the fish had been resting on the downstream grate for 3 s |
| 6 | The final bulk velocity of the fish, time the fish had been swimming, the weight of the fish and the body length of the fish were recorded |
| 7 | The Ucrit value was calculated: $$U_{crit} = U_f + \Delta U \times \frac{T_f}{\Delta T}$$ |

$$U_{crit} = U_f + \Delta U \times \frac{T_f}{\Delta T} \qquad \text{(D-1)}$$

where $U_f$ is the penultimate velocity, $T_f$ is the amount of time that the fish swam in the final increment, $\Delta T$ is the total time increment (5 min) and $\Delta U$ is the water velocity increment. Herein all the velocity data are bulk velocities: i.e., cross-sectional averaged velocities.

Only one individual was tested at a time and all tests were conducted with a water temperature at 24 C. Two boundary roughness conditions were used: rough bed and smooth sidewalls (Configuration 2), and rough bed and rough left sidewall (Configuration 3) (Fig. D-1). During each test, photographs and movies were taken to document the fish swimming behaviour in relation to the boundary roughness.

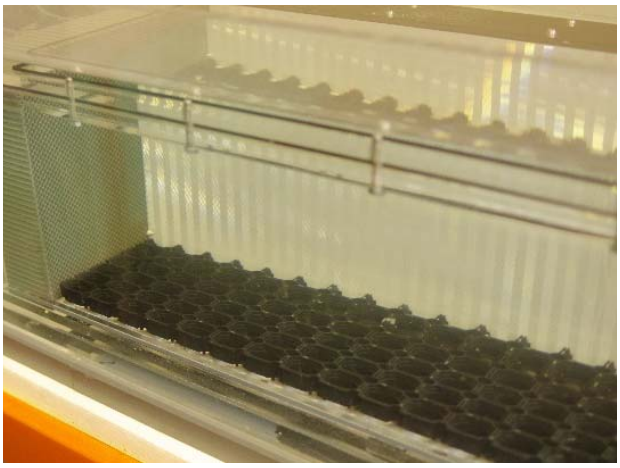

(A) Configuration 2: rough bed and smooth sidewalls

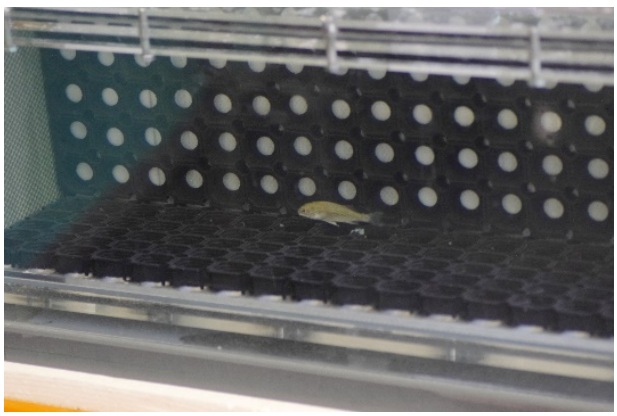

(B) Configuration 3: rough bed, and combination of rough and smooth sidewalls - Note juvenile *Bidyanus bidyanus* swimming close to the corner between rough bed and rough sidewall

Fig. D-1 - Roughness configurations in the recirculating water tunnel

Table D-2 - Fish swimming performance results with rough boundary conditions

| Fish ID | Water temperature (C) | Configuration | Final Velocity (m/s) | $U_f$ (m/s) | $\Delta U$ (m/s) | Time swum (s) | $T_f$ (s) | $\Delta T$ (s) | $U_{crit}$ (m/s) | Weight (g) | Body length (mm) |
|---|---|---|---|---|---|---|---|---|---|---|---|
| big R:RR | 24.5 | Rough bed & smooth sidewalls | 0.887 | 0.845 | 0.042 | 5495 | 95 | 300 | 0.858 | 44.1 | 130.6 |
| L:RY | 24 | Rough bed & smooth sidewalls | 0.760 | 0.718 | 0.042 | 4547 | 47 | 300 | 0.724 | 14.1 | 93.6 |
| L:YY | 23 | Rough bed & smooth sidewalls | 0.633 | 0.591 | 0.042 | 3836 | 235 | 300 | 0.624 | 14.3 | 93 |
| L:YR | 24 | Rough bed & smooth sidewalls | 0.675 | 0.633 | 0.042 | 4166 | 586 | 300 | 0.716 | 9.5 | 81.5 |
| med R:RR | 23.5 | Rough bed & smooth sidewalls | 1.096 | 1.053 | 0.043 | 6622 | 22 | 300 | 1.057 | 14.3 | 97.3 |
| "Big Momma" | 23.5 | Rough bed & smooth sidewalls | 0.930 | 0.887 | 0.043 | 5728 | 28 | 300 | 0.891 | 73.8 | 95.8 |
| Small R:RR | 23.5 | Rough bed & smooth sidewalls | 0.718 | 0.675 | 0.042 | 4556 | 56 | 300 | 0.683 | 7.5 | 82 |
| med R:RR | 24 | Rough bed & sidewall | 0.604 | 0.580 | 0.024 | 5187 | 87 | 300 | 0.587 | 14.1 | 97.3 |
| "Big Momma" | 23.5 | Rough bed & sidewall | 0.529 | 0.505 | 0.024 | 4498 | 298 | 300 | 0.529 | 75.1 | 95.8 |
| Small R:RR | 24.25 | Rough bed & sidewall | 0.628 | 0.604 | 0.024 | 5681 | 259 | 300 | 0.625 | 9.2 | 82 |
| med R:RR | 24.5 | Rough bed & sidewall | 0.628 | 0.604 | 0.024 | 5598 | 198 | 300 | 0.620 | 39.4 | 97.3 |
| L:RY | 24 | Rough bed & sidewall | 0.529 | 0.505 | 0.024 | 4427 | 227 | 300 | 0.523 | 13.8 | 93.6 |
| L:YR | 23.5 | Rough bed & sidewall | 0.318 | 0.290 | 0.028 | 1839 | 39 | 300 | 0.294 | 8.9 | 81.5 |

Notes: $U_f$: final velocity at which the fish swum for the full time increment (m/s), $\Delta U$: velocity increment (m/s), $T_f$: time swum at the maximum velocity (s), $\Delta T$: time increment (s); Grey shade: rough bed and sidewall configuration 3.

D.2 BASIC RESULTS

During the fish swimming experiments, visual observations of the fish swimming patterns were conducted. For low velocities the majority of fish would swim in the corner at the bottom of the inside wall (Configurations 2 & 3) (Fig. D-1B). For larger velocities, the fish swam in the top corner (Fig. D-2), likely caused by the recirculating flume design. Some fish would move around trying to find lower velocity areas. Overall the experiments showed that the fish tested preferred to swim in regions of low velocity, enabling them a longer effort with minimum fatigue in these areas.

The final results are presented in Table D-2. For Silver Perch juveniles, the characteristic speed $U_{crit}$ was consistently larger with the rough bottom (Configuration 2), than with the rough bed and wall (Configuration 3). This is illustrated in Figure D-3. The finding is counter-intuitive, but it is believed to be linked to the non-uniform velocity distribution in the test section and the existence of some recirculation region in the upstream top left corner of the test section.

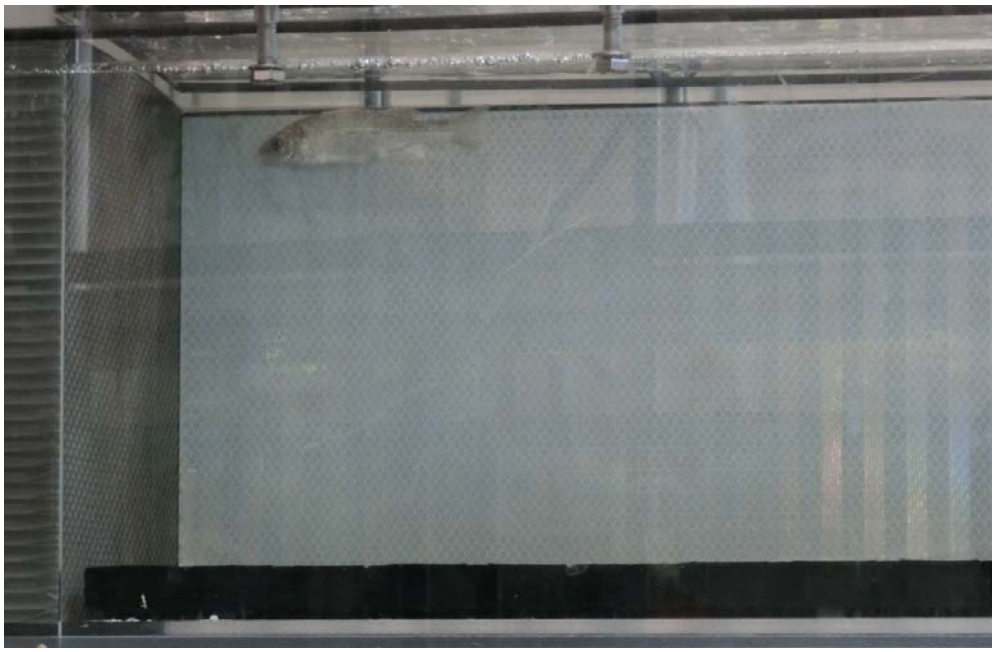

Fig. D-2 - Typical swimming location of juvenile Silver Perch in the upstream top left corner of the test section - Flow direction from left to right, rough bed configuration (Configuration 2)

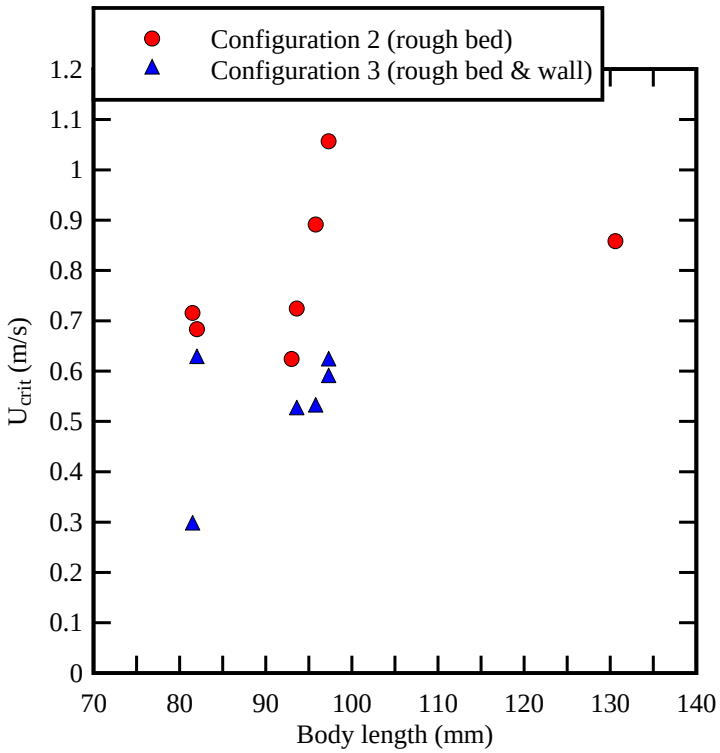


Fig. D-3 - Critical velocity $U_{crit}$ as a function of the body length for juvenile Silver Perch

# REFERENCES


APELT, C.G., and XIE, Q. (1995). "Turbulent Flow in Irregular Channels." *Proc. 12th Australasian Fluid Mechanics Conference AFMC*, Sydney, Australia, Vol. 1, pp. 179-182.

APELT, C.G., and XIE, Q. (2011). "Measurements of the Turbulent Velocity Field in a Non-Uniform Open Channel." *Proc. 34th IAHR World Congress*, Brisbane, Australia, 26 June-1 July, Engineers Australia Publication, Eric VALENTINE, Colin APELT, James BALL, Hubert CHANSON, Ron COX, Rob ETTEMA, George KUCZERA, Martin LAMBERT, Bruce MELVILLE and Jane SARGISON Editors, pp. 3338-3345 (ISBN 978-0-85825-868-6).

BAKI, A.B., ZHU, D.Z., and RAJARATNAM, N. (2014). "Mean Flow Characteristics in a Rock-ramp-type Fish Pass." *Journal of Hydraulic Engineering*, ASCE, Vol. 140, No. 2, pp. 156-168.

BATES. K. (2000). "Fishway guidelines for Washington State." *Washington Department of Fish and Wildlife*, 57 pages.

BRESSE, J.A. (1860). "Cours de Mécanique Appliquée Professé à l'Ecole des Ponts et Chaussées." ('Course in Applied Mechanics lectured at the Pont-et-Chaussées Engineering School.') *Mallet-Bachelier*, Paris, France (in French).

BRETON, F/, BAKI, A.B.M., LINK, O. ZHU, D.Z., and RAJARATNAM, N. (2013). "Flow in nature-like fishway and its relation to fish behaviour." *Canadian Journal of Civil Engineering*, Vol. 40, pp. 567–573.

BRETT, J.R. (1964). "The respiratory metabolism and swimming performance of young sockeye salmon." *Journal of the Fisheries Research Board of Canada*, Vol. 21, pp. 1183-1226.

BRIGG, A.S., and GALAROWICZ, T.L. (2013). "Fish Passage through Culverts in Central Michigan Warmwater Streams." *North American Journal of Fisheries Management*, Vol. 33, pp. 652-664.

British Standard (1943). "Flow Measurement." *British Standard Code BS 1042:1943*, British Standard Institution, London.

CASSAN, L., TIEN, T.D., COURRET, D., LAURENS, P., and DARTUS, D. (2014). "Hydraulic Resistance of Emergent Macroroughness at Large Froude Numbers: Design of Nature-like Fishpasses." *Journal of Hydraulic Engineering*, ASCE, Vol. 140, Paper 04014043, 9 pages.

CHANSON, H. (2004). "The Hydraulics of Open Channel Flow: An Introduction." *Butterworth-Heinemann*, 2nd edition, Oxford, UK, 630 pages (ISBN 978 0 7506 5978 9).

CHANSON, H. (2008). "Acoustic Doppler Velocimetry (ADV) in the Field and in Laboratory: Practical Experiences." *Proceedings of the International Meeting on Measurements and Hydraulics of Sewers IMMHS'08*, Summer School GEMCEA/LCPC, 19-21 Aug. 2008, Bouguenais, Frédérique LARRARTE and Hubert CHANSON Editors, Hydraulic Model Report No. CH70/08, Div. of Civil Engineering, The University of Queensland, Brisbane, Australia, Dec., pp. 49-66 (ISBN 9781864999280).

CHANSON, H. (2009). "Applied Hydrodynamics: An Introduction to Ideal and Real Fluid Flows." *CRC Press*, Taylor & Francis Group, Leiden, The Netherlands, 478 pages.

CHANSON, H. (2010). "Unsteady Turbulence in Tidal Bores: Effects of Bed Roughness." *Journal of Waterway, Port, Coastal, and Ocean Engineering*, ASCE, Vol. 136, No. 5, pp. 247-256 (DOI: 10.1061/(ASCE)WW.1943-5460.0000048).

CHANSON, H., TREVETHAN, M., and AOKI, S. (2008). "Acoustic Doppler Velocimetry (ADV) in Small Estuary: Field Experience and Signal Post-Processing." *Flow Measurement and Instrumentation*, Vol. 19, No. 5, pp. 307-313 (DOI: 10.1016/j.flowmeasinst.2008.03.003).

CHANSON, H., TREVETHAN, M., and KOCH, C. (2007). "Turbulence Measurements with Acoustic Doppler Velocimeters. Discussion." *Journal of Hydraulic Engineering*, ASCE, Vol. 133, No. 11, pp. 1283-1286 (DOI: 10.1061/(ASCE)0733-9429(2005)131:12(1062)).

CHANSON, H., and UYS, W. (2016). "Baffle Designs to facilitate Fish Passage in Box Culverts: A Preliminary Study." *Proceedings of 6th IAHR International Symposium on Hydraulic Structures ISHS2016*, Portland Oregon, USA, 27-30 June, 8 pages.

CHOW, V.T. (1959). "Open Channel Hydraulics." *McGraw-Hill*, New York, USA.

DAVID, L., CALLUAUD, D., PINEAU, G., and TEXIER, A. (2012). "Fishway Hydrodynamics and Global Approaches for insuring the Upstream Migration around Dams." *Proc. 4th IAHR International Symposium on Hydraulic Structures*, APRH - Associação Portuguesa dos Recursos Hídricos (Portuguese Water Resources Association), J. MATOS, S. PAGLIARA & I. MEIRELES Eds., 9-11 February 2012, Porto, Portugal, Paper 4, 15 pages (CD-ROM).

DJENIDI, L., ELAVARASAN, R., and ANTONIA, R.A. (1999). "The Turbulent Boundary Layer over Transverse Square Cavities." *Journal of Fluid Mechanics*, Vol. 395, pp. 271-294.

DOCHERTY, N.J., and CHANSON, H. (2010). "Characterisation of Unsteady Turbulence in Breaking Tidal Bores including the Effects of Bed Roughness." *Hydraulic Model Report No. CH76/10*, School of Civil Engineering, The University of Queensland, Brisbane, Australia, 112 pages (ISBN 9781864999884).

DOCHERTY, N.J., and CHANSON, H. (2012). "Physical Modelling of Unsteady Turbulence in Breaking Tidal Bores." *Journal of Hydraulic Engineering*, ASCE, Vol. 138, No. 5, pp. 412-419 (DOI: 10.1061/(ASCE)HY.1943-7900.0000542).

FAIRFULL, S., and WITHERIDGE, G. (2003). "Why do fish need to cross the road? Fish passage requirements for waterway crossings." *NSW Fisheries*, Cronulla NSW, Australia, 14 pages.

FINELLI, C.M., HART, D.D., and FONSECA, D.M. (1999). "Evaluating the Spatial Resolution of an Acoustic Doppler Velocimeter and the Consequences for Measuring Near-Bed Flows." *Limnology & Oceanography*, Vol. 44, No. 7, pp. 1793-1801.

GIBSON, A.H. (1909). "On the depression of the filament of maximum velocity in a stream flowing through an open channel." *Proceedings Royal Society of London Series A*, Vol. 82, pp. 149-159.

GORING, D.G., and NIKORA, V.I. (2002). "Despiking Acoustic Doppler Velocimeter Data." *Journal of Hydraulic Engineering*, ASCE, Vol. 128, No. 1, pp. 117-126. Discussion: Vol. 129, No. 6, pp. 484-489.

HEASLIP, B.M. (2015). "Substrate Roughnening Improves Swimming Performance of Two Small-bodied Riverine Fish Species: Implications for Culvert Design." *Honours thesis*, The University of Queensland, School of Biological Sciences, Brisbane, Australia, 32 pages.

HEE, M. (1969). "Hydraulics of Culvert Design Including Constant Energy Concept." *Proc. 20th Conf. of Local Authority Engineers*, Dept. of Local Govt, Queensland, Australia, paper 9, pp. 1-27.

HENDERSON, F.M. (1966). "Open Channel Flow." *MacMillan Company*, New York, USA.

HOTCHKISS, R. (2002). "Turbulence investigation and reproduction for assisting downstream migrating juvenile salmonids, Part I." *BPA Report DOE/BP-00004633-I*, Bonneville Power administration, Portland, Oregon, 138 pages.

HUGHES, S.A. (1993). "Physical Models and Laboratory Techniques in Coastal Engineering." *Advanced Series on Ocean Engineering*, Vol. 7, World Scientific Publ., Singapore, 568 pages.

HUNT, M., CLARK, S., and TKACH, R. (2012). "Velocity Distributions near the Inlet of Corrugated Steep Pipe Culverts." *Canadian Journal of Civil Engineering*, Vol. 39, pp. 1243-1251.

JOHNSON, M.F., and RICE, S.P. (2014). "Animal Perception in Gravel-bed Rivers: Scales of Sensing and Environmental Controls on Sensory Information." *Canadian Journal of Fisheries and Aquatic Sciences*, Vol. 71, pp. 945-057.

KNIGHT, D.W., DEMETRIOU, J.D., and HAMED, M.E. (1984). "Boundary Shear in Smooth Rectangular Channels." *Journal of Hydraulic Engineering*, ASCE, Vol. 110. No. 4, pp. 405-422.

LACEY, R.W.J., and RENNIE, C.D. (2012). "Laboratory Investigation of Turbulent Flow Structure around a Bed-mounted Cube at Multiple Flow Stages." *Journal of Hydraulic Engineering*, ASCE, Vol. 138, No. 1, pp. 71-84.

LEMMIN, U., and LHERMITTE, R. (1999). "ADV Measurements of Turbulence: can we Improve their Interpretation ? Discussion" *Journal of Hydraulic Engineering*, ASCE, Vol. 125, No. 6, pp. 987-988.

LENG, X., and CHANSON, H. (2014). "Propagation of Negative Surges in Rivers and Estuaries: Unsteady Turbulent Mixing and the Effects of Bed Roughness." *Hydraulic Model Report No. CH93/13*, School of Civil Engineering, The University of Queensland, Brisbane, Australia, 108 pages (ISBN 9781742720999).

LIGGETT, J.A. (1994). "Fluid Mechanics." *McGraw-Hill*, New York, USA.

LIU, M., ZHU, D., and RAJARATNAM, N. (2002). "Evaluation of ADV Measurements in Bubbly Two-Phase Flows." *Proc. Conf. on Hydraulic Measurements and Experimental Methods*, ASCE-EWRI & IAHR, Estes Park, USA, 10 pages (CD-ROM).

LIU, M.M., RAJARATNAM, N., and ZHU, D,Z. (2006). "Mean flow and turbulence structure in vertical slot fishways." *Journal of Hydraulic Engineering*, ASCE, Vol. 139, No. 4, pp. 424-432.

McLELLAND, S.J., and NICHOLAS, A.P. (2000). "A New Method for Evaluating Errors in High-Frequency ADV Measurements." *Hydrological Processes*, Vol. 14, pp. 351-366.

MACINTOSH, J.C. (1990). "Hydraulic Characteristics in Channels of Complex Cross-Section." *Ph.D. thesis*, Univ. of Queensland, Dept. of Civil Eng., Australia, Nov., 487 pages.

NEZU, I., and NAKAGAWA, H. (1993). "Turbulence in Open-Channel Flows." *IAHR Monograph*, IAHR Fluid Mechanics Section, Balkema Publ., Rotterdam, The Netherlands, 281 pages.

NEZU, I. AND RODI, W. (1985). "Experimental Study on Secondary Currents in Open Channel Flow." *Proceedings 21st IAHR Biennial Congress*, Melbourne, Australia, pp. 114-119.

NIKORA, V.I., ABERLE, J., BIGGS, B.J.F., JOWETT, I.G., and SYKES, J.R.E. (2003). "Effects of Fish Size, Time-to-Fatigue and Turbulence on Swimming Performance: a Case Study of *Galaxias Maculatus*." *Journal of Fish Biology*, Vol. 63, pp. 1365-1382.

NOVAK, P., and CABELKA, J. (1981). "Models in Hydraulic Engineering. Physical Principles and Design Applications." *Pitman Publ.*, London, UK, 459 pages.

NOVAK, P., GUINOT, V., JEFFREY, A., and REEVE, D.E. (2010). "Hydraulic Modelling - an Introduction." *CRC Press*, Taylor & Francis, London, UK, 599 pages.

OLSEN, A. and TULLIS, B. (2013). "Laboratory Study of Fish Passage and Discharge Capacity in Slip-Lined, Baffled Culverts." *Journal of Hydraulic Engineering*, ASCE, Vol. 139, No. 4, pp. 424–432

PAPANICOLAOU, A.N., and TALEBBEYDOKHTI, N. (2002). Discussion of "Turbulent open-channel flow in circular corrugated culverts." *Journal of Hydraulic Engineering*, ASCE, Vol. 128, No. 5, pp. 548–549.

PAVLOV, D.S., LUPANDIN, I.A., and SKOROBOGATOV, M.A. (2000). "The effects of flow turbulence on the behavior and distribution of fish." *Jl Ichthyol*, Vol. 40, pp. S232-S261.

PERRY, A.E., LIM, K.L., and HENBEST, S.M. (1987). "An experimental study of the turbulence structure in smooth- and rough-wall boundary layers." *Journal of Fluid Mechanics*, Vol. 177, pp. 437-466.

RODGERS, E.M., CRAMP, R.L., GORDOS, M., WEIER, A., FAIRFALL, S., RICHES, M., and FRANKLIN, C.E. (2014). "Facilitating upstream passage of small-bodied fishes: linking the thermal dependence of swimming ability to culvert design." *Marine and Freshwater Research*, Vol. 65, pp. 710-719 (DOI: 10.1071/MF13170).

SCHLICHTING, H. (1979). "Boundary Layer Theory." *McGraw-Hill*, New York, USA, 7th edition.

SIMON, B., and CHANSON, H. (2013). "Turbulence Measurements in Tidal Bore-like Positive Surges over a Rough Bed." *Hydraulic Model Report No. CH90/12*, School of Civil Engineering, The University of Queensland, Brisbane, Australia, 176 pages (ISBN 9781742720685).

TAMBURRINO, A., and GULLIVER, J.S. (2007). "Free-Surface Visualization of Streamwise Vortices in a Channel Flow." *Water Resources Research*, Vol. 43, Paper W11410, doi:10.1029/2007WR005988.

TARRADE, L., MANCEAU, R., TEXIER, A., DAVID, L., and LARINIER, M. (2005). "Etude numérique des écoulements hydrodynamiques turbulents dans une passe à poissons." *Proceedings of the 17ème Congrès Français de Mécanique*, Troyes, France (in French).

TREVETHAN, M., CHANSON, H., and BROWN, R. (2008). "Turbulence Characteristics of a Small Subtropical Estuary during and after some Moderate Rainfall." *Estuarine Coastal and Shelf Science*, Vol. 79, No. 4, pp. 661-670 (DOI: 10.1016/j.ecss.2008.06.006).

VOULGARIS, G., and TROWBRIDGE, J.H. (1998). "Evaluation of the Acoustic Doppler Velocimeter (ADV) for Turbulence Measurements." *Jl Atmosph. and Oceanic Tech.*, Vol. 15, pp. 272-289.

WAHL, T.L. (2003). "Despiking Acoustic Doppler Velocimeter Data. Discussion." *Journal of Hydraulic Engineering*, ASCE, Vol. 129, No. 6, pp. 484-487.

WANG, R.W., DAVID, L., and LARINIER, M. (2010). "Contribution of experimental fluid mechanics to the design of vertical slot fish passes." *Knowl Manag Aquat Ecosyst*, Vol. 396, No. 02, 21 pages.

WARREN, M.L., Jr., and PARDEW, M.G. (1998). "Road crossings as barriers to small-stream fish movement." *Transactions of the American Fisheries Society* 127:637–644

YASUDA, Y. (2011). "Guideline of Fishway for Engineers." *Corona Publishing*, NPO Society for Fishway in Hokkaido, Japan, 154 pages (in Japanese)

XIE, Q. (1998). "Turbulent Flows in Non-Uniform Open Channels: Experimental Measurements and Numerical Modelling." *Ph.D. thesis*, Dept. of Civil Eng., University Of Queensland, Australia, 339 pages.

Bibliography

ALBAYRAK, I., and LEMMIN, U. (2011). "Secondary Currents and Corresponding Surface Celocity patterns in a Turbulent Open-Channel Flow over a Rough Bed." *Journal of Hydraulic Engineering*, ASCE, Vol. 137, No. 11, pp. 1318-1334.

CHANSON, H. (2004). "Environmental Hydraulics of Open Channel Flows." *Elsevier-Butterworth-Heinemann*, Oxford, UK, 483 pages (ISBN 978 0 7506 6165 2).

NEZU, I., and RODI, W. (1986). "Open-Channel Flow Measurements with a Laser Doppler Anemometer." *Journal of Hydraulic Engineering*, ASCE, Vol. 112, No. 5, pp. 335-355.

NEZU. I., TOMINAGA, A., and NAKAGAWA, H. (1993). "Field Measurements of Secondary Currents in Straight Rivers." *Journal of Hydraulic Engineering*, ASCE, Vol. 119, No. 5, pp. 598-614 (DOI: 10.1061/(ASCE)0733-9429(1993)119:5(598)).

RAJARATNAM, N., and MURALIDHAR, D. (1969). "Boundary shear stress distribution in rectangular open channels." *La Houille Blanche*, No. 6, pp. 603-610 (DOI: http://dx.doi.org/10.1051/lhb/1969047).

RODRIGUEZ, J.E., and GARCIA, M.H. (2008). "Laboratory Measurements of 3-D Flow Patterns and Turbulence in Straight Open Channel with Rough Bed." *Journal of Hydraulic Research*, IAHR, Vol. 46, No. 4, pp. 454-465.

STEFFLER, P.M., RAJARATNAM, N. and PETERSON, A.W. (1985). "LDA Measurements in an Open Channel." *Journal of Hydraulic Engineering*, ASCE, Vol. 111, No. 1, pp. 119-130.

SHUKRY, A. (1950). "Flow around Bends in an Open Flume." *Transactions*, ASCE, Vol. 115, Paper No. 2411, pp. 751-779.

WYZGA, B., AMIROWICZ, A., RADECKI-PAWLIK, A., and ZAWIEJSKA, J. (2009). "Hydromorphological Conditions, Potential Fish Habitats and the Fish Community in a

Mountain River subjected to variable Human Impacts, the Czarny Dunajec, Polish Carpathians." *River Research and Applications*, Vol. 25, No. 5, pp. 517–536 (DOI: 10.1002/rra.1237).

WYZFA, B., AMIROWICZ, A., OGLECKI, P., HAJDUKIEWICZ, H., RADECKI-PAWLIK, A., , ZAWIEJSKA, J., and MIKUS, P. (2014). "Response of fish and benthic invertebrate communities to constrained channel conditions in a mountain river: Case study of the Biała, PolishCarpathians." *Limnologica*, Vol. 46, pp. 58- 69 (DOI: 10.1016/j.limno.2013.12.002).

YANG, S.Q., TAN, S.K., and WANG, X.K. (2012). "Mechanism of secondary currents in open channel flows." *Journal of Geophysical Research*, Vol. 117, Paper F04014, 13 pages (DOI: 10.1029/2012JF002510).

Open Access Repositories

| | |
|---|---|
| OAIster | {http://www.oaister.org/} |
| UQeSpace | {http://espace.library.uq.edu.au/} |

Bibliographic reference of the Report CH103/16

The Hydraulic Model research report series CH is a refereed publication published by the School of Civil Engineering at the University of Queensland, Brisbane, Australia.

The bibliographic reference of the present report is:

WANG, H., BECKINGHAM, L.K., JOHNSON, C.Z., KIRI, U.R., and CHANSON, H. (2016). "Interactions between Large Boundary Roughness and High Inflow Turbulence in Open channel: a Physical Study into Turbulence Properties to Enhance Upstream Fish Migration." *Hydraulic Model Report No. CH103/16*, School of Civil Engineering, The University of Queensland, Brisbane, Australia, 74 pages (ISBN 978-1-74272-156-9).

The Report CH103/16 is available, in the present form, as a PDF file on the Internet at UQeSpace:

http://espace.library.uq.edu.au/

It is listed at:

http://espace.library.uq.edu.au/list/author_id/193/

# HYDRAULIC MODEL RESEARCH REPORT CH

The Hydraulic Model Report CH series is published by the School of Civil Engineering at the University of Queensland. Orders of any reprint(s) of the Hydraulic Model Reports should be addressed to the School Secretary.

School Secretary, School of Civil Engineering, The University of Queensland
Brisbane 4072, Australia - Tel.: (61 7) 3365 3619 - Fax: (61 7) 3365 4599
Url: http://http://www.civil.uq.edu.au// Email: enquiries@civil.uq.edu.au

| **Report CH** | **Unit price** | Quantity | **Total price** |
|---|---|---|---|
| WANG, H., BECKINGHAM, L.K., JOHNSON, C.Z., KIRI, U.R., and CHANSON, H. (2016). "Interactions between Large Boundary Roughness and High Inflow Turbulence in Open channel: a Physical Study into Turbulence Properties to Enhance Upstream Fish Migration." Hydraulic Model Report No. CH103/16, School of Civil Engineering, The University of Queensland, Brisbane, Australia, 74 pages (ISBN 978-1-74272-156-9). | AUD$60.00 | | |
| REUNGOAT, D., LENG, X., and CHANSON, H. (2016). "Impact of Successive Tidal Bores in the Arcins Channel, Garonne River in August-September-October 2015." *Hydraulic Model Report No. CH102/16*, School of Civil Engineering, The University of Queensland, Brisbane, Australia, 266 pages (ISBN 978-1-74272-155-2). | AUD$60.00 | | |
| LENG, X., and CHANSON, H. (2016). "Unsteady Turbulent Velocity Profiling in Open Channel Flows and Tidal Bores using a Vectrino Profiler." *Hydraulic Model Report No. CH101/15*, School of Civil Engineering, The University of Queensland, Brisbane, Australia, 118 pages (ISBN 978-1-74272-145-3). | AUD$60.00 | | |
| WANG, H., and CHANSON, H. (2016). "Velocity Field in Hydraulic Jumps at Large Reynolds Numbers: Development of an Array of Two Dual-Tip Phase-detection Probes." *Hydraulic Model Report No. CH100/15*, School of Civil Engineering, The University of Queensland, Brisbane, Australia, 77 pages (ISBN 978 1 74272 143 9). | AUD$60.00 | | |
| SUARA. K., BROWN, R., and CHANSON, H. (2015). "Turbulence and Mixing in the Environment: Multi-Device Study in a Sub-tropical Estuary." *Hydraulic Model Report No. CH99/15*, School of Civil Engineering, The University of Queensland, Brisbane, Australia, 167 pages (ISBN 978 1 74272 138 5). | AUD$60.00 | | |
| LENG, X., and CHANSON, H. (2015). "Unsteady Turbulence during the Upstream Propagation of Undular and Breaking Tidal Bores: an Experimental Investigation." *Hydraulic Model Report No. CH98/15*, School of Civil Engineering, The University of Queensland, Brisbane, Australia, 235 pages & 4 video movies (ISBN 978 1 74272 135 4). | AUD$60.00 | | |
| ZHANG, G., and CHANSON, H. (2015). "Hydraulics of the Developing Flow Region of Stepped Cascades: an Experimental Investigation." *Hydraulic Model Report No. CH97/15*, School of Civil Engineering, The University of Queensland, Brisbane, Australia, 76 pages (ISBN 978 1 74272 134 7). | AUD$60.00 | | |

| | | | |
|---|---|---|---|
| LENG, X., and CHANSON, H. (2014). "Turbulent Advances of Breaking Bores: Experimental Observations." *Hydraulic Model Report No. CH96/14*, School of Civil Engineering, The University of Queensland, Brisbane, Australia, 40 pages (ISBN 978 1 74272 130 9). | AUD$40.00 | | |
| WANG, H, MURZYN, F., and D., CHANSON, H. (2014). "Pressure, Turbulence and Two-Phase Flow Measurements in Hydraulic Jumps." Hydraulic Model Report No. CH95/14, School of Civil Engineering, The University of Queensland, Brisbane, Australia, 154 pages (ISBN 9781742720616 9781742721064). | AUD$60.00 | | |
| REUNGOAT, D., CHANSON, H., and KEEVIL, C. (2014). "Turbulence, Sedimentary Processes and Tidal Bore Collision in the Arcins Channel, Garonne River (October 2013)." *Hydraulic Model Report No. CH94/14* School of Civil Engineering, The University of Queensland, Brisbane, Australia, 145 pages (ISBN 9781742721033). | AUD$60.00 | | |
| LENG, X., and CHANSON, H. (2014). "Propagation of Negative Surges in Rivers and Estuaries: Unsteady Turbulent Mixing including the Effects of Bed Roughness." *Hydraulic Model Report No. CH93/13*, School of Civil Engineering, The University of Queensland, Brisbane, Australia, 108 pages (ISBN 9781742720944). | AUD$60.00 | | |
| WUTHRICH, D., and CHANSON, H. (2014). "Aeration and Energy Dissipation over Stepped Gabion Spillways: a Physical Study." *Hydraulic Model Report No. CH92/13*, School of Civil Engineering, The University of Queensland, Brisbane, Australia, 171 pages and 5 video movies (ISBN 9781742720944). | AUD$60.00 | | |
| WANG, H., and CHANSON, H. (2013). "Free-Surface Deformation and Two-Phase Flow Measurements in Hydraulic Jumps". *Hydraulic Model Report No. CH91/13*, School of Civil Engineering, The University of Queensland, Brisbane, Australia, 108 pages (ISBN 9781742720746). | AUD$60.00 | | |
| SIMON, B., and CHANSON, H. (2013). "Turbulence Measurements in Tidal Bore-like Positive Surges over a Rough Bed". *Hydraulic Model Report No. CH90/12*, School of Civil Engineering, The University of Queensland, Brisbane, Australia, 176 pages (ISBN 9781742720685). | AUD$60.00 | | |
| REUNGOAT, D., CHANSON, H., and CAPLAIN, B. (2012). "Field Measurements in the Tidal Bore of the Garonne River at Arcins (June 2012)." Hydraulic Model Report No. CH89/12, School of Civil Engineering, The University of Queensland, Brisbane, Australia, 121 pages (ISBN 9781742720616). | AUD$60.00 | | |
| CHANSON, H., and WANG, H. (2012). "Unsteady Discharge Calibration of a Large V-Notch Weir." *Hydraulic Model Report No. CH88/12*, School of Civil Engineering, The University of Queensland, Brisbane, Australia, 50 pages & 4 movies (ISBN 9781742720579). | AUD$60.00 | | |
| FELDER, S., FROMM, C., and CHANSON, H. (2012). "Air Entrainment and Energy Dissipation on a 8.9° Slope Stepped Spillway with Flat and Pooled Steps." *Hydraulic Model Report No. CH86/12*, School of Civil Engineering, The University of Queensland, Brisbane, Australia, 82 pages (ISBN 9781742720531). | AUD$60.00 | | |
| FELDER, S., and CHANSON, H. (2012). "Air-Water Flow Measurements in Instationary Free-Surface Flows: a Triple Decomposition Technique." *Hydraulic Model Report No. CH85/12*, School of Civil Engineering, The University of Queensland, Brisbane, Australia, 161 pages (ISBN 9781742720494). | AUD$60.00 | | |
| REICHSTETTER, M., and CHANSON, H. (2011). "Physical and Numerical Modelling of Negative Surges in Open Channels." *Hydraulic Model Report No. CH84/11*, School of Civil Engineering, The University of Queensland, Brisbane, Australia, 82 pages (ISBN 9781742720388). | AUD$60.00 | | |

| | | | |
|---|---|---|---|
| BROWN, R., CHANSON, H., McINTOSH, D., and MADHANI, J. (2011). "Turbulent Velocity and Suspended Sediment Concentration Measurements in an Urban Environment of the Brisbane River Flood Plain at Gardens Point on 12-13 January 2011." *Hydraulic Model Report No. CH83/11*, School of Civil Engineering, The University of Queensland, Brisbane, Australia, 120 pages (ISBN 9781742720272). | AUD$60.00 | | |
| CHANSON, H. "The 2010-2011 Floods in Queensland (Australia): Photographic Observations, Comments and Personal Experience." *Hydraulic Model Report No. CH82/11*, School of Civil Engineering, The University of Queensland, Brisbane, Australia, 127 pages (ISBN 9781742720234). | AUD$60.00 | | |
| MOUAZE, D., CHANSON, H., and SIMON, B. (2010). "Field Measurements in the Tidal Bore of the Sélune River in the Bay of Mont Saint Michel (September 2010)." *Hydraulic Model Report No. CH81/10*, School of Civil Engineering, The University of Queensland, Brisbane, Australia, 72 pages (ISBN 9781742720210). | AUD$60.00 | | |
| JANSSEN, R., and CHANSON, H. (2010). "Hydraulic Structures: Useful Water Harvesting Systems or Relics." *Proceedings of the Third International Junior Researcher and Engineer Workshop on Hydraulic Structures (IJREWHS'10)*, 2-3 May 2010, Edinburgh, Scotland, R. JANSSEN and H. CHANSON (Eds), Hydraulic Model Report CH80/10, School of Civil Engineering, The University of Queensland, Brisbane, Australia, 211 pages (ISBN 9781742720159). | AUD$60.00 | | |
| CHANSON, H., LUBIN, P., SIMON, B., and REUNGOAT, D. (2010). "Turbulence and Sediment Processes in the Tidal Bore of the Garonne River: First Observations." *Hydraulic Model Report No. CH79/10*, School of Civil Engineering, The University of Queensland, Brisbane, Australia, 97 pages (ISBN 9781742720104). | AUD$60.00 | | |
| CHACHEREAU, Y., and CHANSON, H., (2010). "Free-Surface Turbulent Fluctuations and Air-Water Flow Measurements in Hydraulics Jumps with Small Inflow Froude Numbers." *Hydraulic Model Report No. CH78/10*, School of Civil Engineering, The University of Queensland, Brisbane, Australia, 133 pages (ISBN 9781742720036). | AUD$60.00 | | |
| CHANSON, H., BROWN, R., and TREVETHAN, M. (2010). " Turbulence Measurements in a Small Subtropical Estuary under King Tide Conditions." *Hydraulic Model Report No. CH77/10*, School of Civil Engineering, The University of Queensland, Brisbane, Australia, 82 pages (ISBN 9781864999969). | AUD$60.00 | | |
| DOCHERTY, N.J., and CHANSON, H. (2010). "Characterisation of Unsteady Turbulence in Breaking Tidal Bores including the Effects of Bed Roughness." *Hydraulic Model Report No. CH76/10*, School of Civil Engineering, The University of Queensland, Brisbane, Australia, 112 pages (ISBN 9781864999884). | AUD$60.00 | | |
| CHANSON, H. (2009). "Advective Diffusion of Air Bubbles in Hydraulic Jumps with Large Froude Numbers: an Experimental Study." *Hydraulic Model Report No. CH75/09*, School of Civil Engineering, The University of Queensland, Brisbane, Australia, 89 pages & 3 videos (ISBN 9781864999730). | AUD$60.00 | | |
| CHANSON, H. (2009). "An Experimental Study of Tidal Bore Propagation: the Impact of Bridge Piers and Channel Constriction." *Hydraulic Model Report No. CH74/09*, School of Civil Engineering, The University of Queensland, Brisbane, Australia, 110 pages and 5 movies (ISBN 9781864999600). | AUD$60.00 | | |
| CHANSON, H. (2008). "Jean-Baptiste Charles Joseph BÉLANGER (1790-1874), the Backwater Equation and the Bélanger Equation." *Hydraulic Model Report No. CH69/08*, Div. of Civil Engineering, The University of Queensland, Brisbane, Australia, 40 pages (ISBN 9781864999211). | AUD$60.00 | | |

| | | | |
|---|---|---|---|
| GOURLAY, M.R., and HACKER, J. (2008). "Reef-Top Currents in Vicinity of Heron Island Boat Harbour, Great Barrier Reef, Australia: 2. Specific Influences of Tides Meteorological Events and Waves." *Hydraulic Model Report No. CH73/08*, Div. of Civil Engineering, The University of Queensland, Brisbane, Australia, 331 pages (ISBN 9781864999365). | AUD$60.00 | | |
| GOURLAY, M.R., and HACKER, J. (2008). "Reef Top Currents in Vicinity of Heron Island Boat Harbour Great Barrier Reef, Australia: 1. Overall influence of Tides, Winds, and Waves." *Hydraulic Model Report CH72/08*, Div. of Civil Engineering, The University of Queensland, Brisbane, Australia, 201 pages (ISBN 9781864999358). | AUD$60.00 | | |
| LARRARTE, F., and CHANSON, H. (2008). "Experiences and Challenges in Sewers: Measurements and Hydrodynamics." *Proceedings of the International Meeting on Measurements and Hydraulics of Sewers*, Summer School GEMCEA/LCPC, 19-21 Aug. 2008, Bouguenais, Hydraulic Model Report No. CH70/08, Div. of Civil Engineering, The University of Queensland, Brisbane, Australia (ISBN 9781864999280). | AUD$60.00 | | |
| CHANSON, H. (2008). "Photographic Observations of Tidal Bores (Mascarets) in France." *Hydraulic Model Report No. CH71/08*, Div. of Civil Engineering, The University of Queensland, Brisbane, Australia, 104 pages, 1 movie and 2 audio files (ISBN 9781864999303). | AUD$60.00 | | |
| CHANSON, H. (2008). "Turbulence in Positive Surges and Tidal Bores. Effects of Bed Roughness and Adverse Bed Slopes." *Hydraulic Model Report No. CH68/08*, Div. of Civil Engineering, The University of Queensland, Brisbane, Australia, 121 pages & 5 movie files (ISBN 9781864999198) | AUD$70.00 | | |
| FURUYAMA, S., and CHANSON, H. (2008). "A Numerical Study of Open Channel Flow Hydrodynamics and Turbulence of the Tidal Bore and Dam-Break Flows." *Report No. CH66/08*, Div. of Civil Engineering, The University of Queensland, Brisbane, Australia, May, 88 pages (ISBN 9781864999068). | AUD$60.00 | | |
| GUARD, P., MACPHERSON, K., and MOHOUPT, J. (2008). "A Field Investigation into the Groundwater Dynamics of Raine Island." *Report No. CH67/08*, Div. of Civil Engineering, The University of Queensland, Brisbane, Australia, February, 21 pages (ISBN 9781864999075). | AUD$40.00 | | |
| FELDER, S., and CHANSON, H. (2008). "Turbulence and Turbulent Length and Time Scales in Skimming Flows on a Stepped Spillway. Dynamic Similarity, Physical Modelling and Scale Effects." *Report No. CH64/07*, Div. of Civil Engineering, The University of Queensland, Brisbane, Australia, March, 217 pages (ISBN 9781864998870). | AUD$60.00 | | |
| TREVETHAN, M., CHANSON, H., and BROWN, R.J. (2007). "Turbulence and Turbulent Flux Events in a Small Subtropical Estuary." Report No. CH65/07, Div. of Civil Engineering, The University of Queensland, Brisbane, Australia, November, 67 pages (ISBN 9781864998993) | AUD$60.00 | | |
| MURZYN, F., and CHANSON, H. (2007). "Free Surface, Bubbly flow and Turbulence Measurements in Hydraulic Jumps." *Report CH63/07*, Div. of Civil Engineering, The University of Queensland, Brisbane, Australia, August, 116 pages (ISBN 9781864998917). | AUD$60.00 | | |
| KUCUKALI, S., and CHANSON, H. (2007). "Turbulence in Hydraulic Jumps: Experimental Measurements." *Report No. CH62/07*, Div. of Civil Engineering, The University of Queensland, Brisbane, Australia, July, 96 pages (ISBN 9781864998825). | AUD$60.00 | | |
| CHANSON, H., TAKEUCHI, M, and TREVETHAN, M. (2006). "Using Turbidity and Acoustic Backscatter Intensity as Surrogate Measures of Suspended Sediment Concentration. Application to a Sub-Tropical Estuary (Eprapah Creek)." *Report No. CH60/06*, Div. of Civil Engineering, The University of Queensland, Brisbane, Australia, July, 142 pages (ISBN 1864998628). | AUD$60.00 | | |

| | | | |
|---|---|---|---|
| CAROSI, G., and CHANSON, H. (2006). "Air-Water Time and Length Scales in Skimming Flows on a Stepped Spillway. Application to the Spray Characterisation." *Report No. CH59/06*, Div. of Civil Engineering, The University of Queensland, Brisbane, Australia, July (ISBN 1864998601). | AUD$60.00 | | |
| TREVETHAN, M., CHANSON, H., and BROWN, R. (2006). "Two Series of Detailed Turbulence Measurements in a Small Sub-Tropical Estuarine System." *Report No. CH58/06*, Div. of Civil Engineering, The University of Queensland, Brisbane, Australia, Mar. (ISBN 1864998520). | AUD$60.00 | | |
| KOCH, C., and CHANSON, H. (2005). "An Experimental Study of Tidal Bores and Positive Surges: Hydrodynamics and Turbulence of the Bore Front." *Report No. CH56/05*, Dept. of Civil Engineering, The University of Queensland, Brisbane, Australia, July (ISBN 1864998245). | AUD$60.00 | | |
| CHANSON, H. (2005). "Applications of the Saint-Venant Equations and Method of Characteristics to the Dam Break Wave Problem." *Report No. CH55/05*, Dept. of Civil Engineering, The University of Queensland, Brisbane, Australia, May (ISBN 1864997966). | AUD$60.00 | | |
| CHANSON, H., COUSSOT, P., JARNY, S., and TOQUER, L. (2004). "A Study of Dam Break Wave of Thixotropic Fluid: Bentonite Surges down an Inclined plane." *Report No. CH54/04*, Dept. of Civil Engineering, The University of Queensland, Brisbane, Australia, June, 90 pages (ISBN 1864997710). | AUD$60.00 | | |
| CHANSON, H. (2003). "A Hydraulic, Environmental and Ecological Assessment of a Sub-tropical Stream in Eastern Australia: Eprapah Creek, Victoria Point QLD on 4 April 2003." *Report No. CH52/03*, Dept. of Civil Engineering, The University of Queensland, Brisbane, Australia, June, 189 pages (ISBN 1864997044). | AUD$90.00 | | |
| CHANSON, H. (2003). "Sudden Flood Release down a Stepped Cascade. Unsteady Air-Water Flow Measurements. Applications to Wave Run-up, Flash Flood and Dam Break Wave." *Report CH51/03*, Dept of Civil Eng., Univ. of Queensland, Brisbane, Australia, 142 pages (ISBN 1864996552). | AUD$60.00 | | |
| CHANSON, H,. (2002). "An Experimental Study of Roman Dropshaft Operation : Hydraulics, Two-Phase Flow, Acoustics." *Report CH50/02*, Dept of Civil Eng., Univ. of Queensland, Brisbane, Australia, 99 pages (ISBN 1864996544). | AUD$60.00 | | |
| CHANSON, H., and BRATTBERG, T. (1997). "Experimental Investigations of Air Bubble Entrainment in Developing Shear Layers." *Report CH48/97*, Dept. of Civil Engineering, University of Queensland, Australia, Oct., 309 pages (ISBN 0 86776 748 0). | AUD$90.00 | | |
| CHANSON, H. (1996). "Some Hydraulic Aspects during Overflow above Inflatable Flexible Membrane Dam." *Report CH47/96*, Dept. of Civil Engineering, University of Queensland, Australia, May, 60 pages (ISBN 0 86776 644 1). | AUD$60.00 | | |
| CHANSON, H. (1995). "Flow Characteristics of Undular Hydraulic Jumps. Comparison with Near-Critical Flows." *Report CH45/95*, Dept. of Civil Engineering, University of Queensland, Australia, June, 202 pages (ISBN 0 86776 612 3). | AUD$60.00 | | |
| CHANSON, H. (1995). "Air Bubble Entrainment in Free-surface Turbulent Flows. Experimental Investigations." *Report CH46/95*, Dept. of Civil Engineering, University of Queensland, Australia, June, 368 pages (ISBN 0 86776 611 5). | AUD$80.00 | | |
| CHANSON, H. (1994). "Hydraulic Design of Stepped Channels and Spillways." *Report CH43/94*, Dept. of Civil Engineering, University of Queensland, Australia, Feb., 169 pages (ISBN 0 86776 560 7). | AUD$60.00 | | |
| POSTAGE & HANDLING (per report) | AUD$10.00 | | |
| GRAND TOTAL | | | |

## OTHER HYDRAULIC RESEARCH REPORTS

| Reports/Theses | Unit price | Quantity | Total price |
|---|---|---|---|
| FELDER, S. (2013). "Air-Water Flow Properties on Stepped Spillways for Embankment Dams: Aeration, Energy Dissipation and Turbulence on Uniform, Non-Uniform and Pooled Stepped Chutes." *Ph.D. thesis*, School of Civil Engineering, The University of Queensland, Brisbane, Australia. | AUD$100.00 | | |
| REICHSTETTER, M. (2011). "Hydraulic Modelling of Unsteady Open Channel Flow: Physical and Analytical Validation of Numerical Models of Positive and Negative Surges." *MPhil thesis*, School of Civil Engineering, The University of Queensland, Brisbane, Australia, 112 pages. | AUD$80.00 | | |
| TREVETHAN, M. (2008). "A Fundamental Study of Turbulence and Turbulent Mixing in a Small Subtropical Estuary." Ph.D. thesis, Div. of Civil Engineering, The University of Queensland, 342 pages. | AUD$100.00 | | |
| GONZALEZ, C.A. (2005). "An Experimental Study of Free-Surface Aeration on Embankment Stepped Chutes." *Ph.D. thesis*, Dept of Civil Engineering, The University of Queensland, Brisbane, Australia, 240 pages. | AUD$80.00 | | |
| TOOMBES, L. (2002). "Experimental Study of Air-Water Flow Properties on Low-Gradient Stepped Cascades." *Ph.D. thesis*, Dept of Civil Engineering, The University of Queensland, Brisbane, Australia. | AUD$100.00 | | |
| CHANSON, H. (1988). "A Study of Air Entrainment and Aeration Devices on a Spillway Model." *Ph.D. thesis*, University of Canterbury, New Zealand. | AUD$60.00 | | |
| POSTAGE & HANDLING (per report) | AUD$10.00 | | |
| GRAND TOTAL | | | |

## CIVIL ENGINEERING RESEARCH REPORT CE

The Civil Engineering Research Report CE series is published by the School of Civil Engineering at the University of Queensland. Orders of any of the Civil Engineering Research Report CE should be addressed to the School Secretary.

School Secretary, School of Civil Engineering, The University of Queensland
Brisbane 4072, Australia
Tel.: (61 7) 3365 3619 Fax: (61 7) 3365 4599
Url: http://http://www.civil.uq.edu.au// Email: enquiries@civil.uq.edu.au

| Recent Research Report CE | Unit price | Quantity | Total price |
|---|---|---|---|

| | | | |
|---|---|---|---|
| CALLAGHAN, D.P., NIELSEN, P., and CARTWRIGHT, N. (2006). "Data and Analysis Report: Manihiki and Rakahanga, Northern Cook Islands - For February and October/November 2004 Research Trips." *Research Report CE161*, Division of Civil Engineering, The University of Queensland (ISBN No. 1864998318). | AUD$10.00 | | |
| GONZALEZ, C.A., TAKAHASHI, M., and CHANSON, H. (2005). "Effects of Step Roughness in Skimming Flows: an Experimental Study." *Research Report No. CE160*, Dept. of Civil Engineering, The University of Queensland, Brisbane, Australia, July (ISBN 1864998105). | AUD$10.00 | | |
| CHANSON, H., and TOOMBES, L. (2001). "Experimental Investigations of Air Entrainment in Transition and Skimming Flows down a Stepped Chute. Application to Embankment Overflow Stepped Spillways." *Research Report No. CE158*, Dept. of Civil Engineering, The University of Queensland, Brisbane, Australia, July, 74 pages (ISBN 1 864995297). | AUD$10.00 | | |
| HANDLING (per order) | AUD$10.00 | | |
| GRAND TOTAL | | | |

Note: Prices include postages and processing.

---

**PAYMENT INFORMATION**

1- VISA Card

| | |
|---|---|
| Name on the card : | |
| Visa card number : | |
| Expiry date : | |
| Amount : | AUD$ ..... |

2- Cheque/remittance payable to: THE UNIVERSITY OF QUEENSLAND and crossed "Not Negotiable".

N.B. For overseas buyers, cheque payable in Australian Dollars drawn on an office in Australia of a bank operating in Australia, payable to: THE UNIVERSITY OF QUEENSLAND and crossed "Not Negotiable".

Orders of any Research Report should be addressed to the School Secretary.

School Secretary, School of Civil Engineering, The University of Queensland
Brisbane 4072, Australia - Tel.: (61 7) 3365 3619 - Fax: (61 7) 3365 4599
Url: http://http://www.civil.uq.edu.au// Email: enquiries@civil.uq.edu.au